

AN INVESTIGATION OF THE PHOTOCHEMISTRY AND
STRUCTURES OF SELECTED SECOND AND THIRD ROW
TRANSITION METAL COMPLEXES

Thesis by
Penny Kristen Eidem

In Partial Fulfillment of the Requirements
for the Degree of
Doctor of Philosophy

California Institute of Technology
Pasadena, California
1981

(Submitted December 8, 1980)

Copyright c by
Penny Kristen Eidem
1980

iii

To

Dr. Judith Saperstein Braun

who helped make this, and so much more, possible

Acknowledgements

Caltech's been most special for the fabulous friends it has brought me. To Cathy Coyle, Ann English, Merrie Jo Johnson, Susan Nunnery, Tom Smith, Dan Straus, and Kathy Yocom, thanks for your love, laughter, and lively art. My parents and pre-Caltech friends are lovingly remembered for more of the same: Dr. Alma Booker, Dana Chapin, Pam Jones Craycroft, Catherine, Corrine, and Walt DeBoer, Charlotte and Ralph Eidem, Herman and Myrtle Eidem, Flo, Mandi, and Ron Glazebrook, Doris and Tom Harris, Irene and Mel Hooper, Roma Jones, Fred Montgomery, Jim Nicholson, Burl, Jean, and Linda Norberg, Kathy Hoylen Petrie, Gregory Ranney, Bill Richardson, Magritte Lee Roos, Michael Thomas, Jason, Mihran, and Vivian Tachdjian, Arnie Villone, and Gary Volk.

For their friendship, support, and expertise a special word of thanks to Jeb Bercaw, Steve Cramer, Zvi Dori, Dave Erwin, Jan Najdzionek, Andy Maverick, Kent Mann, Steve Milder, Steve Rice, T. Pat Smith, Dave Tyler, Jay Winkler, and all past and present members of the Gray Group.

The fabulous staff people have been generous with their time and so much more. Many thanks to Rose Alvarez, Fred Beal, Charlie Beebe, Fran Bennett, Louis Borbon, Sue Brittenham, Pat Bullard, Rhonda Campbell, Elmer Clarke, Tom Dunn, Anita Duran, Brax Evans, Gabor Faluti, Roy Harris, Siegfried Jenner, Ed Lohr, Emily Mazurek, Ernie Moore, Eric Sigal, and Bill Schuelke.

Jen Burkhart deserves a special acknowledgment and thank you for typing this thesis. I've enjoyed our conversations.

Last, but not least, many thanks to my leader, HBG, for his humor, insight, and support and for always trying to be a nice guy.

ABSTRACT

Examination of the electronic spectrum of IrCl_6^{3-} has led to a reassignment of the electronic transitions involved. The band at 206 nm, formerly assigned as the spin allowed π_L to metal e_g transition, is shown to be $1t_{1u}(\sigma) \rightarrow 2e_g(z^2, x^2-y^2)$ [$^1A_{1g} \rightarrow ^1T_{1u}$]. Low temperature spectra revealed the presence of additional features at 250 and 278 nm. These are ascribed to the $1t_{2u}(\pi) \rightarrow 2e_g(z^2, x^2-y^2)$ [$^1A_{1g} \rightarrow ^1T_{1u}$] and $1t_{2u}(\pi) \rightarrow 2e_g(z^2, x^2-y^2)$ [$^1A_{1g} \rightarrow ^3T_{1u}$] transitions, respectively. Irradiation ($\lambda = 254$ nm) of 1-12 M HCl solutions of IrCl_6^{3-} yields IrCl_6^{2-} and H_2 . Since the excited state populated at this wavelength has been shown to be ligand to metal charge transfer in nature, the reactive intermediate is proposed to be an Ir(II) species with a chlorine atom still formally bound. Photolysis of the reaction product, IrCl_6^{2-} in HCl results in the formation of IrCl_6^{3-} and Cl_2 . This reaction prevails regardless of wavelength of excitation. The reactive state is again LMCT in nature. Coupling of these reactions effects a reversible photochemical hydrohalic acid splitting catalyst.

The photochemistry of Mo(III), Mo(IV), Mo(V) in aqueous solution was investigated, and these ions were shown to be photochemically inert. Structural characterizations via Raman spectroscopy and X-ray absorption edge and EXAFS were undertaken. The Mo(II) structure is shown to be a quadruply

bound dinuclear species. The Mo(III) is singly bonded with hydroxy bridges. Data for the Mo(V) ion are typical for oxobridged dinuclear compounds. In strong acid, Mo(IV) is shown to exist as a trinuclear species. As the pH of the medium is increased, the Mo-Mo amplitude decreased, indicating possible cluster fragmentation. In basic solution, a major structural change occurs. The presence of halide ions had no effect on the spectra.

$\text{Ru}_3(\text{CO})_{12}$ reacts photochemically in the presence of olefins, CO, and H_2 to catalyze the hydroformylation reaction. Typical yields are 1.5×10^{-3} moles of aldehydes in a 2:1 linear to branched chain ratio. A heterogeneous catalyst can also be effected by photoinduced fragmentation of the cluster in the presence of PV4P. Attachment of a Ru-CO moiety was confirmed by IR and elemental analysis. The first step in catalyst activation was shown to be formation of $\text{Ru}(\text{CO})_4$ olefin with a quantum yield of 0.03 for 1-pentene. Subsequent steps involved formation of a hydrido-olefin complex, rearrangement to a hydrido alkyl, "CO insertion," and reductive elimination of aldehyde. Olefin isomerization and alkane production are also seen under reaction conditions. Formation of larger ruthenium carbonyl clusters led to catalyst deactivation. Photolysis of $\text{Ru}_3(\text{CO})_{12}$ in the presence of H_2 led to the formation of $\alpha\text{H}_4\text{-Ru}_4(\text{CO})_{12}$. This molecule can also effect catalysis of the hydroformylation reaction, although yields are an order of magnitude less than for the parent cluster.

TABLE OF CONTENTS

Chapter 1	The Photochemistry and Electronic Spectra of IrCl_6^{3-} and IrCl_6^{2-}	1
Chapter 2	The Photochemistry and Structural Determination of Molybdenum Aquo Ions	60
Chapter 3	Photochemical Hydroformylation Using Triruthen- iumdodecacarbonyl as a Homogeneous and a Hetero- geneous Catalyst	131
Chapter 4	Propositions	198

Chapter 1

The Photochemistry and Electronic Spectra of IrCl_6^{3-} and IrCl_6^{2-}

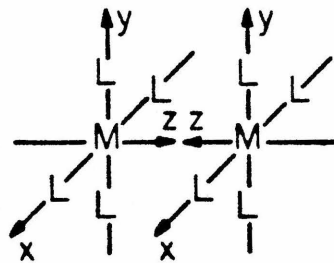
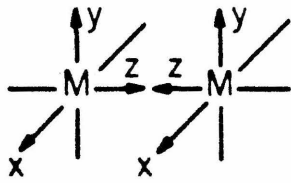
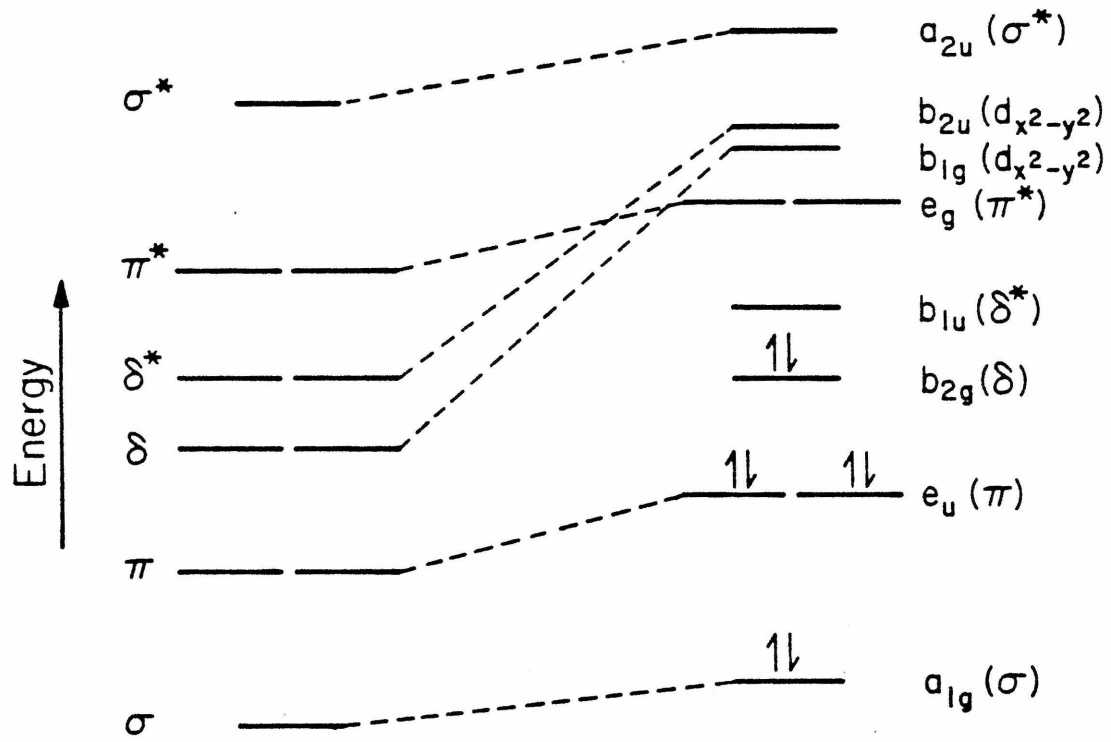
Abstract: Examination of the electronic spectrum of IrCl_6^{3-} has led to a reassignment of the electronic transitions involved. The band at 206 nm, formerly assigned as the spin allowed π_L to metal e_g transition, is shown to be $1_{t_{1u}}(\sigma) \rightarrow 2e_g(z^2, x^2-y^2) [^1A_{1g} \rightarrow ^1T_{1u}]$. Low temperature spectra revealed the presence of additional features at 250 and 278 nm. These are ascribed to the $1_{t_{1u}}(\pi) \rightarrow 2e_g(z^2, x^2-y^2) [^1A_{1g} \rightarrow ^1T_{1u}]$ and $1_{t_{2u}}(\pi) \rightarrow 2e_g(z^2, x^2-y^2) [^1A_{1g} \rightarrow ^3T_{1u}]$ transitions, respectively. Irradiation ($\lambda = 254$ nm) of 1-12 M HCl solutions of IrCl_6^{3-} yields IrCl_6^{2-} and H_2 . Since the excited state populated at this wavelength has been shown to be π ligand to metal charge transfer in nature, the reactive intermediate is proposed to be an Ir(II) species with a chlorine atom still formally bound. Photolysis of the reaction product, IrCl_6^{2-} in HCl results in formation of IrCl_6^{3-} and Cl_2 . This reaction prevails, although quantum yields vary, regardless of wavelength of excitation. The reactive state is again LMCT in nature. Coupling of these reactions effects a reversible photochemical hydrohalic acid splitting catalyst.

The photoredox reactions of Cr^{2+} ,^{1,2} Fe^{2+} ,³⁻⁶ V^{2+} ,⁴ Eu^{2+} ,⁷⁻⁹ Ce^{3+} ,¹⁰ Co^{2+} ,⁴ and Cu^+ ¹¹ in aqueous solution yield molecular hydrogen and an oxidized metal species. Although the formation of a hydrated electron via a charge transfer to solvent (CTTS) state has been proposed, this type of mechanism has been unequivocally established only for Cr^{2+} ,¹²⁻¹⁴ $\text{Fe}(\text{CN})_6^{4-}$,¹²⁻¹⁴ $\text{W}(\text{CN})_8^{4-}$,¹²⁻¹⁴ $\text{Mo}(\text{CN})_8^{4-}$,¹²⁻¹⁴ and CuCl_2^- .¹¹ Recently, metal cluster compounds such as $\text{Mo}_2(\text{SO}_4)_4^{4-}$,¹⁵ $\text{Mo}_2\text{Cl}_8^{4-}$,¹⁶ $\text{Mo}_2(\text{aq})^{4+}$,¹⁶ and $\text{Rh}_4(\text{br})_8^{6+}$ ¹⁷ (br = 1,3-diisocyanopropane) have been shown to effect the photochemical reduction of protons in aqueous solution. The mechanisms of these photoredox reactions have not been elucidated in any detailed sense.

Our interest in this area centered originally on the aqueous photochemistry of $\text{Re}_2\text{X}_8^{2-}$ (X = Cl, Br). Both complexes are diamagnetic, have an unusually short Re-Re bond, and show an eclipsed rotational configuration. These phenomena were first explained by Cotton¹⁸ who proposed that a $d^4 - d^4$ complex such as $\text{Re}_2\text{X}_8^{2-}$ possesses a quadruple metal-metal bond ($\sigma^2 \pi^4 \delta^2$). As shown in the molecular orbital scheme in Figure 1, σ , π , and δ bonding and antibonding orbitals may be generated from the appropriate linear combinations of the d_{z^2} , (d_{xz} , d_{yz}) and d_{xy} orbitals, respectively. While the exact position of the ${}^1A_{1g} \rightarrow {}^1A_{2u}$ ($\delta\delta^*$) transition has been the subject of much controversy, it is now well established that this transition in $\text{Re}_2\text{Cl}_8^{2-}$ falls at 680 nm.¹⁹ Assignments of the electronic absorption

Figure 1

Molecular orbital scheme for $\text{Re}_2\text{X}_8^{2-}$



spectrum are given in Table 1.

A previous study of the photochemistry of $\text{Re}_2\text{Cl}_8^{2-}$ showed that irradiation led to cleavage of the quadruple bond, resulting in monomeric products.²⁰ Photolyses ($\lambda < 366 \text{ nm}$) in CH_3CN yielded trans- $[\text{ReCl}_4(\text{CH}_3\text{CN})_2]^-$ and $\text{ReCl}_3(\text{CH}_3\text{CN})_3$ as the primary and secondary photoproducts, respectively. Although definitive evidence was lacking, the most likely mechanism invokes association of acetonitrile to the excited state, thereby assisting dimer fragmentation.

To see if $\text{Re}_2\text{Cl}_8^{2-}$ might undergo redox rather than substitution photochemistry, irradiations were carried out in HCl solutions (12 M). Ultraviolet light ($\lambda < 366 \text{ nm}$) led to the production of hydrogen and the chloro-bridged $\text{Re}_2\text{Cl}_9^{2-}$ species, as identified by the electronic absorption spectrum. The fact that a one-electron oxidized binuclear complex was produced implies that dissociation to mononuclear fragments does not occur in this medium. If it had, both $\text{Re}_2\text{Cl}_9^{2-}$ and Re_2Cl_9^- would have been observed, and none of the latter was evident. For photolysis ($\lambda < 366 \text{ nm}$) of $\text{Re}_2\text{Br}_8^{2-}$ in 48% HBr, molecular hydrogen was again produced, but the oxidized metal species in this case was Re_2Br_9^- . In this case it is probable that secondary photolysis occurred, as $\text{Re}_2\text{Br}_9^{2-}$ is strongly absorbing in the region of irradiation, and it is also photosensitive. The overlapping spectra (Table 2) and each of any isosbestic points, however, preclude identification of any intermediates.

Table 1. Electronic Spectral Data and Assignments for $\text{Re}_2\text{Cl}_8^{2-}$.

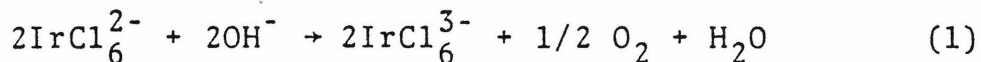
λ (nm)	${}^1A_{1g} \rightarrow$
680	${}^1A_{2u}(\delta \rightarrow \delta^*)$
478	${}^1A_{1u}[\delta \rightarrow d_{x^2-y^2}(b_{1g})]$
423	${}^1E_g(\pi \rightarrow \delta^*)$
370, 355	${}^1A_{2u}[e_g \pi_{ } \text{ and } \pi_{\perp}(\text{halide}) \rightarrow \delta^*]$
280	${}^1A_{2u}[\text{Cl}(\pi_{\perp}) \rightarrow \delta^*]$
255	${}^1A_{1g} \rightarrow {}^1A_{2u}$

Table 2. Electronic Spectral Data for $\text{Re}_2\text{Br}_8^{2-}$, Re_2Br_9^- , and $\text{Re}_2\text{Br}_9^{2-}$.

Complex	λ (nm)	($\text{l} \cdot \text{mol}^{-1} \text{cm}^{-1}$)
$\text{Re}_2\text{Br}_8^{2-}$	715	14,500
	470	238
	418	3,440
	376	3,220
Re_2Br_9^-	725	560
	396	18,000
$\text{Re}_2\text{Br}_9^{2-}$	718	1,200
	469	7,000
	418	10,800
	388	11,000

The $\text{Re}_2\text{X}_9^{2-}$ and Re_2X_9^- complexes ($\text{X} = \text{Cl}, \text{Br}$) are ineffective as oxidizing agents and cannot be readily reduced to the starting material, $\text{Re}_2\text{X}_8^{2-}$. Also, the quantum yields for hydrogen production are extremely low ($\ll 10^{-4}$) and any reasonable degree of conversion required continued irradiation for several days. Accordingly, we turned our attention to halo complexes of other heavy metals.

The chloro complexes of iridium seemed logical candidates for investigation. Both IrCl_6^{3-} and IrCl_6^{2-} have been studied extensively as thermal redox reagents,²¹⁻⁴² the latter being a powerful oxidant ($E_0 = 0.867 \text{ v}$). Previous work on the thermal aqueous chemistry of IrCl_6^{2-} has also indicated that it undergoes spontaneous reduction in alkaline or weakly acidic solution:⁴³



Thus, if IrCl_6^{2-} and H_2 could be produced by irradiation of IrCl_6^{3-} under the right conditions, a homogeneous, photodriven water splitting system would be available for detailed study. The goal of our work was to define the conditions under which photochemical water splitting by $\text{IrCl}_6^{3-/2-}$ could be achieved, and to begin mechanistic investigations of this model system.

To date only cursory investigation of the photochemistry of these complexes has been made. A report by Sleight and Hare indicated that IrCl_6^{2-} undergoes aquation in neutral or

acidic solution with no media or wavelength dependence apparent.⁴⁴ Conflicting results were obtained by Moggi, et al., who found both redox and aquation photochemistry, the products varying with the wavelength of irradiation and the concentration of Cl^- present.⁴⁵ In a flash photolysis study of IrCl_6^{3-} , Adamson postulated that ultraviolet irradiation of this complex results in solvated electron formation.⁴⁶ Although Jørgensen had assigned the transition involved as being ligand to metal charge transfer in nature,⁴⁷ Adamson suggested that it was, in fact, charge transfer to solvent. Owing to these conflicting results, we reinvestigated the electronic spectra of these complexes in parallel with our photochemical studies. The results of both the spectroscopic and photochemical experiments are presented in this chapter.

Experimental

Na_3IrCl_6 , Na_2IrCl_6 , and H_2^{18}O (99% isotopically pure) were purchased from Alfa Chemical Company. Ultra-pure HCl or HCl distilled from hydroxylamine was used to minimize Cl_2 content.

Electronic absorption spectra and spectral changes were recorded with either a Cary 17 or a Cary 219 spectrophotometer. Low temperature spectra were obtained using a C.T.I. 21 cryocooler. Infrared spectra were recorded with a Beckman IR-12 instrument. A 250 watt Hg-Xe lamp in

conjunction with Corning cut-off on solution band pass filters was used for visible irradiations. A low pressure Hg lamp was used for 254 nm irradiations.

Ferrioxilate actinometry was used for quantum yield determinations at 254, 313, 366, 420, and 488 nm. The procedure was modified to adopt precautions recently advised by Bowman and Demas.⁴⁸ Quantum yields for IrCl_6^{3-} oxidation were determined by monitoring the appearance of the 488 nm band of IrCl_6^{2-} . Differential quantum yields for IrCl_6^{2-} photolyses were calculated from the tangents of concentration versus time plots for the decrease in absorbance of IrCl_6^{2-} at 488 nm. In order to minimize secondary photoreactions, only a small percent of the initial complex was decomposed.

Photolyses were done in special two arm evacuable cells equipped with Kontes quick-release valves. Solutions to be photolyzed were either freeze-thaw-degassed six times or purged with Argon prior to irradiation. In a typical experiment 7×10^{-3} M IrCl_6^{3-} or 4×10^{-4} M IrCl_6^{2-} M was irradiated in an HCl solution. Typical photon fluxes were 2.7×10^{-6} , 6.9×10^{-8} , 4.5×10^{-8} , 3.1×10^{-7} , and 1.3×10^{-7} einsteins per minute for 254, 315, 420, and 480 nm, respectively.

Conventional flash photolysis was performed on an apparatus constructed at Caltech. This consists of a Xenon Corporation N851C flashlamp fired by a Model 457 micropulser (energy = 36-100 J/flash), $\tau_{1/2} \approx 5 \mu\text{s}$). The sample was placed in a 15 cm pathlength quartz cell, and Corning cut-off

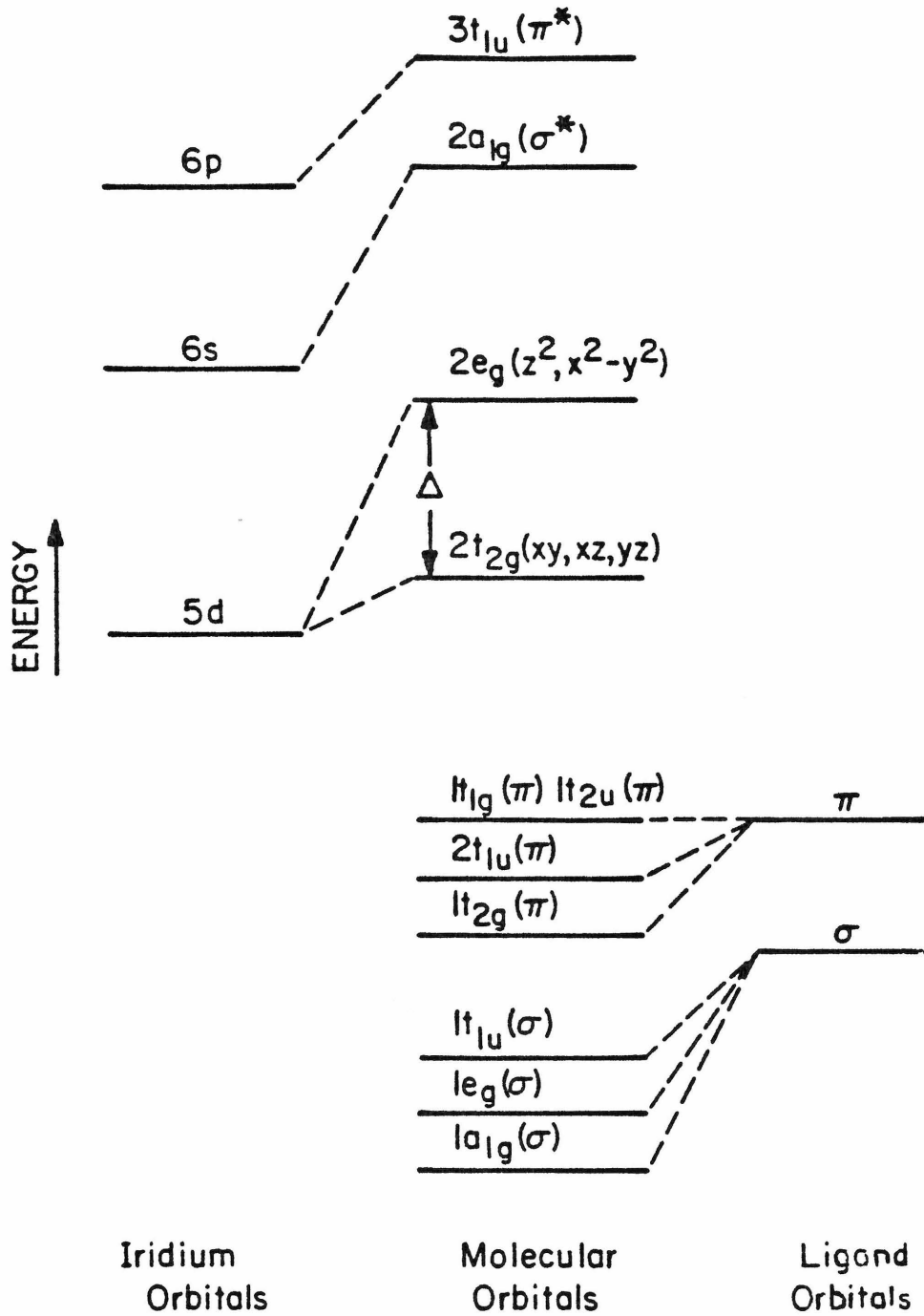
filters were used to isolate spectral regions. The monitoring beam was the output of a 200 watt Hg-Xe lamp; detection employed an Oriel 7240 1/4 meter monochromator and a Hamamatsu R928 photomultiplier. The signal was displayed on either a Tektronix 549 storage oscilloscope with Type W plug in or on a Hewlett-Packard 700 SB x-y recorder after storage in a Biomation 805 transient waveform recorder.

Hydrogen and oxygen were qualitatively determined by mass spectral data. Quantitative measurements of H_2 were done as follows. The total volume of gas evolved was measured by Toepler pumping the stirred, photolyzed solution into a known volume and manometrically measuring the pressure. The gases were then passed through a heated CuO column. This oxidized H_2 to H_2O , which was condensed in a liquid nitrogen trap. The amount of H_2 was completed by differences. Typically, 10 torr of H_2 were collected and the measurements were reproducible to $\pm 6\%$. Mass spectral analyses for $^{18}O_2$ were made on samples of $IrCl_6^{2-}$ in $H_2^{18}O$ into which a known volume of HCl gas had been condensed.

Results and Discussion

Electronic Spectra of $IrCl_6^{3-}$ and $IrCl_6^{2-}$. A generalized molecular orbital energy level diagram suitable for discussion of both iridium complexes is shown in Figure 2. The $IrCl_6^{3-}$ complex has a low spin d^6 electronic configuration, the highest filled level is $2t_{2g}^6$ (xy, xz, yz). Thus the

Figure 2
Molecular orbital scheme for IrCl_6^{2-}

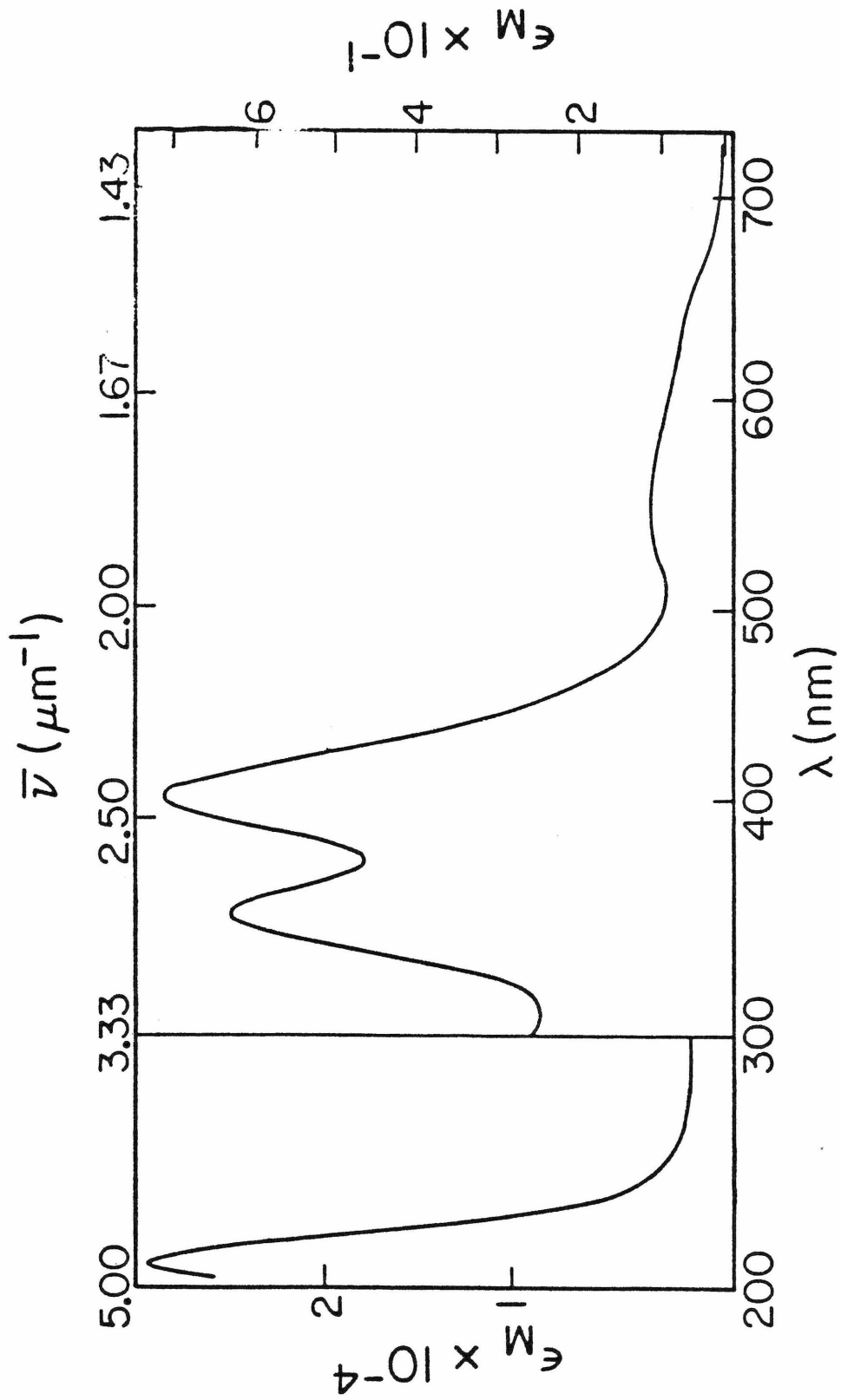


ground state is designated as $^1A_{1g}$. The first excited state configuration for a d - d transition is $[2t_{2g}(xy,xz,yz)]^5 [2e_g(z^2,x^2-y^2)]^1$, which gives rise to $^1T_{1g}$ and $^1T_{2g}$ and $^3T_{1g}$ and $^3T_{2g}$ excited states. Transitions from $^1A_{1g}$ to these states give rise to four weak absorption bands in the 650-350 nm region of the spectrum of IrCl_6^{3-} (Figure 3). The two relatively weak bands observed at 615 ($\epsilon = 7.5$) and 560 ($\epsilon = 10$) have been assigned by Jørgensen to the spin-forbidden transitions, whereas those at 415 ($\epsilon = 76$) and 356 nm ($\epsilon = 64$) to the two spin-allowed ones.⁴⁹ This assignment scheme is consistent with the fact that the extinction coefficients are lower for the spin-forbidden bands, and that the triplets fall at lower energies than the singlets. An excellent fit to the transition energies is obtained by taking the following values for the octahedral splitting (Δ) and electron-repulsion parameters: $\Delta = 28\ 110$; $B = 250$; $C = 4020\ \text{cm}^{-1}$. Calculated and observed energies of the ligand field states are as follows: $^1T_{2g}$, 28,090 (calcd), 28,090 (obsd); $^1T_{1g}$, 24,090 (calcd), 24,096 (obsd); $^3T_{2g}$, 18,050 (calcd), 17,857 (obsd); $^3T_{1g}$, 16,050 (calcd), 16,260 cm^{-1} (obsd).

The intense, high energy band at 206 nm (Figure 3) was assigned by Jørgensen as the spin allowed π to e_g transition.⁴⁷ Adamson, however, has criticized this assignment on the basis of a flash photolysis study as mentioned earlier.⁴⁶ Photolyzed solutions of IrCl_6^{3-} under an atmosphere of N_2O yielded IrCl_6^{2-} and N_2 , the products expected upon solvated

Figure 3

Electronic absorption spectrum of IrCl_6^{3-}



electron formation. Although the quantum yield for reaction (0.031) was an order of magnitude smaller than those for other complexes studied, and the purported solvated electron was not observed spectroscopically, Adamson suggested the transition to be charge transfer to solvent in nature.

Flash photolysis studies in our laboratory showed no transient ascribable to $e^-(aq)$ although this could be explained by lifetime limitations of the apparatus. To test for charge transfer to solvent character, spectra of $IrCl_6^{3-}$ were recorded in various solvent systems and at different temperatures. According to a detailed analysis of CTTS bands by Blandemeyer and Fox,⁵⁰ there are a number of unique characteristics which can be used to diagnose this type of transition. These include 1) a blue shift of several nanometers when the solvent is changed from H_2O to D_2O ; 2) a blue shift when organic solutes and solvents are added; 3) a blue shift for a large increase in ionic strength; and, 4) a very slight red shift as the temperature is increased. At a given temperature, different E_{max} values for a given ion in a range of solvents reflect differences in the radius of the solvent cavity (which may be viewed as the radius of the excited state orbital). As the radius increases (corresponding to an increase in the number of cavities available for electron solvation), the transition energy decreases. At higher temperatures, there is more disorder of solvent molecules, resulting in a larger excited state radius and a

greater number of available sites for the solvated electron. The high energy shift or E_{\max} on replacing water by deuterium oxide is in agreement with the generally accepted viewpoint that water and deuterium oxide are very similar in their properties, except those of the latter are comparable to water at lower temperatures, i.e., more structural order exists. The effects of added solutes or cosolvents on charge transfer to solvent spectra have been extensively investigated but are not well understood in any quantitative fashion. It is known, however, that E_{\max} increases when electron acceptor molecules are removed from the solvent shell (by dilution, substitution, or ion pairing), as would be expected from simple theoretical considerations. The main result of our studies is that the 206 nm band in the IrCl_6^{3-} spectrum is insensitive to environmental perturbations (Table 3). Thus, at least for the transition that gives a 206 nm peak, a CTTS assignment is inappropriate.

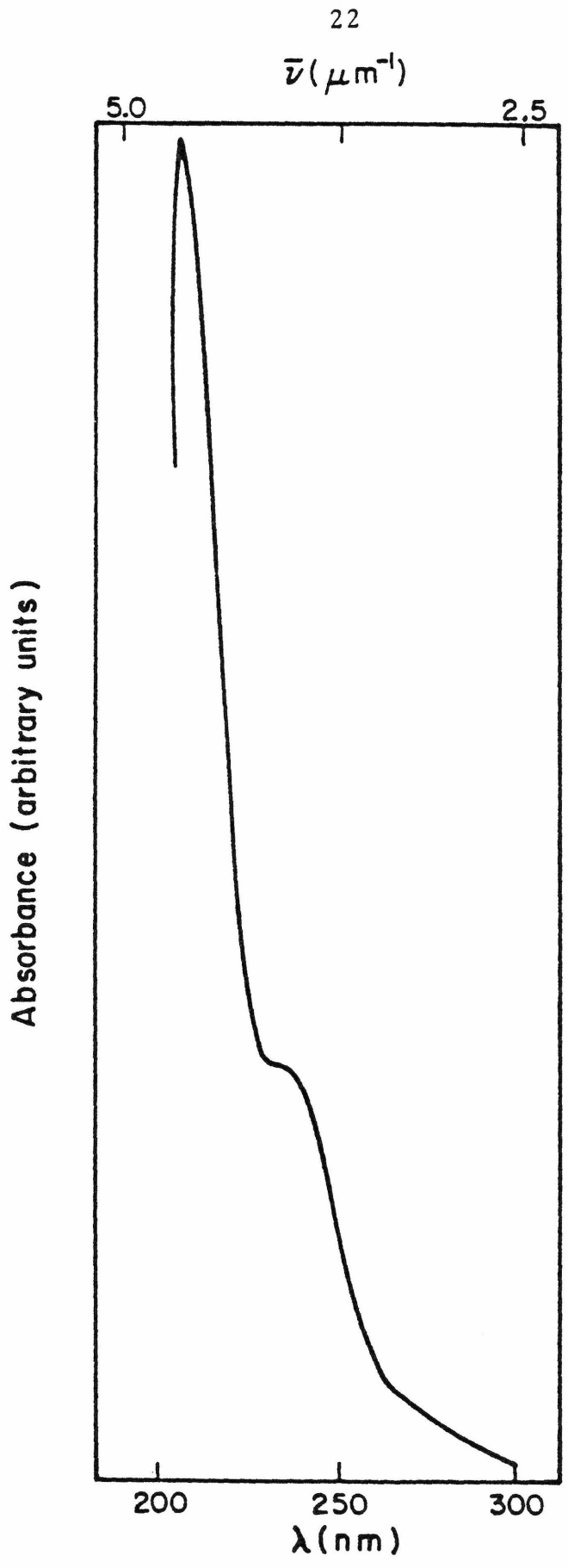
It was noted, however, that the band in question is extremely broad, tailing out considerably toward low energy. Because this large bandwidth suggested the possibility of an additional transition(s), low temperature spectra were recorded. Figure 4 shows the spectrum of IrCl_6^{3-} in a 50% LiCl glass at 60 K. The band at 206 nm has sharpened and intensified, but more interesting is the appearance of a new feature at ca. 245 nm and a shoulder at ca. 265 nm. If either of these features is ascribable to a charge transfer

Table 3. Studies of the 206 nm Band in the IrCl_6^{3-} Spectrum

<u>Solute</u>	<u>Experiment</u>	<u>λ_{max} (nm)</u>
3.38×10^{-5} M IrCl_6^{3-} 0.25 M Cl^- 0.20 M Li^+ 0.05 M NH_4^+	H_2O solution (25°C)	205.3
3.38×10^{-5} M IrCl_6^{3-} 1.0 M Cl^- 0.05 M NH_4^+ 0.95 M Li^+	H_2O solution (25°C) MeOH solution (25°C)	205.0 206.0
3.38×10^{-5} M IrCl_6^{3-} 1.0 M Cl^- 1.0 M H^+	$\text{H}_2\text{O}/1.0$ M sucrose solution (25°C) H_2O solution (25°C)	205.2 206.0
3.38×10^{-5} M IrCl_6^{3-} 1.0 M Cl^- 1.0 M H^+	H_2O solution (25°C) H_2O solution (50°C)	205.3 205.3
3.38×10^{-5} M IrCl_6^{3-} 1.0 M Cl^- 1.0 M H^+	H_2O solution (25°C) $\text{H}_2\text{O}/2\text{M}$ HClO_4 solution (25°C)	205.0 204.0

Figure 4

LiCl glass spectrum of IrCl_6^{3-} at 60K



to solvent transition, it should disappear in the solid state. Figure 5 shows a KCl pellet spectrum of IrCl_6^{3-} at 16 K. All three bands are still present in this medium; therefore, none could result from a CTTS state. The high energy band at 206 nm has not changed position, whereas red shifts of ca. 800 and 1800 cm^{-1} are observed for the less prominent features (these now appear at 250 and 278 nm, respectively).

An assignment of these new bands may be made by analogy to Mason's interpretation of the spectrum of the isoelectronic PtCl_6^{2-} (Table 4).⁵¹ Two intense high energy bands are observed at 266 and 202 nm in the PtCl_6^{2-} spectrum. Both sharpen and increase in maximum molar extinction as the temperature is lowered, which is characteristic of a fully allowed transition. The detailed assignment of the 266 nm band is the $1t_{2u}(\pi) \rightarrow 2e_g(z^2, x^2-y^2) [{}^1A_{1g} \rightarrow {}^1T_{1u}]$. The second band, observed at 202 nm in acetonitrile, is more intense than the first. The band is ascribed to an LMCT transition, but one involving ligand σ orbitals: $1t_{1u}(\sigma) \rightarrow 2e_g(z^2, x^2-y^2) [{}^1A_{1g} \rightarrow {}^1T_{1u}]$. The bands in IrCl_6^{3-} must result from analogous transitions as given in Table 5. The 206 nm band is $1t_{1u}(\sigma) \rightarrow 2e_g(z^2, x^2-y^2) [{}^1A_{1g} \rightarrow {}^1T_{1u}]$, the 250 nm band the $1t_{2u}(\pi) \rightarrow 2e_g(z^2, x^2-y^2) [{}^1A_{1g} \rightarrow {}^1T_{1u}]$. The shoulder at 278 nm is undoubtedly the $1t_{2u}(\pi) \rightarrow 2e_g(z^2, x^2-y^2) [{}^1A_{1g} \rightarrow {}^3T_{1u}]$ transition. These assignments are consistent both with the intensities and energies of the bands.

Figure 5

KCl pellet spectrum of IrCl_6^{3-} at 15K

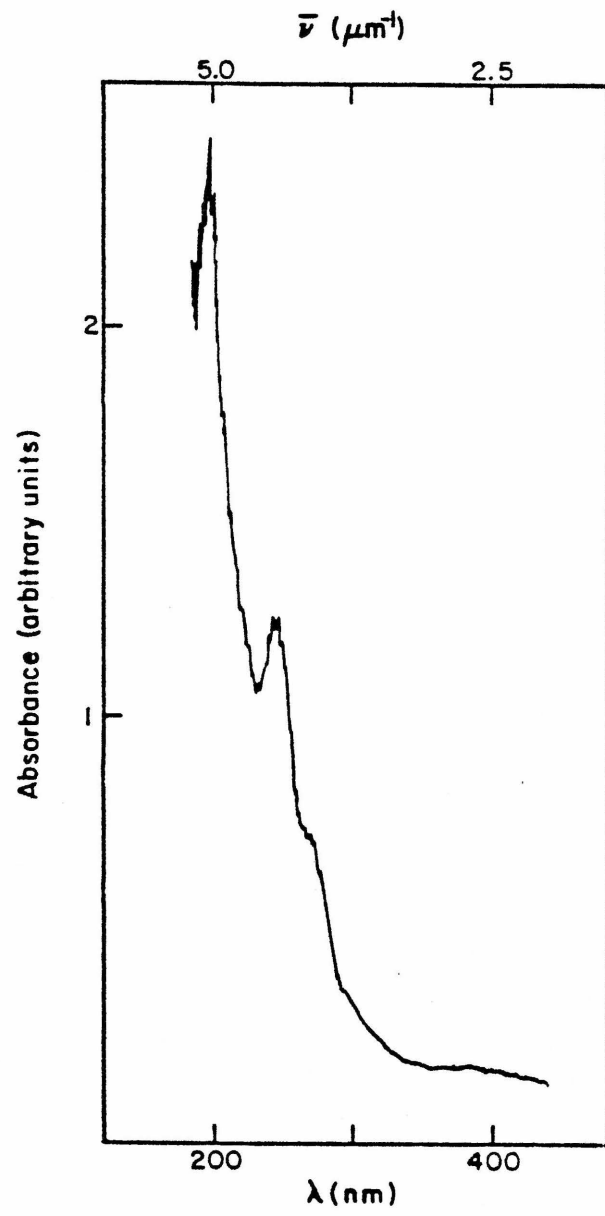


Table 4. Electronic Spectral Data and Assignments for PtCl_6^{2-} ^a

DMF	$2\text{CH}_3\text{-THF-ClH}_3\text{OH}$					$\frac{1}{A_{1g}^+}$ $3T_{1g}$ or T_{1g} $3T_{2g}$
	$\frac{\text{CH}_3\text{CN}}{\text{CH}_3\text{OH}}$	$\frac{\text{CH}_3\text{OH}}$	$\frac{300 \text{ K}}$	$\frac{77 \text{ K}}$	$\frac{\text{CH}_2\text{Cl}_2}$	
465 (69)	463 (65)	461 (58)	468 (52)	483 (27) ^b	459 (74)	
366 (530) ^b	361 (455) ^b	360 (470) ^b	358 (470) ^b	379 (200) ^b	365 (490) ^b	$1T_{1g}$ $1T_{2g}$ $1T_{1u}$ $1T_{1u}$
	270 (28,800)	265 (27,500)	266 (24,100)	271 (28,800)	269 (30,500)	
	202 (69,000)					

^a λ (nm), ϵ ($\text{l mol}^{-1}\text{cm}^{-1}$)

^bshoulder (ϵ for the λ given)

Table 5 Electronic Spectral Data and Assignments for
 IrCl_6^{3-}

<u>H₂O/298 K</u>	<u>KCL/15 K</u>	<u>$1A_{1g} \rightarrow$</u>
615	b	$3T_{1g}$
560	b	$3T_{2g}$
415	b	$1T_{1g}$
356	b	$1T_{2g}$
	278 ^c	$3T_{1u}$
	250	$1T_{1u}$
206	206	$1T_{1u}$

^a_λ (nm)

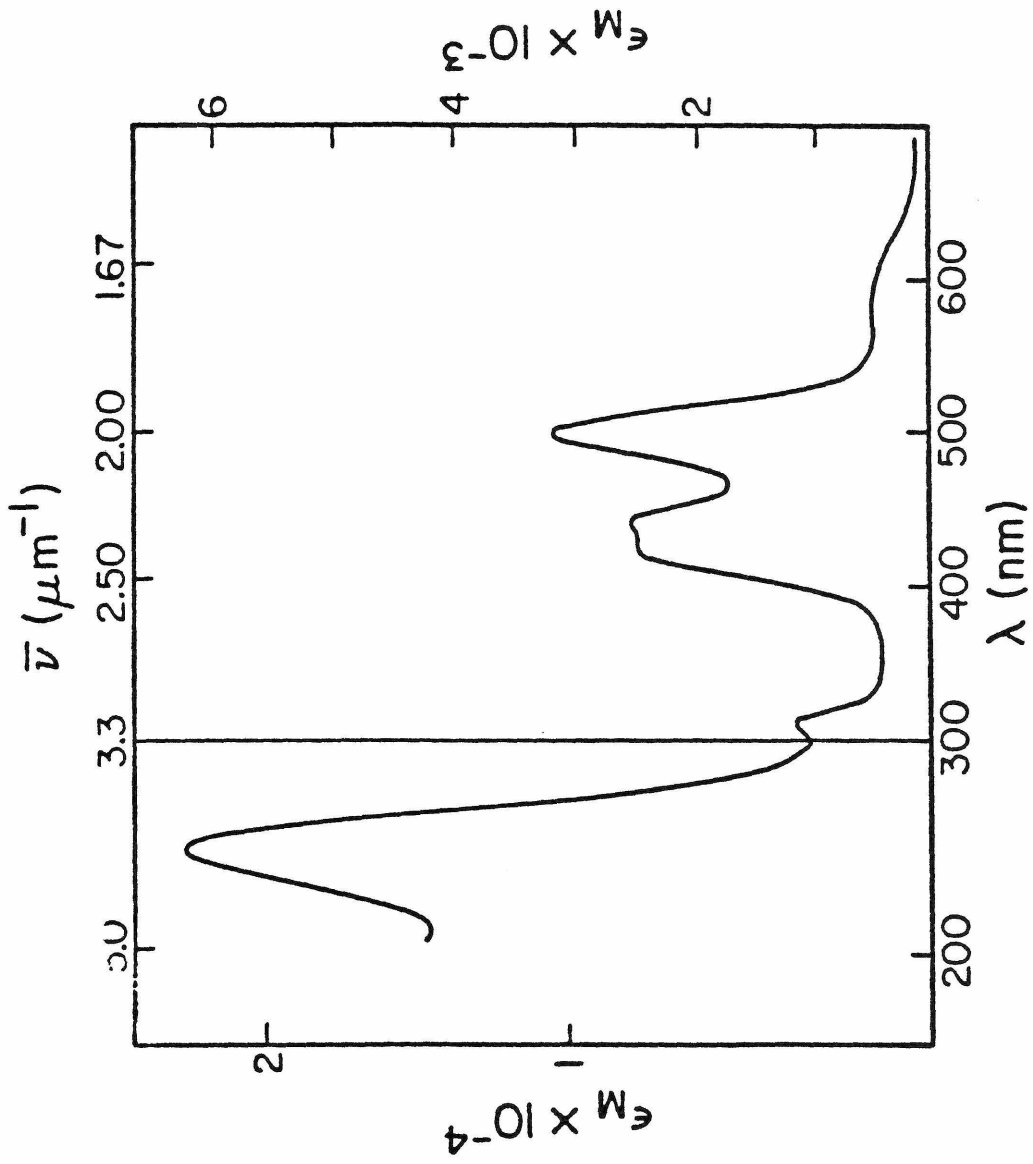
^b not measured

^c shoulder

IrCl_6^{2-} . The electronic absorption spectrum of IrCl_6^{2-} is shown in Figure 6. An interpretation of this spectrum can be developed from the molecular orbital scheme given earlier (Figure 2). The ground state electron configuration of IrCl_6^{2-} is $2t_{2g}(xy,xz,yz)^5$ yielding a $2T_{2g}$ state. The ligand field transitions $[2t_{2g}(xy,xz,yz)]^4 [2e_g(z^2,x^2-y^2)]^1$ are at 360 ($\epsilon = 300$) and 306 nm ($\epsilon = 1180$). Due to the presence of one t_{2g} hole, ligand to metal charge transfer bands occur in the visible region of the spectrum. The $\pi \rightarrow t_{2g}$ transitions are at 590 ($\epsilon = 410$), 487 ($\epsilon = 3280$), 434 ($\epsilon = 2560$), and 410 nm ($\epsilon = 2410$). The π to e_g

Figure 6

Electronic absorption spectrum of IrCl_6^{2-}

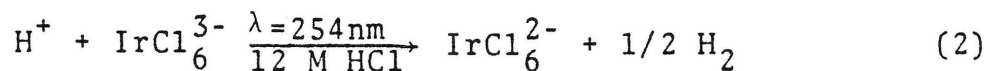


transition is at 232 nm ($\epsilon = 21,600$). These assignments are summarized for clarity in Table 6.⁴⁷

Table 6. Electronic Spectral Data and Assignments for IrCl_6^{2-}

<u>λ (nm)</u>	<u>ϵ ($\ell \text{ mol}^{-1} \text{ cm}^{-1}$)</u>	<u>Transition</u>
590	410	$\pi \rightarrow t_{2g}$
487	3280	$\pi \rightarrow t_{2g}$
434	2560	$\pi \rightarrow t_{2g}$
410	2410	$\pi \rightarrow t_{2g}$
360	300	$t_{2g} \rightarrow e_g$
306	1180	$t_{2g} \rightarrow e_g$
232	21600	$\pi \rightarrow e_g$

Photochemistry. Irradiation (254 nm) of a 12 M HCl solution of IrCl_6^{3-} (6.7×10^{-3} M) at room temperature results in the disappearance of IrCl_6^{3-} and the appearance of IrCl_6^{2-} (Figure 7). Hydrogen evolution accompanies the formation of IrCl_6^{2-} , according to Equation 2:



Exhaustively photolyzed solutions were Toepler-pumped for hydrogen and IrCl_6^{2-} was analyzed by spectrophotometric methods (Table 7), confirming the stoichiometry above.

The quantum yields for the reaction are extremely sensitive to proton concentration (Table 8). A Stern-Volmer

Figure 7

Spectral changes upon irradiation ($\lambda=254$ nm) of 5.5×10^{-3} M
 IrCl_6^{3-} in 12 M HCl

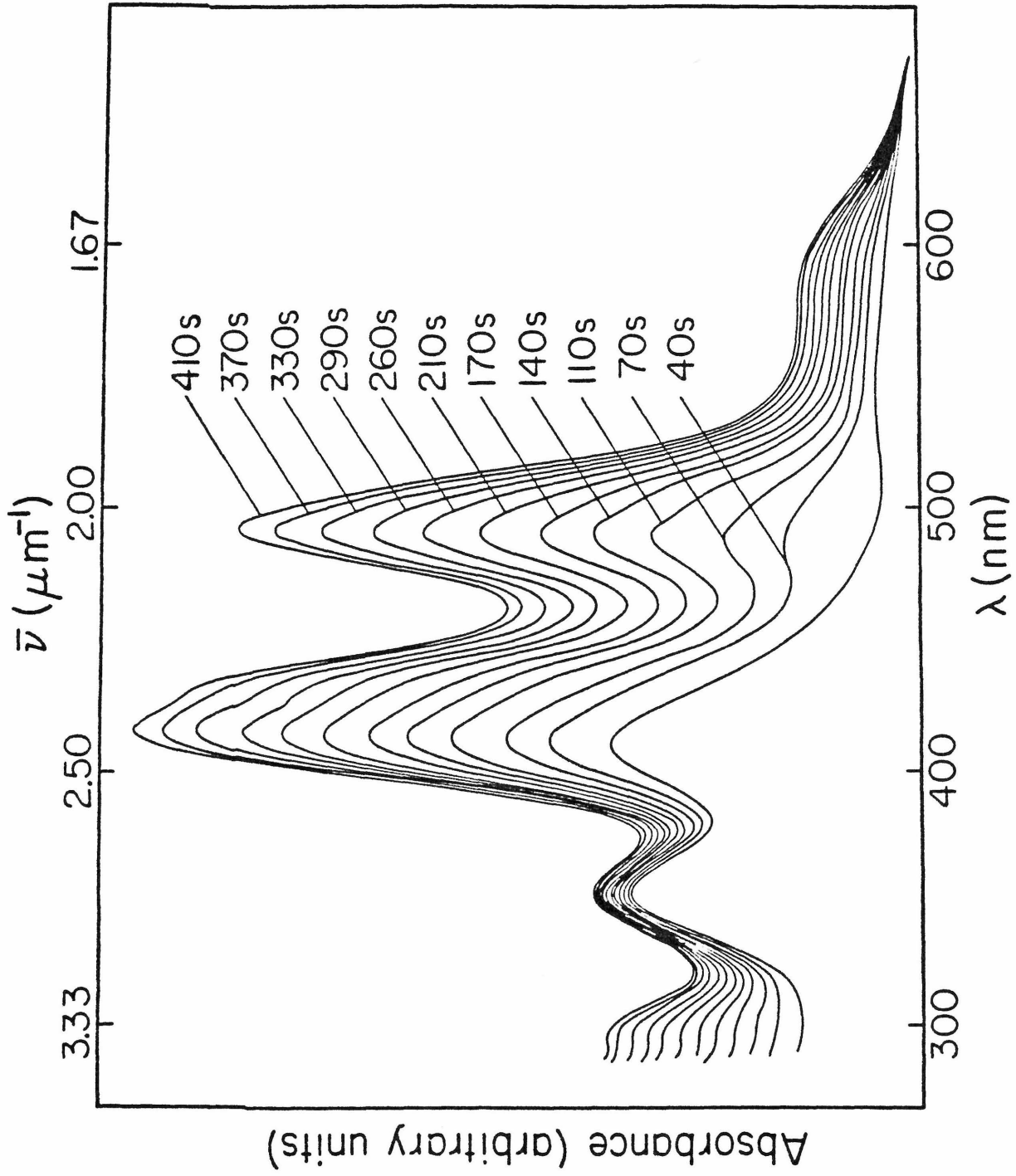


Table 7. Analysis of the IrCl_6^{3-} Photoreaction in 12 M HCl
(254 nm irradiation)

<u>IrCl_6^{2-} (moles)</u>	<u>H_2 (moles)</u>	<u>Ratio $\text{H}_2:\text{IrCl}_6^{2-}$</u>
1.24×10^{-5}	6.93×10^{-6}	0.56
1.02×10^{-5}	5.12×10^{-6}	0.50

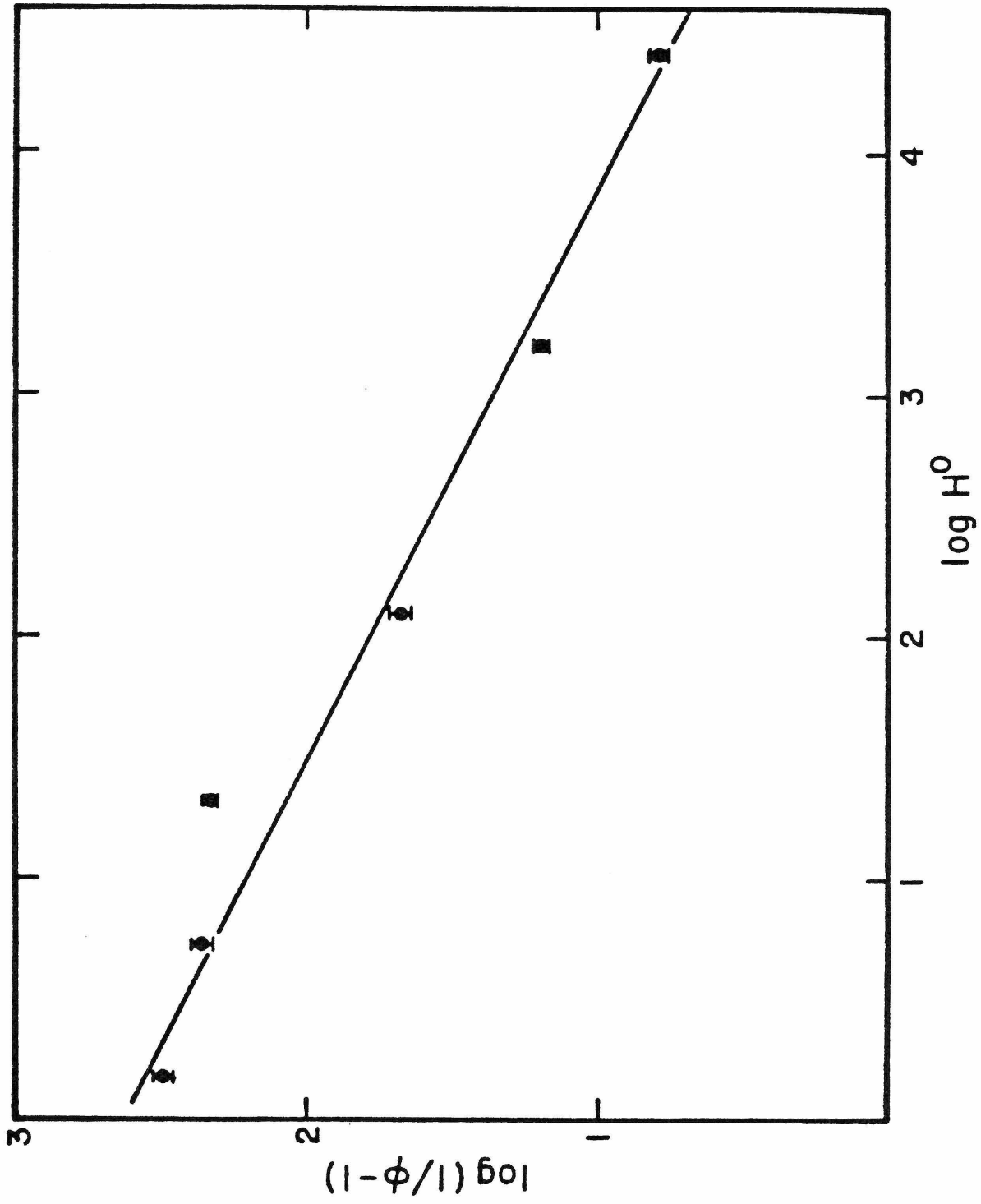
Table 8. Quantum Yields for IrCl_6^{2-} Formation from IrCl_6^{3-}
($\lambda = 254$ nm) in HCl Solutions

<u>HCl Concentration (moles/liter)</u>	<u>ϕ</u>
12.0	0.28
9.0	0.127
6.0	0.0411
4.0	0.00921
2.0	0.00868
1.0	0.00653

plot (Figure 8) of quantum yield versus hydronium ion concentration shows the two are directly related. Evidently, at high proton activity, the photoprocess resulting in H_2 production is much more efficient, possibly due to proton association with ground state IrCl_6^{3-} . Proton concentration dependence for photohydrogen production is also seen for $\text{Fe}(\text{CN})_6^{4-}$,⁵² a case in which the ground state species is assumed to exist in a protonated form at low pH.^{53,54}

Figure 8

Stern Volmer plot of quantum yield vs. Hydronium ion activity



The protonation of IrCl_6^{3-} has been investigated by potentiometric pH titration in aqueous solution. As seen from Figure 9, there is no evidence for protonation in the pH range 1-7 individual points on the titration curve of IrCl_6^{3-} coincided with an analogous blank titration of pure water. Pertinent calculations indicate that all three ionization constants of H_3IrCl_6 must be larger than 0.1 in order to account for the results obtained. We were not able to study the position of the 206 nm band at higher HCl concentrations (1-12 M), owing to the strong absorption of Cl^- in this region. We can only speculate that protonation of IrCl_6^{3-} becomes important at high acid concentrations, thereby explaining the marked effect on the rate of photoconversion of IrCl_6^{3-} to IrCl_6^{2-} and H_2 . This is consistent with the results for $\text{Fe}(\text{CN})_6^{4-}$ ($\text{HFe}(\text{CN})_6^{3-}$) mentioned earlier.

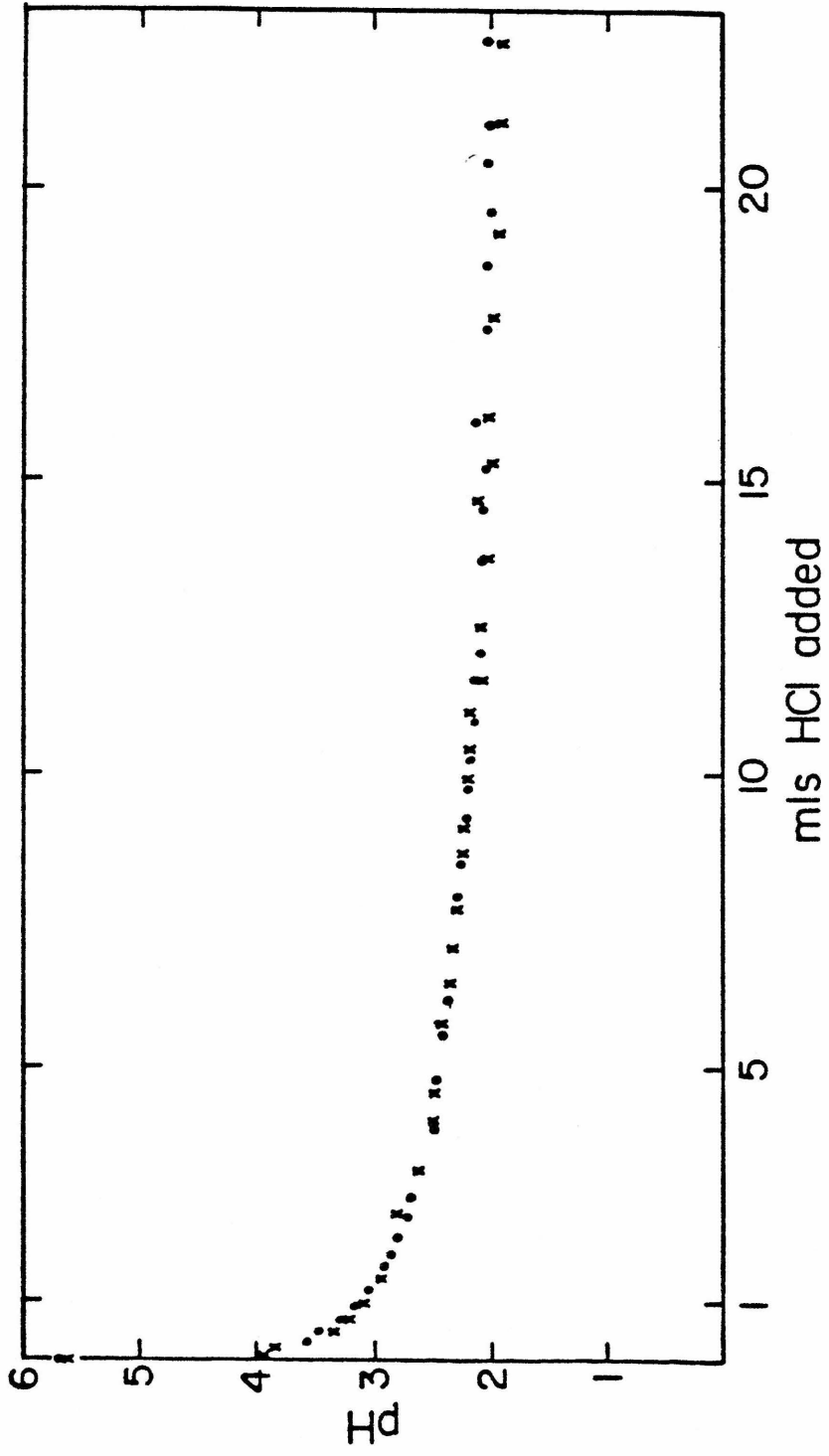
The quantum yields are also highly wavelength dependent (Table 9), photoredox behavior being predominantly a high

Table 9. Wavelength-dependent Quantum Yields for IrCl_6^{2-} Formation from IrCl_6^{3-} in 12 M HCl

<u>Irradiation (nm)</u>	<u>ϕ</u>	<u>Excitation</u>
254	0.28	$\pi_L(t_{1u}) \rightarrow \sigma_M^*(e_g)$
313	10^{-4}	$\pi_L(t_{1u}) \rightarrow \sigma_M^*(e_g)$
366	ϕ	$\pi_M^*(t_{2g}) \rightarrow \sigma_M^*(e_g)$
420	ϕ	$\pi_M^*(t_{2g}) \rightarrow \sigma_M^*(e_g)$

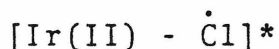
Figure 9

Protonation titration of 100 ml of $1.0 \times 10^{-3} \text{ M IrCl}_6^{3-}$ with
.1 F HCl ✕ and pure water ●



energy phenomenon ($\lambda = 254 \text{ nm}$). Our identification of the π_{Cl^-} to e_g transitions in the IrCl_6^{3-} spectrum is particularly crucial in the interpretation of this photochemistry.

Transitions to the $^1T_{1u}$ and $^3T_{1u}$ states are located at 250 and 278 nm in the solid state spectrum. Because ultraviolet irradiations were carried out at 254 nm, one or both of these excited state configurations must be responsible for the resultant redox chemistry. Direct excitation to either state is possible. The triplet could also be populated by rapid intersystem crossing from $^1T_{1u}$. Both excited states have $\text{Ir(II)}-\text{Cl}\cdot$ character, corresponding to the configuration $2t_{2g}(xy,xz,yz)^6 2e_g(z^2,x^2-y^2)^1$ for Ir:

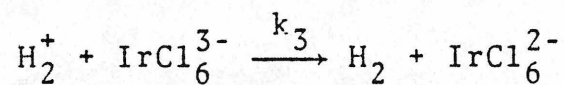
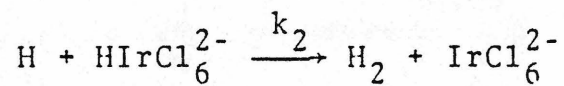
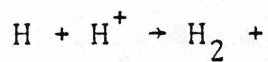
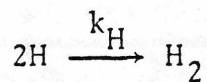
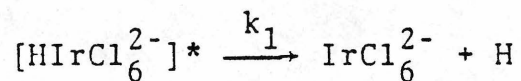
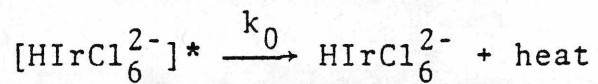
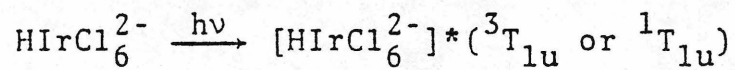
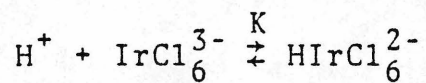


These excited states of IrCl_6^{3-} may return to the ground state or react with their immediate environment to yield IrCl_6^{2-} and a reduced species. Chlorine atoms are not released from these excited states, as evidenced by the fact that Cl_2^- was not observed in flash photolyses studies.

In strong acid solutions, IrCl_6^{3-} undoubtedly is in equilibrium with HIrCl_6^{2-} , $\text{H}_2\text{IrCl}_6^-$, and possibly H_3IrCl_6 . We envision the photochemistry as in Figure 10 (for simplicity HIrCl_6^{2-} is considered the reactive species). This scheme is consistent with the variation in quantum yields with proton activity. If absorption of light by HIrCl_6^{2-} resulting in hydrogen atom formation is the rate limiting step, the

Figure 10

Scheme for the IrCl_6^{3-} photoreaction to give IrCl_6^{2-} and H_2



mechanism is also in accord with the observations that the reaction rate is first order in IrCl_6^{3-} and quantum yields are independent of light intensity (Table 10). Finally,

Table 10. Quantum Yields for IrCl_6^{2-} Production from IrCl_6^{3-} as a Function of IrCl_6^{3-} Concentration and Light Intensity

$[\text{IrCl}_6^{3-}]$ (moles/liter)	Light Intensity (Einsteins/minute)	ϕ
2.30×10^{-3}	4.78×10^{-7}	0.283 ^a
1.18×10^{-3}	4.78×10^{-7}	0.279 ^a
6.70×10^{-3}	4.78×10^{-7}	0.280
6.70×10^{-3}	2.66×10^{-6}	0.276

^a ϕ corrected for the fraction of light absorbed

this scheme explains Adamson's flash photolysis results, because photogenerated hydrogen atoms could reduce N_2O .

Although photoredox chemistry does occur at longer wavelengths ($\lambda = 313$ nm), the quantum yields are extremely small ($\phi < 10^{-4}$). We interpret this in terms of the small relative population of the LMCT states upon excitation at lower energies. Irradiation into the ligand field bands ($\lambda = 366$ or 420 nm) results in aquation rather than oxidation of the metal center.

Prolonged photolyses of IrCl_6^{3-} resulted in a marked decrease in the rate of oxidation, possibly due to competitive light absorption by IrCl_6^{2-} . The extinction

Table 11. Reaction Conditions and Results of Previous Photochemical Studies of IrCl_6^{2-}

Investigators	IrCl_6^{2-} Concentration (moles/liter)	Wavelength of Excitation (nm)	Solvent System	Predominant Product	ϕ
Sleight and Hare	0.5 - 2.0	broad band	H_2O	$\text{IrCl}_5(\text{H}_2\text{O})^-$	not given
	0.5 - 2.0	broad band	$\text{HCl}(1-6\text{M})$	$\text{IrCl}_5(\text{H}_2\text{O})^-$	not given
Moggi, et al.	2.5×10^{-4}	254	2.5 N HClO_4	$\text{IrCl}_5(\text{H}_2\text{O})^-$	2.5×10^{-2}
			without Cl^-	$\text{IrCl}_5(\text{H}_2\text{O})^{2-}$	10^{-3}
	1.0×10^{-3}	313	2.5 N HClO_4	$\text{IrCl}_5(\text{H}_2\text{O})^-$	1.0×10^{-2}
			without Cl^-	IrCl_6^{3-}	2.0×10^{-2}
1.0×10^{-3}	365	2.5 N HClO_4	$\text{IrCl}_5(\text{H}_2\text{O})^-$	1.0×10^{-3}	
		without Cl^-	IrCl_6^{3-}	5.0×10^{-3}	
	433	2.5 N HClO_4	$\text{IrCl}_5(\text{H}_2\text{O})^-$	5.0×10^{-5}	
		without Cl^-	IrCl_6^{3-}	1.0×10^{-4}	
1.0×10^{-3}	495	2.5 N HClO_4	$\text{IrCl}_5(\text{H}_2\text{O})^-$	5.0×10^{-5}	
		without Cl^-	$\text{IrCl}_5(\text{H}_2\text{O})^{2-}$	5.0×10^{-5}	
			with 1.2 M Cl^-	$\text{IrCl}_5(\text{H}_2\text{O})^{2-}$	5.0×10^{-5}

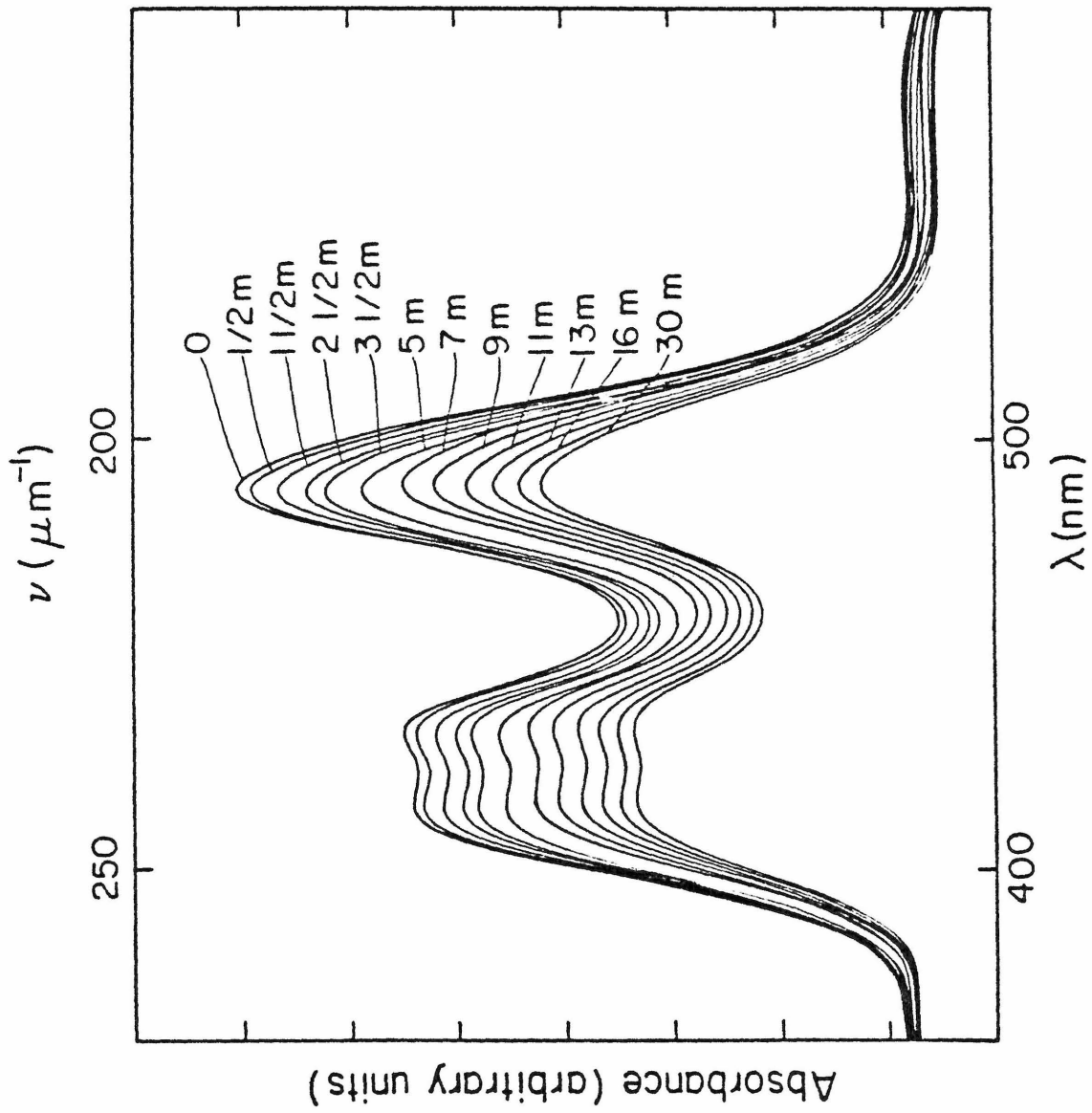
coefficients at 254 nm are 958 and 7548 for IrCl_6^{3-} and IrCl_6^{2-} respectively, so secondary photolysis seemed likely. Previous studies on the photochemistry of IrCl_6^{2-} had led to conflicting results. Sleight and Hare⁴⁴ indicated that only aquation products are obtained upon photolysis, irrespective of reaction conditions. Contrary to these findings, Moggi, *et al.*,⁴⁵ claimed both aquation and reduction products as a result of irradiation, the relative yield varying with both wavelength and media. The results of these earlier studies are summarized in Table 11.

It was obvious at this point that investigation of IrCl_6^{2-} under reaction conditions identical with those for the photoreaction of IrCl_6^{3-} to produce IrCl_6^{2-} and H_2 was necessary. Irradiation at $\lambda = 254$ nm for 30 minutes in 6 M HCl led to the spectral changes shown in Figure 11. If a reaction to form $\text{IrCl}_6(\text{H}_2\text{O})^-$ had occurred, isosbestic points should have appeared at 386, 417, 437, and 518 nm; but, in fact, the absorbance only decreased over the entire spectral region examined. Because absorbances due to $\text{IrCl}_5(\text{H}_2\text{O})^-$ have extinction coefficients comparable to IrCl_6^{2-} , whereas those of IrCl_6^{3-} and its aquation products are orders of magnitude less, it may be concluded that only redox chemistry resulted from irradiation. The reduced species were easily identifiable, as Ir(III) complexes of the type $\text{IrCl}_x(\text{H}_2\text{O})_{6-x}^{3-x}$ are quantitatively oxidized by Cl_2 to the corresponding Ir(IV) complex without any change in inner sphere structure. On

Figure 11

Spectral changes upon irradiation ($\lambda=254\text{nm}$) of 6.7×10^{-4} M

IrCl_6^{2-} in 6 M HCl



bubbling Cl_2 through the photolyzed solutions, the spectrum returned to that of zero time, indicating the product to be IrCl_6^{3-} .

Irradiations at longer wavelengths led to similar results, as may be seen from the quantum yields given in Table 13. No evidence for aquation products was obtained in experiments in which the IrCl_6^{2-} concentrations were 6.7×10^{-4} M. As was the case for IrCl_6^{3-} , the rates of reaction diminish with time. Neither a correction for interfilter

Table 13. Wavelength-Dependent Quantum Yields for Conversion of IrCl_6^{2-} to IrCl_6^{3-} in 6 M HCl.

Irradiation	(nm)	ϕ	Excitation
254		0.128	$\pi_L(t_{1u}) \rightarrow \sigma_m^*(eg)$
313		0.107	$\pi_M^*(t_{2g}) \rightarrow \sigma_M^*(eg)$
366		0.090	$\pi_M^*(t_{2g}) \rightarrow \sigma_M^*(eg)$
420		0.0159	$\pi_L(t_{2u}) \rightarrow \pi_M^*(t_{2g})$
488		0.00361	$\pi_L(t_{1u}) \rightarrow \pi_M^*(t_{2g})$

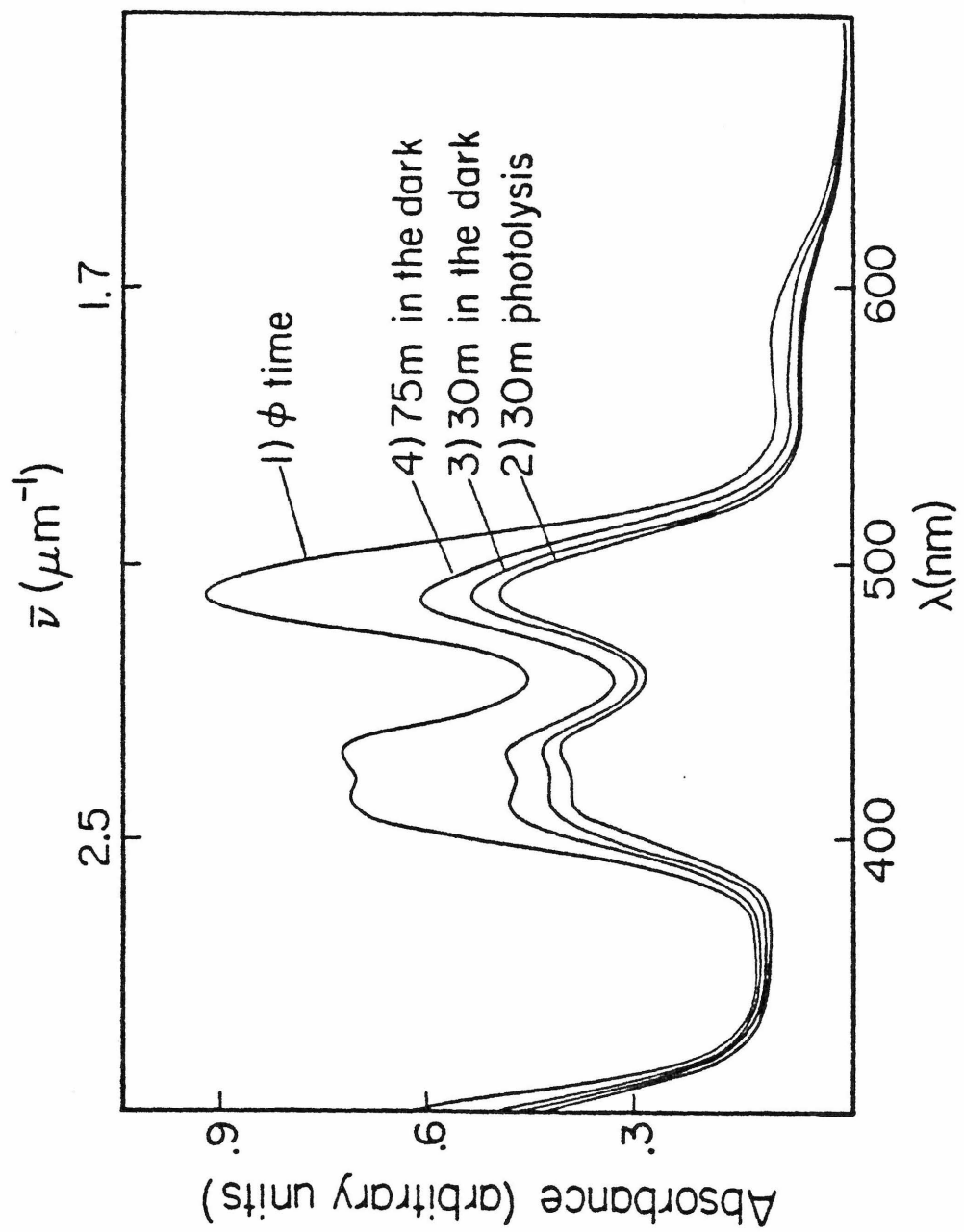
effects nor one for secondary photolysis, however, explains the marked decrease in reaction rate. Evidently, prolonged photolysis results in steady state concentrations that cannot be altered by further irradiation. Of the two possible oxidation products, Cl_2 and O_2 , only the former will back react rapidly with IrCl_6^{3-} to form IrCl_6^{2-} . Unfortunately, with the exception of $\text{C}_2\text{O}_4^{2-}$, conventional $\text{Cl}\cdot$ or Cl_2 trapping

agents cannot survive the reaction medium. While $C_2O_4^{2-}$ reacts thermally with $IrCl_6^{2-}$ to produce $IrCl_6^{3-}$, there is a dramatic rate increase upon irradiation ($\lambda > 300$ nm) suggesting the presence of chlorine atoms. More informative is the fact that irradiated solutions will back react in the absence of light. The spectra in Figure 12 show $IrCl_6^{2-}$ (6.7×10^{-4} M) in 6 M HCl prior to photolysis, after 30 minutes irradiation, and after 30 minutes dark reaction. Exposure to light results in a bleaching of the spectrum; cessation of irradiation results in the reappearance of $IrCl_6^{2-}$, suggesting the presence of Cl_2 in the solution. Mass spectral measurements did not reveal any Cl_2 , but this is not surprising because Cl_2 is extremely soluble in HCl (over two liters of gas per liter of solution). What is more, most of the Cl_2 produced would have been reduced by $IrCl_6^{3-}$. Experiments with $H_2^{18}O$ and HCl gas as the reaction medium showed no evidence for $^{18}O_2$ formation, providing further proof that the oxidation product is Cl_2 .

The photochemical behavior of $IrCl_6^{2-}$ is related to the enhanced oxidizing power of $[IrCl_6^{2-}]^*$. The ground state is a strong oxidant ($E = 0.867$ v, varying with the solvent), and electronic excitation increases the driving force for reduction to $IrCl_6^{3-}$. In 6M HCl it appears that both LMCT and ligand field transitions result in photoredox chemistry. At first blush these findings seem to conflict with previous investigations. However, on closer analysis these conflicts

Figure 12

Spectral changes upon irradiation ($\lambda > 300$ nm) of 6.7×10^{-4} M
in 6 M HCl (30 minutes) and due to subsequent thermal back
reaction (30 minutes)



disappear, as the reaction conditions are so different. Sleight and Hare observed only aquation products from photolysis of IrCl_6^{2-} . However, at their IrCl_6^{2-} concentrations (2.0 to 0.5 M), any Cl_2 produced would have been scavenged immediately, yielding no net redox chemistry. Moggi, et al., saw both aquation and redox chemistry at lower IrCl_6^{2-} concentrations (10^{-4} M), the relative importance of the processes being a function of Cl^- concentration. Specifically, photoaquation is the predominant mode in the absence of Cl^- ; whereas with 1.2 M Cl^- present, the main reaction is photoreduction. This is consistent with our results: at low IrCl_6^{2-} concentration (6.7×10^{-4} M) and high Cl^- concentration (6 M), redox chemistry is the sole mode of reaction.

Because thermal aquations and anations are very slow processes, it would seem that a common intermediate is responsible for both possible products, with reaction conditions influencing which is obtained. A possible reaction mechanism is shown for LMCT excitation in Figure 13. The excited state is an Ir(III) complex with a chlorine atom still formally bound. Because IrCl_6^{2-} is known to undergo both inner and outer sphere electron transfer, the latter may be invoked in the presence of Cl^- . This also explains why no Cl_2 is seen upon flash photolysis, as the Ir-Cl bond remains intact.

The photoreactions of IrCl_6^{2-} at 254 nm are summarized in

Figure 13

Scheme for IrCl_6^{2-} photoreaction to give IrCl_6^{3-} and Cl_2

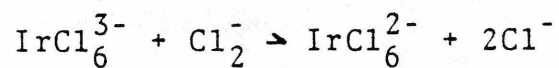
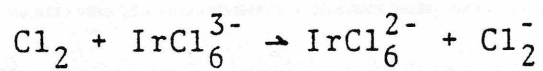
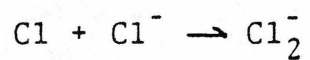
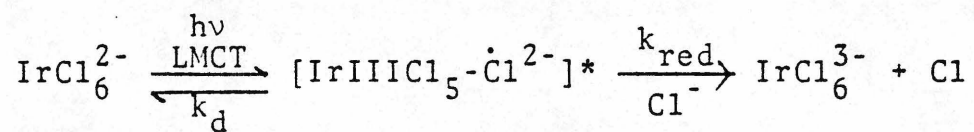
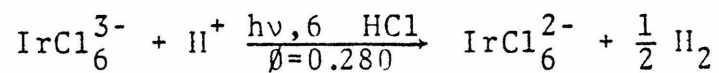
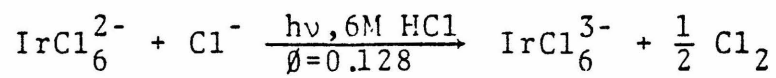


Figure 14. In 6 M HCl, photolysis of IrCl_6^{2-} results in the formation of IrCl_6^{3-} and Cl_2 . When the concentration of IrCl_6^{3-} becomes large enough for competitive light absorption, it undergoes secondary photolysis to yield IrCl_6^{2-} and H_2 , as confirmed by mass spectral measurements. In this medium the $\text{IrCl}_6^{2-}/3-$ couple is a true photochemical catalyst for proton reduction and chloride oxidation. Completion of a water splitting cycle in this system can be achieved under conditions where chlorine oxidizes water to oxygen.

Based on our findings, it is clear that the photochemistry of the $\text{IrBr}_6^{2-}/3-$ system should be studied. The charge transfer transitions are considerably red shifted in these complexes (Table 14),^{47,49} suggesting that it might be possible to produce hydrogen and bromine from HBr at relatively long excitation wavelengths by a photoredox scheme analogous to that given in Figure 14 for the $\text{HCl}/\text{IrCl}_6^{3-}/2-/\text{H}_2/\text{Cl}_2$ system.

Figure 14

The photoreactions of IrCl_6^{3-} and IrCl_6^{2-} in 6 M HCl



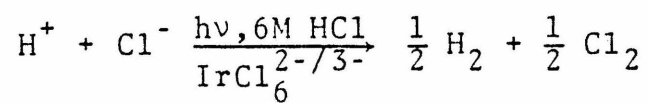


Table 14. Electronic Spectral Data and Assignments for
 IrBr_6^{2-} and IrBr_6^{3-}

Complex	λ (nm)	ϵ ($\ell \cdot \text{mol}^{-1} \text{cm}^{-1}$)	Transition
IrBr_6^{2-}	860	800	$\pi \rightarrow t_{2g}$
	745	1570	$\pi \rightarrow t_{2g}$
	700	2350	$\pi \rightarrow t_{2g}$
	673	2520	$\pi \rightarrow t_{2g}$
	583	3220	$\pi \rightarrow t_{2g}$
	545	1780	$\pi \rightarrow t_{2g}$
	509	1530	$\pi \rightarrow t_{2g}$
	318	8000	$\pi \rightarrow e_g$
	270	17,000	$\pi \rightarrow e_g$
IrBr_6^{3-}	597	27	$t_{2g} \rightarrow e_g$
	447	232	$t_{2g} \rightarrow e_g$
	387	198	$t_{2g} \rightarrow e_g$
	272	12,000	$\pi \rightarrow e_g$
	243	20,000	$\pi \rightarrow e_g$

References

1. E. Collinson, F. S. Dainton, and M. A. Malati, Trans. Faraday Soc., 55, 2097 (1959).
2. M. W. Rophael and M. A. Malati, J. Inorg. Nucl. Chem., 37, 1326 (1975).
3. R. H. Potterhill, O. J. Walker, and J. Weiss, Proc. R. Soc. London, Ser. A., 156, 561, (1936).
4. F. S. Dainton and D. G. L. James, J. Chem. Phys., 48, C17, (1951).
5. L. J. Heidt, M. G. Mullin, W. B. Martin, Jr., and A. M. Johnson-Beatly, J. Phys. Chem., 66, 336 (1962).
6. P. L. Airey and F. S. Dainton, Proc. R. Soc. London, Ser. A, 291, 340 (1966).
7. D. L. Douglas and D. M. Yost, J. Chem. Phys., 17, 1345 (1949).
8. Y. Haas, G. Stein, and R. Tenne, Isr. J. Chem. 10, 529, (1972).
9. D. D. Davis, K. L. Stevenson, and G. K. King, Inorg. Chem., 16, 670 (1977).
10. L. J. Heidt and A. F. Mcmillan, J. Am. Chem. Soc., 76, 2135 (1954).
11. D. D. Davis, K. L. Stevenson, and C. R. Davis, J. Am. Chem. Soc., 100, 5344 (1978).
12. V. Balzani and V. Carassiti, "Photochemistry of Coordination Compounds," Academic Press, 1970, and references therein.
13. P. C. For, R. E. Hintze, and J. D. Petersen in "Concepts of Inorganic Photochemistry," ed. by A. W. Adamson and P. D. Fleischauer, John Wiley and Sons, 1975, and references therein.

14. M. Fox, "Concepts of Inorganic Photochemistry," ed. by A. W. Adamson and P. D. Fleischauer, John Wiley and Sons, 1975, and references therein.
15. D. K. Erwin, G. L. Geoffrey, H. B. Gray, G. S. Hammond, E. I. Solomon, W. C. Trogler, and A. A. Zagars, J. Am. Chem. Soc., 99, 3260 (1977).
17. K. R. Mann, N. S. Lewis, V. M. Miskowski, D. K. Erwin, G. S. Hammond, and H. B. Gray, J. Am. Chem. Soc., 99, 5525 (1977).
18. F. A. Cotton, Accounts Chem. Res., 2, 240 (1969).
19. W. C. Trogler, C. D. Cowman, H. B. Gray, and F. A. Cotton, J. Am. Chem. Soc., 99, 2993 (1977).
20. G. L. Geoffrey, H. B. Gray, and G. S. Hammond, J. Am. Chem. Soc., 96, 5565 (1974).
21. J. P. Birk, Inorg. Chem., 16, 1381 (1977).
22. G. R. Cayley, R. S. Taylor, R. K. Wharton, and A. G. Sykes, Inorg. Chem., 16, 1377 (1977).
23. E. Pelizzetti, E. Mentasti, E. Pramauro, Inorg. Chem., 17, 1181 (1978).
24. A. G. Sykes and R. N. F. Thorneley, J. Chem. Soc. (A), 232 (1970).
25. G. D. Owens, K. L. Chellappa, D. W. Margerum, Inorg. Chem., 18 (1979).
26. J. Y. Chen, H. C. Gardner and J. K. Kochi, J. Am. Chem. Soc., 98, 6150 (1976).
27. K. K. Sengupta and P. K. Sen, Inorg. Chem., 18, 979 (1979).
28. E. Pelizzetti, E. Mentasti, and C. Baiocchi, J. Phys. Chem., 80, 2979 (1976).

29. J. Y. Chen and J. K. Kochi, J. Am. Chem. Soc., 99, 1450 (1977).
30. R. J. Campion, N. Purdie and N. Sutin, Inorg. Chem, 3, 1091 (1964).
31. H. C. Gardner and J. K. Kochi, J. Am. Chem. Soc, 97, 1855 (1975).
32. T. T. Tsou and J. K. Kochi, J. Am. Chem. Soc, 100, 1634 (1978).
33. R. N. F. Thorneley and A. G. Sykes, J. Chem Soc (A), 1036 (1970).
34. K. K. Sengupta, U. Chatterjee, and P. K. Sen, Indian J. Chem, 16B, 767 (1978).
35. A. B. Soares, R. S. Taylor, and A. G. Sykes, Inorg. Chem., 17, 496 (1978).
36. M. H. Ford-Smith and J. J. Habeeb, J. Chem. Soc. Dalton, 461 (1973).
37. R. Cecil and J. S. Littler, J. S. Littler, J. Chem. Soc. (B), 1420 (1968).
38. R. Cecil, A. J. Fear, and J. S. Littler, J. Chem. Soc. (B), 632 (1970).
39. R. Cecil, J. S. Littler, and G. Easton, J. Chem. Soc (B), 626 (1970).
40. H. N. Po, H. Eran, Y. Kim, and L. Byrd, Inorg. Chem, 18, 197 (1979).
41. J. P. Birk, Inorg. Chem., 17, 504 (1978).
42. G. A. Rechnitz and J. E. McClure, Anal. Chem., 36, 2265 (1964).
43. D. A. Fine, Inorg. Chem., 8, 1914 (1969).
44. T. P. Sleight and C. R. Hare, Inorg. Nucl. Chem. Let., 4, 165 (1968).
45. L. Moggi, G. Varani, M. F. Manfrin, and V. Balzani, Inorg. Chim Acta, 4, 335 (1970).
46. W. L. Waltz and A. W. Adamson, J. Phys. Chem., 73, 4250 (1969).
47. C. K. Jørgensen, Mol. Phys., 2, 309 (1959).
48. W. D. Bowman and J. N. Demas, J. Phys. Chem., 80, 2434 (1976).

49. C. K. Jorgensen, Acta. Chem. Scand., 500 (1956).
50. M. J. Blandameyer and M. F. Fox, Chem. Rev., 70, 59 (1970).
51. D. L. Swihar and W. R. Mason, Inorg. Chem., 9, 1749 (1970).
52. P. L. Airey and F. S. Dainton, Pro. Roy Soc. A, 340 (1966).
53. F. S. Dainton and P. L. Airey, Nature, 1190 (1965).
54. J. Jordan and G. J. Ewing, Inorg. Chem., 1, 587 (1962).

Chapter 2

Photochemistry and Structural Determination of
Molybdenum Aquo Ions

Abstract: The photochemistry of Mo(III), Mo(IV), and Mo(V) in aqueous solution was investigated, and these ions were shown to be photochemically inert in a variety of media. Since the exact speciation of these complexes in solution was not known, a structural characterization via Raman spectroscopy and X-ray absorption edge and extended X-ray absorption fine structure (EXAFS) studies was undertaken. Vibrational modes predominately Mo-Mo stretching in character were seen at ca. 200 cm^{-1} in the Raman spectra of $\text{Mo}_2\text{O}_4(\text{aq})^{2+}$ and $\text{Na}_4\text{Mo}_6\text{O}_{28}(\text{EDTA})_3 \cdot 14\text{H}_2\text{O}$. For these two complexes and $\text{Cs}_2\text{Mo}_3\text{O}_4^{2-}$, $(\text{C}_2\text{O}_4)_3(\text{H}_2\text{O})_3$ and $\text{Mo}_3\text{O}_4(\text{aq})^{4+}$ ring stretching frequencies appear in the 700, 400, and 300 cm^{-1} regions of the spectra. A molybdenyl vibration was seen at ca. 900 cm^{-1} for $\text{Mo}_2\text{O}_4^{2-}(\text{aq})^{2+}$. X-ray absorption edge and EXAFS data were collected for Mo(V), Mo(III), and Mo(II) in aqueous acidic solutions; Mo(IV) was examined under a variety of conditions including varying pH and anion environments. The Mo(II) structure is shown to be consistent with a quadruply bound dinuclear species. Although electronically capable of multiple metal-metal bonds, the Mo(III) ion appears to exist as a singly bonded species with two hydroxy bridges. Data for the Mo(V) aquo ion are typical for oxobridged dinuclear Mo(V) compounds. Evidence for a molybdenyl functionality is also seen. Because of the controversy over the nature of Mo(IV), a variety of aqueous samples was investigated. In strong acid solution, the ion is shown to exist as a trinuclear

species $\text{Mo}_3\text{O}_4(\text{aq})^{4+}$. As the pH of the medium is increased, the Mo-Mo amplitude decreased, indicating possible cluster fragmentation. In basic solution, a major structural change occurs. The presence of halide ions had no effect on the spectra.

Part A

Photochemistry and Acid Cryoscopy and Raman Studies

Decomposition of water into H_2 and O_2 via visible photolysis has generated much interest as a means of solar energy storage. Since the electronic absorption spectrum of water does not overlap the solar spectrum at the surface of the earth, transition metal complexes that absorb visible radiation have been employed to catalyze the reaction. Unfortunately, the formation of water derived radicals often imposes high threshold energies and decreases the efficiency of the system. This can be avoided, however, if the catalyst and substrate are arranged in appropriate molecular structures such as a binuclear coordination compound. As depicted in Figure 1, formation of H_2 , O_2 or H_2O_2 rather than radical species is possible due to geometrical restraints on excited state configuration.

In light of the above, an investigation was made of the photocatalytic capabilities of molybdenum aquo ions. Previous work indicated that photolysis of $Mo_2(aq)^{4+}$ in acidic solution yields $Mo_2(-OH)_2(aq)^{4+}$ and H_2 .¹ It was thought that either this MoIII dimer or the MoIV or MoV analogues might be capable of oxidizing water to form O_2 and a reduced metal species. The structures proposed for these ions (Figure 2) seem ideal for oxygen production; all three have hydroxy or oxo bridges, coordinated waters, and two metal centers capable of variable oxidation states in close proximity. The electronic absorption spectra show transitions in the visible as reported in Table 1,²

Figure 1

Schematic representation of O_2 , H_2O_2 , and H_2 production
from H_2O via binuclear transition metal complexes

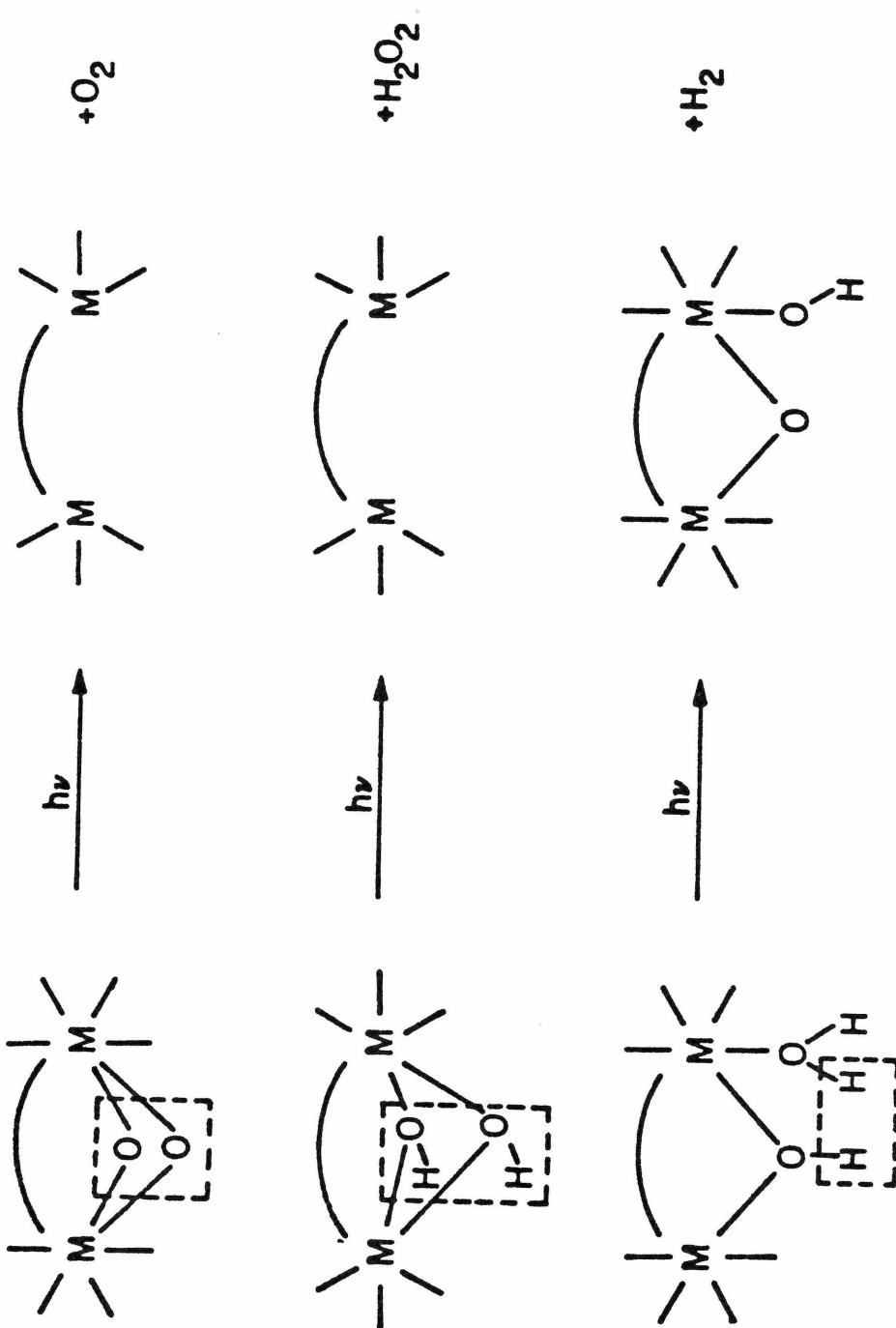
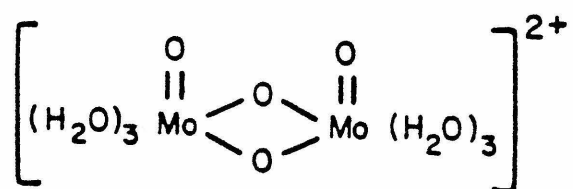
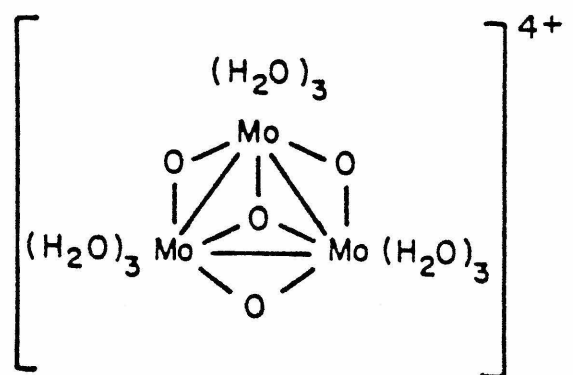


Figure 2

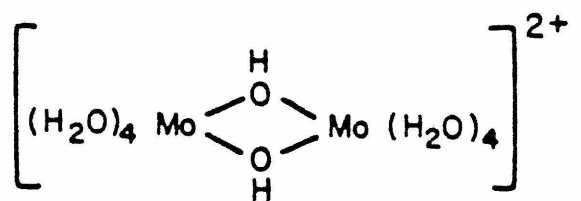
Proposed structures of $\text{Mo}_2(\mu\text{-OH})(\text{aq})^{4+}$, $\text{Mo}_3\text{O}_4\text{aq}^{4+}$
and $\text{Mo}_2\text{O}_4(\text{aq})^{2+}$



Mo V



Mo IV



Mo III

indicating that low energy light might be used to initiate the reaction.

Unfortunately, photolyses of these ions under various conditions proved them to be photochemically inert (Table 2). This is reasonable upon structural considerations and examination of the transitions involved. For all three complexes some type of metal-metal bonding has been evoked. This coupled with the presence of oxo or hydroxy bridges makes fragmentation unlikely. Furthermore the lowest energy transitions have been ascribed to being metal localized ($\sigma \rightarrow \pi n$)³, making redox photochemistry derived from this state not probable. Higher energy irradiation is also unlikely to yield net photochemistry as transitions are delocalized electronically over several centers.

In view of this lack of photoreactivity, we focused our attention on definitive structural characterizations of the aquo ions by X-ray absorption edge and extended X-ray absorption fine structure (EXAFS) analysis. In particular, the Mo(IV) aquo ion was of interest as the structure of this ion plagued researchers in the past. Work by Ardon and Pernick^{4,5} led to the formulation of a binuclear $\text{Mo}_2\text{O}_4^{4+}$ species, but this was disputed by Sykes and coworkers⁶ who favored a mononuclear structure MoO^{2+} or $\text{Mo}(\text{OH}_2)_2^{2+}$. Initial X-ray absorption edge and EXAFS data from our laboratory indicated yet another possibility--that the ion existed as a trimer. To complement this work, Raman and acid cryoscopy

Table 1. Spectral Data for Electronic Absorption Bands in
Mo Aquo Ions

	$\lambda_{\text{max}}(\text{nm})$	$\epsilon(\text{l mol}^{-1}\text{cm}^{-1})$
$\text{Mo}_2(\mu\text{-OH})_2(\text{aq})^{4+}$	360	306
	572	39
	624	43
$\text{Mo}_3\text{O}_4(\text{aq})^{4+}$ (acidic solution)	505	60
$\text{Mo}(\text{IV})(\text{aq})$ (basic solution)	575	80
$\text{Mo}_2\text{O}_4(\text{aq})^{2+}$	254	1999
	293	1727
	390	50

Table 2. Reaction conditions for photolyses of Mo(V), Mo(IV) and Mo(III) aquo ions.

Aquo Ion	Medium	Wavelength Irradiation	Result
Mo(V)	1-3 M HCl	broad band	no reaction
Mo(IV)	1-3 M HCl	broad band	no reaction
	1-3 M HMS	broad band	no reaction
	pH .5-2 HCl	broad band	no reaction
	pH .5-2 HMS	broad band	no reaction
	5 M NaOH	broad band	no reaction
Mo(III)	1-3 M HCl	broad band	no reaction

studies were made in pursuit of the elusive nature of Mo(IV) in aqueous solution. These are described herein.

Experimental

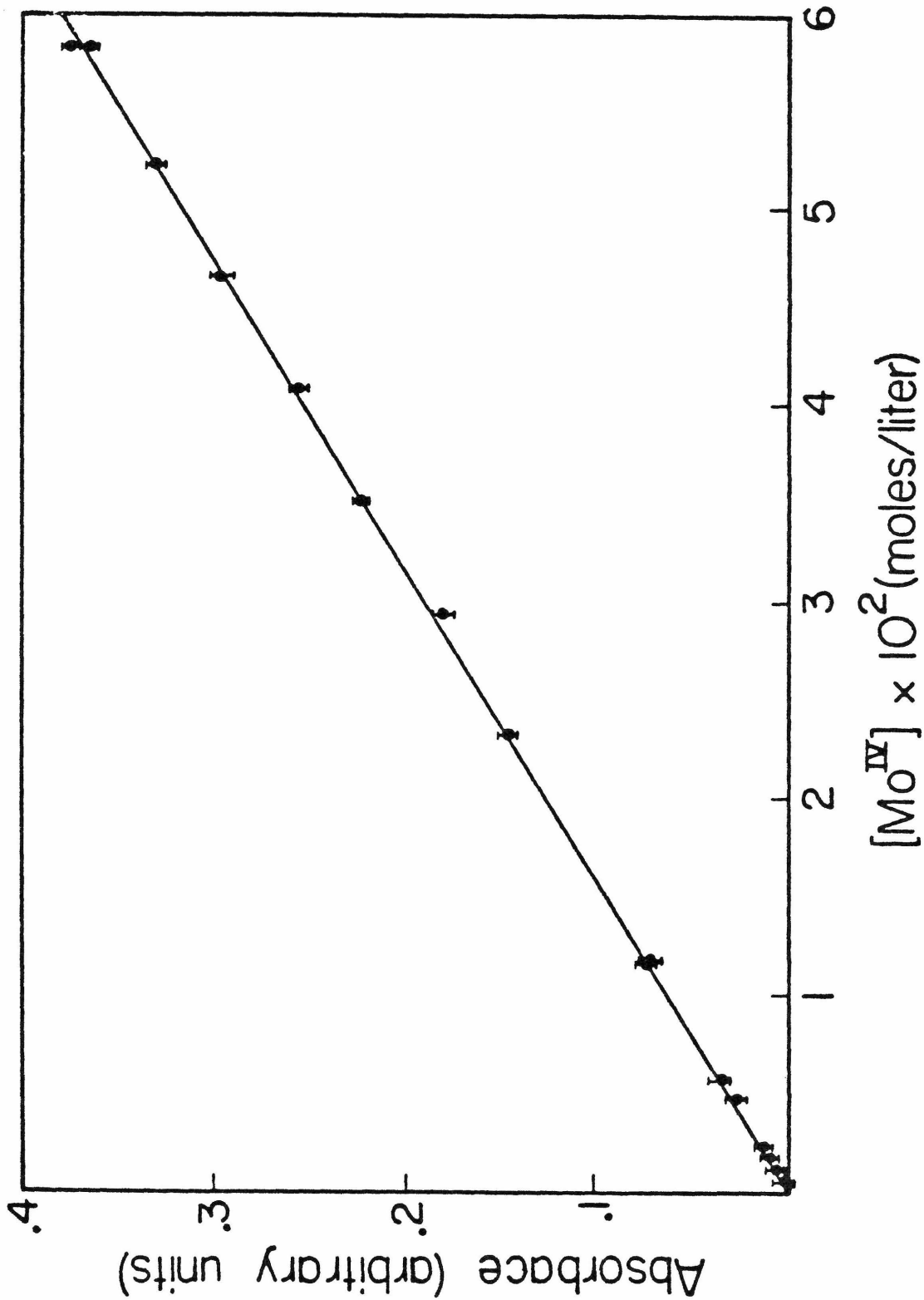
Aqueous Mo(IV) was prepared by the method of Ardon and Pernick.⁴ A Beer's Law study (Figure 3) of this ion indicated that only a single species was existent in solution. Aqueous Mo(V) was prepared by reduction over mercury.⁷ The compounds $\text{Na}_4\text{Mo}_6\text{O}_8 (\text{EDTA})_3 \cdot 14\text{H}_2\text{O}$ ⁸ and $\text{Cs}_2\text{Mo}_3\text{O}_4 (\text{C}_2\text{O}_4)_3 (\text{H}_2\text{O})_3$ ⁹ were prepared by literature methods.

Ion and cryoscopy experiments, Mo(IV) was concentrated on a Dowex 50 X2 cation-exchange column followed by elution in 5.1 M aqueous trifluoroacetic acid. At this concentration the acid has a eutectic freezing point of $-22.465 \pm .005^\circ\text{C}$. Using a copper constantin thermocouple and a digital microvolt voltmeter, this temperature corresponds to a reading of $78.1 \pm 5.2 \mu\text{v}$. Standard calibration curves were made using Zn^{2+} and Fe^{2+} as solutes. The freezing point of each solution was measured ten times by the procedure in Reference 10, yielding average values good to $\pm 6 \mu\text{v}$.

Aerated aqueous solutions of $\text{Na}_4\text{Mo}_6\text{O}_8 (\text{EDTA})_3 \cdot 14\text{H}_2\text{O}$ and $\text{Cs}_2\text{Mo}_3\text{O}_4 (\text{C}_2\text{O}_4)_3 (\text{H}_2\text{O})_3$ and 3 M HCl solutions of the Mo(IV) and Mo(V) aquo ions were used for Raman studies. A Spex 14018 double monochromator with 2400 lines/mm holographic gratings in conjunction with a spectrophysics 170 Ar^+ ion laser were used to record the Raman data. Detection was by

Figure 3

Beer's law plot for varying concentrations of $\text{Mo}_3\text{O}_4\text{aq}^{4+}$
in 3M HMS



standard photon counting techniques using associated Spex electronics and a Spex SCAMP SC-30 data processor.

The 5145 Å excitation line was used for $\text{Mo}_3\text{O}_4(\text{aq})^{4+}$ and $\text{Cs}_2\text{Mo}_3\text{O}_4(\text{C}_2\text{O}_4)_3(\text{H}_2\text{O})_3$ data collection, the 4545 Å excitation line for $\text{Mo}_2\text{O}_4(\text{aq})^{2+}$ and $\text{Na}_4\text{Mo}_6\text{O}_8(\text{EDTA})_3 \cdot 14\text{H}_2\text{O}$. Spectra obtained using the 4545 Å excitation line were complicated by numerous plasma lines, a spectrum of which has been included (Figure 4) for clarity. All frequency measurements were calibrated by using the emission spectrum of CCl_4 .

The electronic spectroscopic data were recorded on a Cary 17 spectrophotometer.

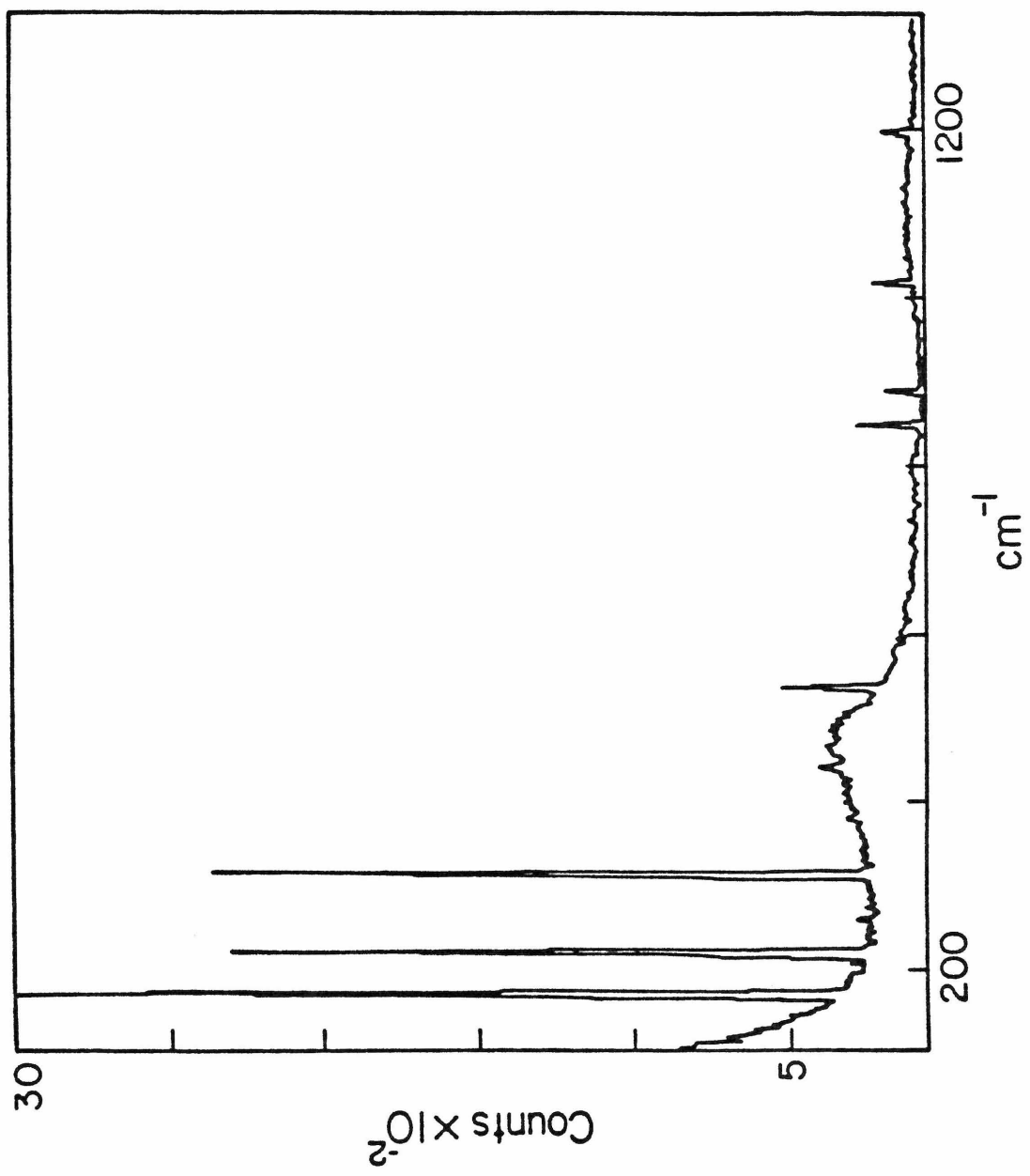
Results and Discussion

Acid Cryoscopy. The degree of polymerization of transition metal ions and other species which are stable only in acidic solutions may be determined by acid cryoscopy.¹¹ This method was employed by Ardon, et al.,¹² in a study of Mo(IV) in aqueous acidic solution. Average molal freezing-point depression constants nearly one-half of the calculated were obtained, thus leading to formulation of a dimeric species.

Because our EXAFS results indicated a trimeric structure, we reinvestigated the acid cryoscopic study above to see if evidence for our formulation might be gleaned. Unfortunately, the data obtained do not permit absolute characterization of the system due to large errors in measurements. This may best be understood by examination of the standard calibration

Figure 4

The Raman spectrum of plasma lines obtained
with 4545 Å excitation line



curve given in Figure 5 for $Zn^{2+}/5.1$ M HTFA. While discrimination can be made between a mononuclear and polynuclear species, the numbers obtained do not permit analysis as to the degree of polymerization. For example, if a solution .1 M in Mo(IV) (the maximum concentration preparable) were analyzed, values of 45.0 ± 5.3 , 53.2 ± 7.2 , and 65.3 ± 6.1 μ v readings should be obtained if the complex exists as a monomer, dimer, or a trimer, respectively. Typical values for Mo(IV) solutions at this concentration were in the 51-67 μ v region. Although one may conclude with surety that some polymerization is existent, the error limits preclude evidence as to the degree.¹³

Raman Spectroscopy. In a further attempt to obtain spectral evidence for the trimeric structure of $Mo_3O_4(aq)^{4+}$, the low frequency Raman spectrum was examined. The symmetry of the proposed species is C_{3v} , thus two Mo-Mo stretches of a_1 and e symmetries are expected. From previous investigations on complexes containing metal-metal bonds, $\mu(Mo-Mo)$ is expected to appear in the 250-100 cm^{-1} region.^{14,15} Similar spectra are anticipated for $Cs_2Mo_2O_4(C_2O_4)_3(H_2O)_3$ and $Na_4Mo_6O_8 \cdot 14H_2O$ complexes, while only one (Mo-Mo) stretch should appear for the dimer $Mo_2O_4(aq)^{2+}$ due to the lower symmetry (e.g., C_{2v}).

The Raman spectra are given in Figures 6-9 and Table 3. Using the 5145 Å excitation line of the Ar⁺ laser, no bands were observed below 340 cm^{-1} for $Mo_3O_4(aq)^{4+}$ or $Cs_2Mo_3O_4^-$

Figure 5

Calibration curve for Zn^{2+} /5.1 M HTFA

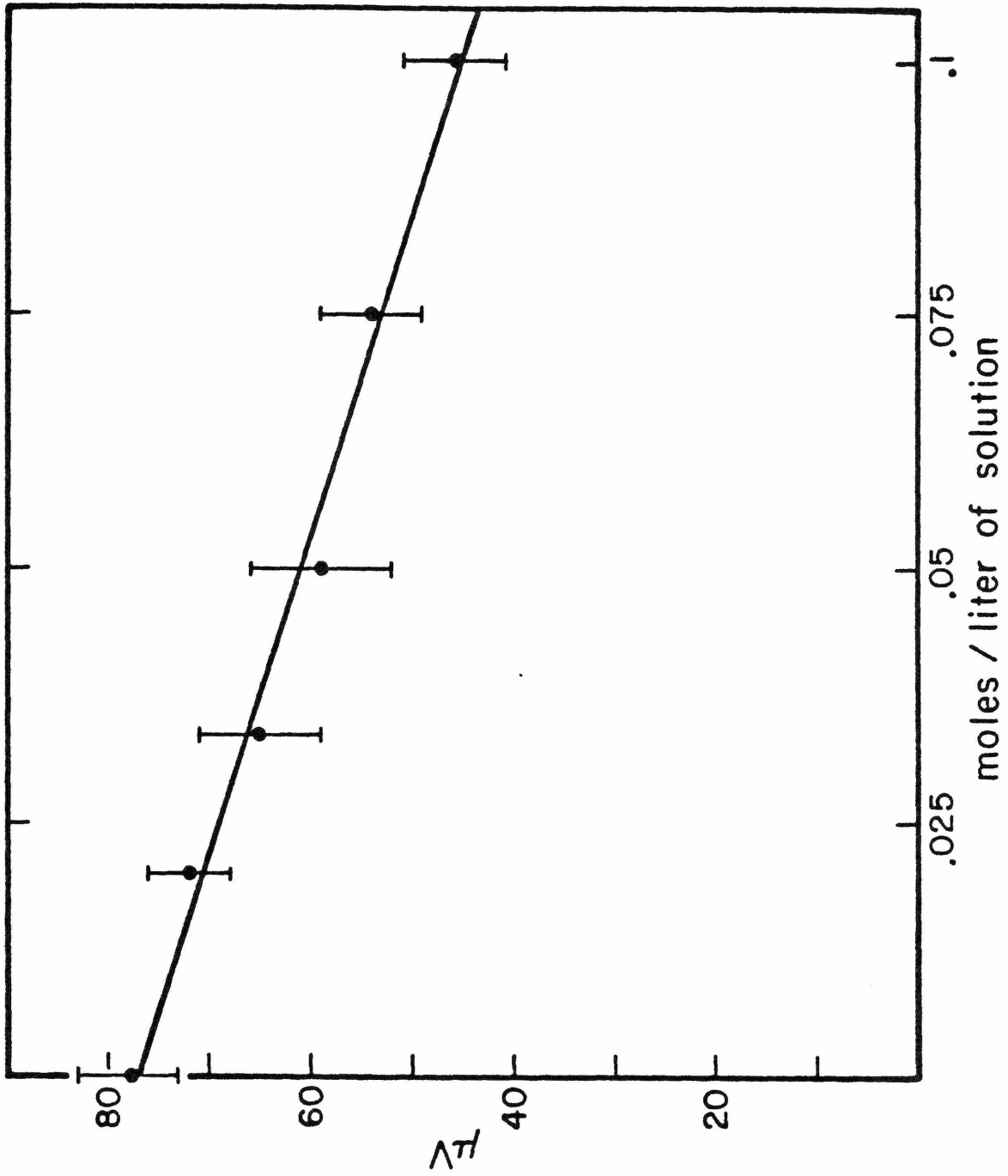


Figure 6*

The Raman spectrum of $\text{Mo}_3\text{O}_4(\text{aq})^{4+}$

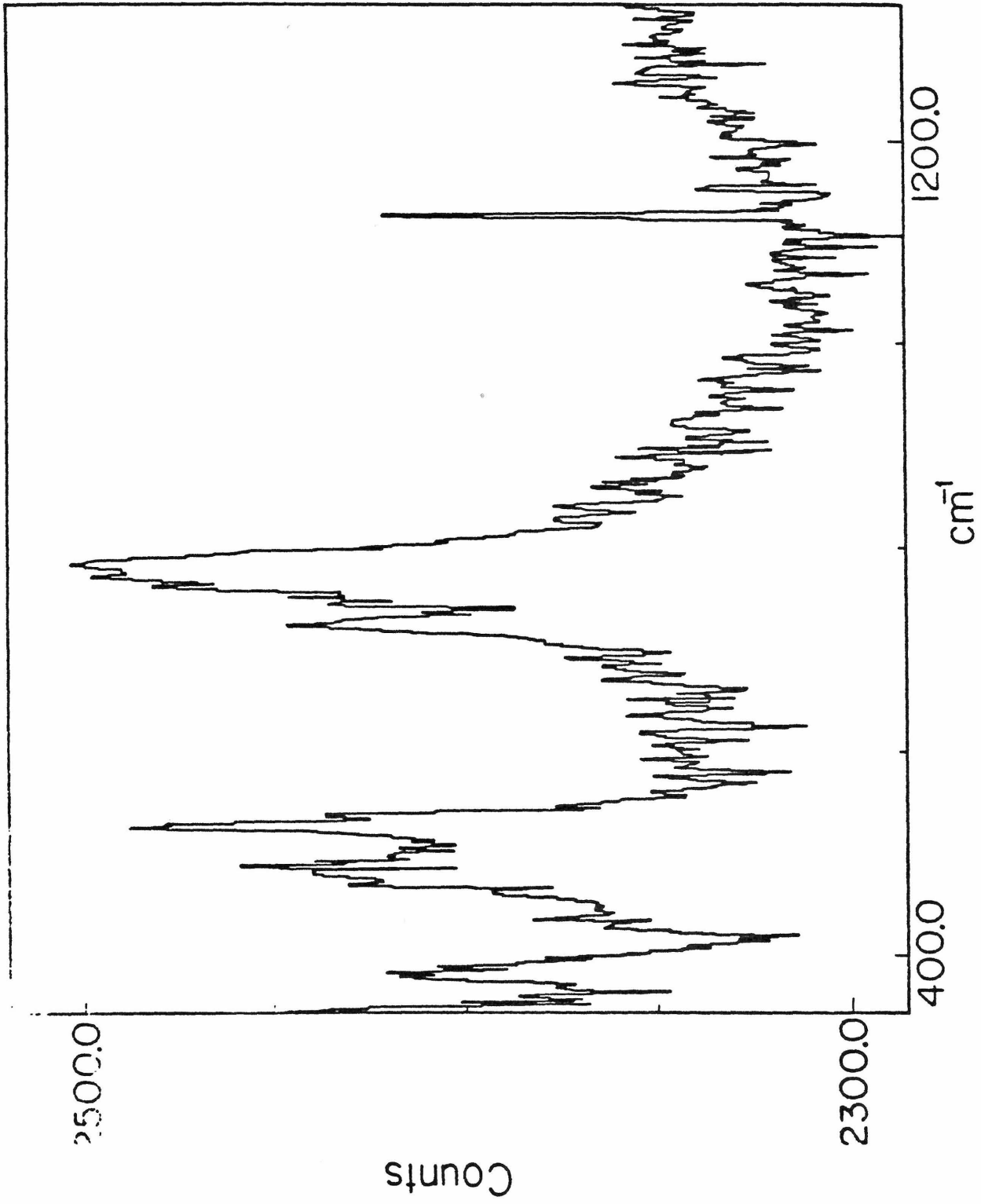


Figure 7

The Raman spectrum of $\text{Cs}_2\text{Mo}_3\text{O}_4(\text{C}_2\text{O}_4)_3(\text{H}_2\text{O})_3$

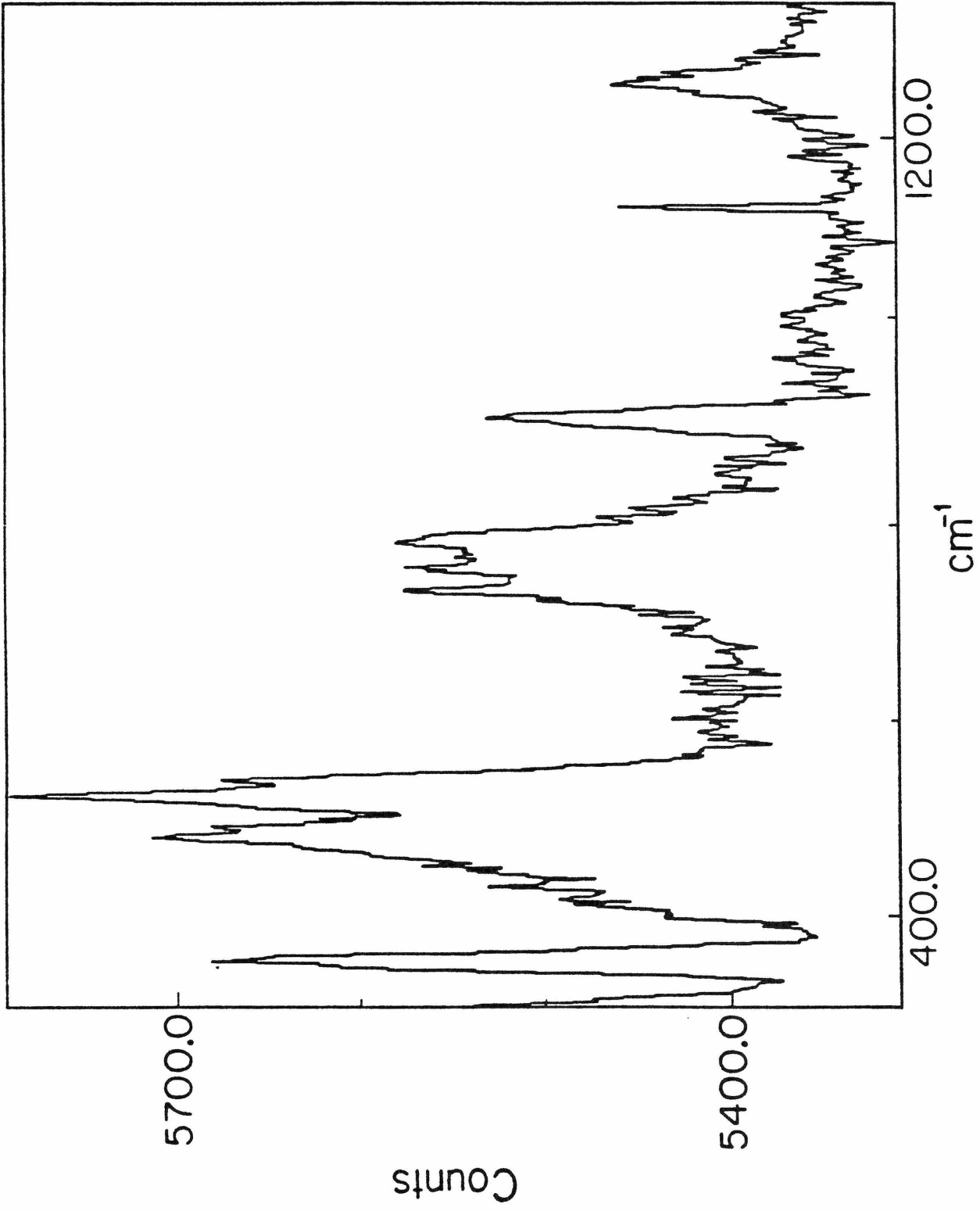


Figure 8

The Raman spectrum of $\text{Mo}_2\text{O}_4(\text{aq})^{2+}$

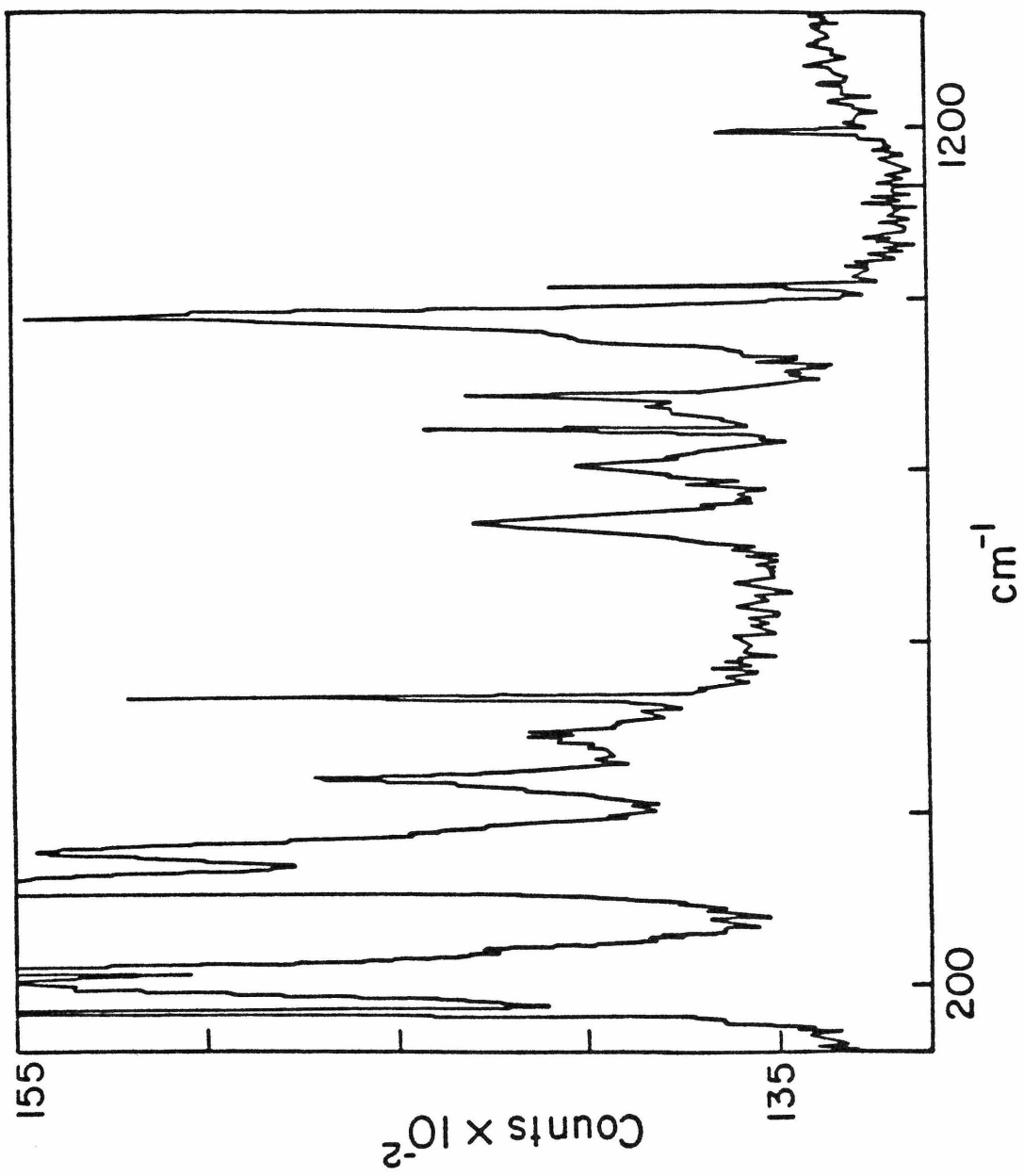


Figure 9

The Raman spectrum of $\text{Na}_4\text{Mo}_6\text{O}_8(\text{EDTA})_3 \cdot 14\text{H}_2\text{O}$

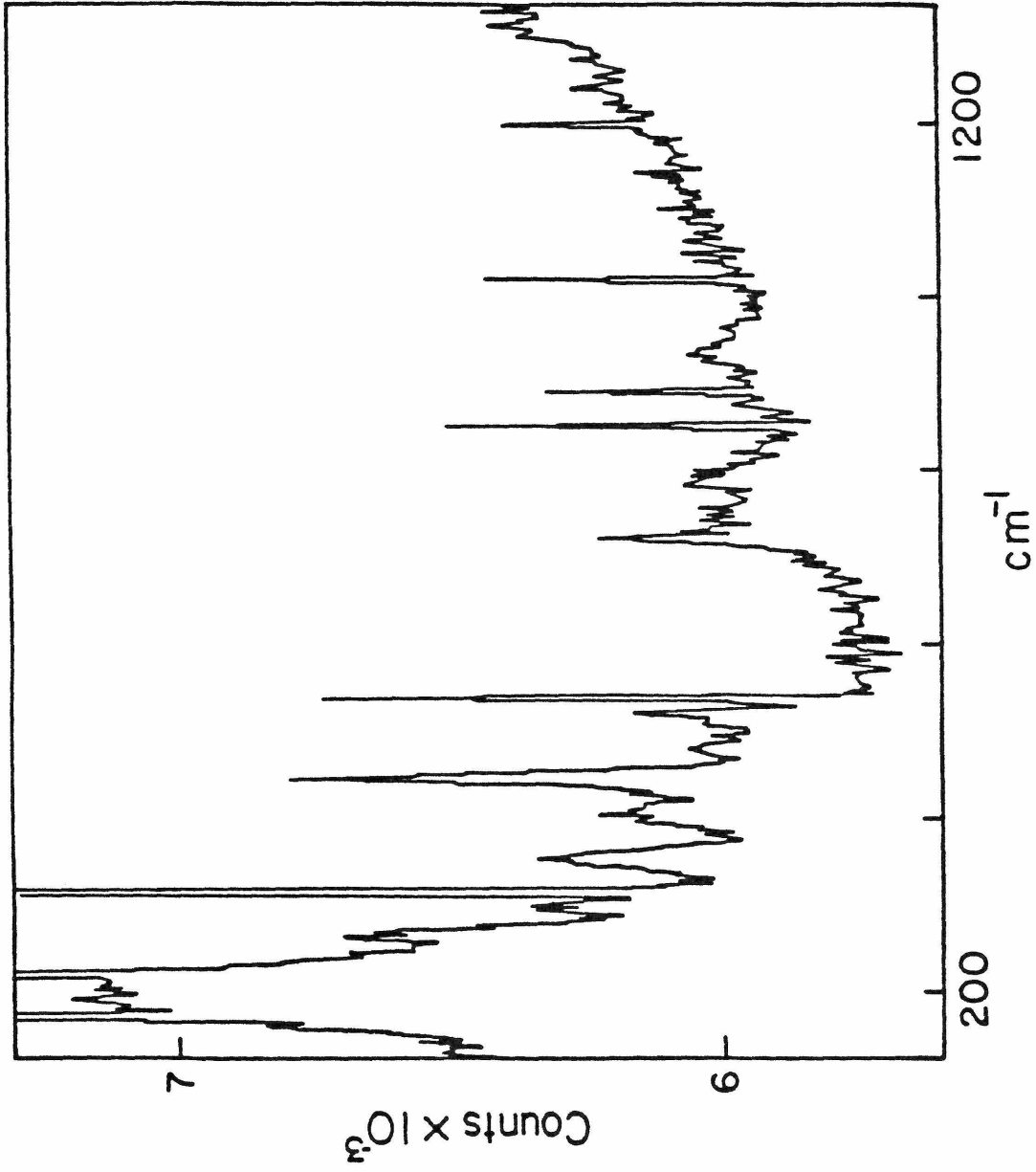


Table 3. Molybdenum-oxygen Terminal and Bridge Vibrational Modes

$\text{Cs}_2\text{Mo}_3\text{O}_4(\text{C}_2\text{O}_4)_3(\text{H}_2\text{O})_3$	353	481	521	736	786	907
$\text{Mo}_3\text{O}_4(\text{aq})^{4+}$	381	488	528	735	791	
$\text{Na}_4\text{Mo}_6\text{O}_8(\text{EDTA})_3 \cdot 14\text{H}_2\text{O}$	194	348	445	516	722	781
$\text{Mo}_2\text{O}_4(\text{aq})^{2+}$	200	342	484	742	806	981

Table 4. Molybdenum-oxygen Terminal and Bridge Vibrational Modes in Mo₂O₄F_x Compounds

(NH ₄) ₄ [Mo ₂ O ₄ F ₆]	No ₄ [Mo ₂ O ₄ F ₆]·3NaF	(NH ₄) ₂ Mo ₂ O ₄ F ₄ (H ₂ O) ₂	[N(CH ₃) ₄] ₂ Mo ₂ O ₄ F ₄				
Ir	Ra	Ir	Ra	Ra			
950vs	950vs	960vs	956vs	973vs	971vs	} ν _{Mo-O} (cm ⁻¹)	
910m	907m	940s	935m	958m	948m		
890m					931m		
735s	733m	763s	753m	745m,b	738vs,b	749m,b	} ν _{Mo₂O₂} (cm ⁻¹)
705sh					775sh	750sh	
505s		516m				515m	} ν _{Mo₂O₂} (cm ⁻¹)
		500m				475s	
	368m		374m	350w	367m	363m	} deformation vibration
			344w	317w	324w	318w	
	237m		250m	290m	298w	210s	} ν _{Mo₂O₂} (Mo-O)
	222m		240w	210vs			

Table 5. Molybdenum-oxygen Terminal and Bridge Vibrational Modes in $\text{Mo}_2\text{O}_4(\text{LL})_2$

Compound	Isotope	IR Spectrum	
		$\nu(\text{Mo}=\text{O})$ (cm^{-1})	$\nu(\text{MoO}_2\text{Mo})$ (cm^{-1})
$\text{Mo}_2\text{O}_4(\text{S}_2\text{PPr}_2)_2$	^{16}O	980vs	732s
		961m	714w
			475m
	^{18}O	934vs	701s
		913m	454m
		[932,914] ^a	[696,679,452] ^a
$\text{Mo}_2\text{O}_4(\text{S}_2\text{CNET}_2)_2$	^{16}O	973vs	730s
		956s	709w
			477m
	^{18}O	926vs	696s
		910s	672w
		[925,909] ^a	455m
		[694,674,454] ^a	

^aCalculated values for ^{18}O vibration

$(C_2O_4)_3(H_2O)_3$. This is probably a result of the cut-off limit due to Raleigh scattering of this intense laser line. On 4545 Å excitation, however, the Raman spectra of $Na_4Mo_6O_8(EDTA)_3 \cdot 14H_2O$ and $Mo_2O_4(aq)^{2+}$ show peaks at 194 and 200 cm^{-1} , respectively. These peaks can be assigned to vibrational modes predominantly symmetric Mo-Mo stretching in character, although there is undoubtedly some oxygen bridge interaction.¹⁴ While it is surprising that no band ascribable to an e mode is evidenced in the spectrum of $Na_4Mo_6O_8(EDTA)_3$, these bands are often weak and difficult to discern.

The remainder of bands given in Table 3 may be assigned to molybdenum-oxygen terminal and bridging modes by comparison with the assignments given by Von Mattes and Lux¹⁶ for Mo_2O_4 fluoro compounds (Table 4) and Newton and McDonald's¹⁷ IR study of $Mo_2O_2X_2(LL)_2$ compounds (Table 5). Both authors assign molybdenyl frequencies in the 900 cm^{-1} region and Mo_2O_2 at somewhat lower energies, 700-400 cm^{-1} . In our study (Table 3), $Mo_2O_4(aq)^{2+}$ with two Mo = O groups exhibits a peak at 981 cm^{-1} , consistent with a molybdenyl assignment, whereas the 907 band for $Cs_2Mo_3O_4(C_2O_4)_3(H_2O)_3$ is due to an oxalate localized vibration.¹⁸ Ring stretching frequencies appear in the 700, 400, and 300 cm^{-1} regions of the spectra. Using the 4545 Å excitation line, another feature was found at approximately 200 cm^{-1} for the $Mo_2O_4(aq)^{2+}$ and $Na_4Mo_6O_8(EDTA)_3 \cdot 14H_2O$ compounds, which again are most likely ascribed to ring stretching modes.

Figure 10

Near and far IR spectrum of $\text{Na}_4\text{Mo}_6\text{O}_8(\text{EDTA})_3 \cdot 14\text{H}_2\text{O}$

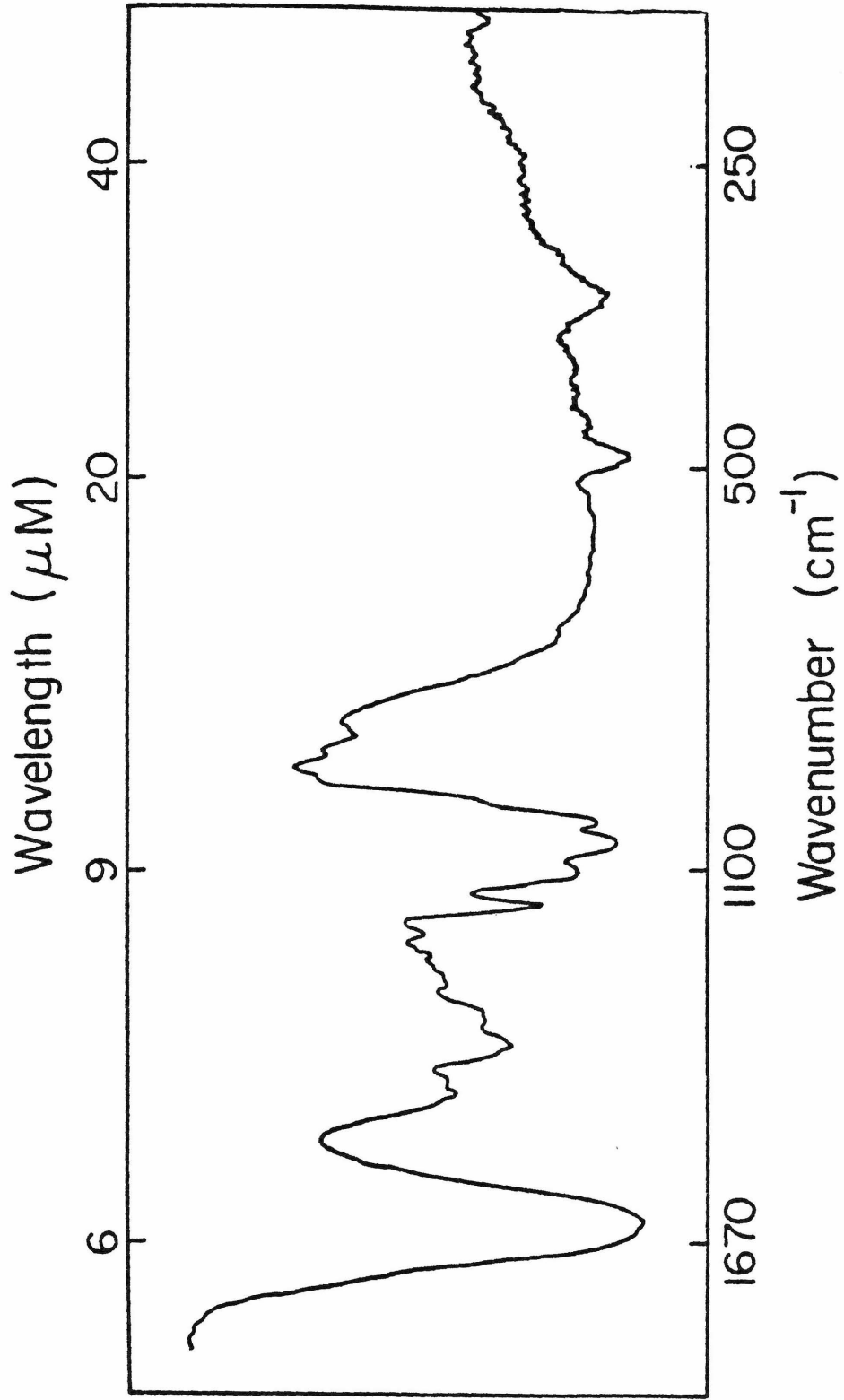
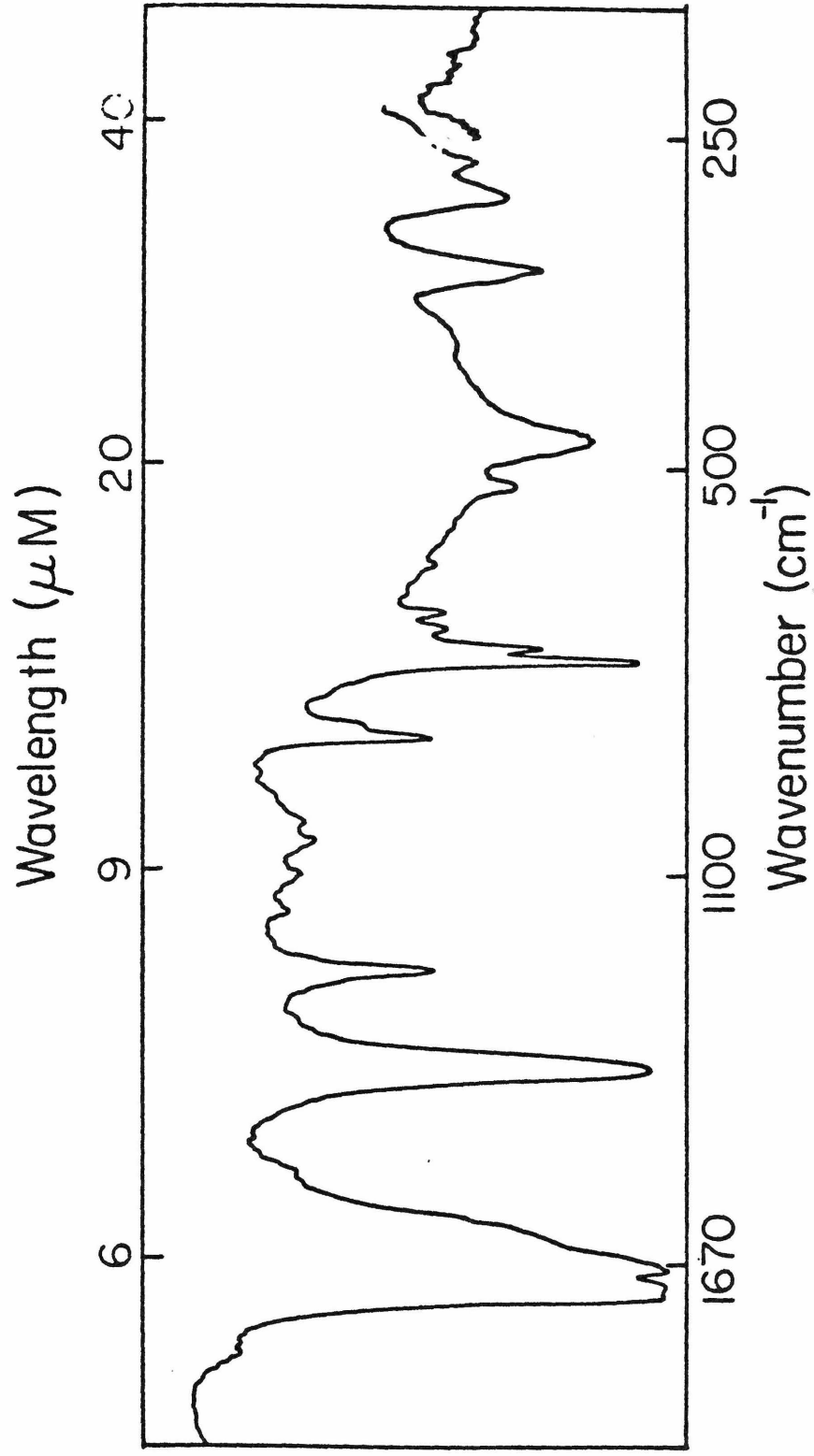


Figure 11

Near and far IR spectrum of $\text{Cs}_2\text{Mo}_3\text{O}_4(\text{C}_2\text{O}_4)_3(\text{H}_2\text{O})_3$



The $\text{Na}_4\text{Mo}_6\text{O}_8(\text{EDTA})_3 \cdot 14\text{H}_2\text{O}$ and $\text{Cs}_2\text{Mo}_3\text{O}_4(\text{C}_2\text{O}_4)_3(\text{H}_2\text{O})_3$ compounds exhibit C_{3v} symmetry in the crystalline state. Thus, both a_1 and e modes should be both IR and Raman allowed. The IR spectrum for $\text{Cs}_2\text{Mo}_3(\text{C}_2\text{O}_4)_3(\text{H}_2\text{O})_3$ (Figure 10) shows a band at 350 as compared with 353 for the Raman. Similarly, the IR spectrum for $\text{Na}_4\text{Mo}_6\text{O}_8(\text{EDTA})_3 \cdot 14\text{H}_2\text{O}$ (Figure 11) shows a band at 355 as compared with 348 for the Raman. It seems likely that this band can be attributed to either an a or e mode for both complexes.

While no conclusive structural evidence for the trimeric nature of $\text{Mo}_3\text{O}_4(\text{aq})^{4+}$ was gained, the infrared and Raman study was informative for location of the $\nu(\text{Mo-Mo})$ at $\sim 200 \text{ cm}^{-1}$, a mutually allowed vibration at $\sim 350 \text{ cm}^{-1}$, and observed similarities between these compounds and other bridging oxygen systems.

References

1. W. C. Trogler, Ph.D. Thesis, California Institute of Technology, 1948.
2. M. Ardon and A. Pernick, J. of Less Common Metals 54, 233-241 (1977).
3. J. R. Winkler, unpublished results.
4. M. Ardon and A. Pernick, J. Am. Chem. Soc. 95, 6871 (1973).
5. M. Ardon and A. Pernick, J. Am. Chem. Soc. 96, 1643 (1974).

6. T. Ramansami, R. S. Taylor and A. G. Sykes, J. Am. Chem. Soc. 97, 5918 (1975).
7. I. M. Kolthoff, Vol. Analysis 3, 92 (1957).
8. A. Bino, F. A. Cotton and Z. Dori, J. Am. Chem. Soc. 101, 3842 (1979).
9. A. Bino, F. A. Cotton and Z. Dori, J. Am. Chem. Soc. 100, 5252 (1978).
10. M. Ardon and G. Yahov, Inorg. Chem. 15, 12 (1976).
11. Ordinary cryoscopy (in water) as well as cryoscopy in a saturated solution of Na_2SO_4 (salzkryoscop) are not suitable for this purpose (cf. ref. 10).
12. M. Ardon, A. Bino and G. Yahov, J. Am. Chem. Soc. 98, 2338 (1976).
13. This was confirmed by Michael Ardon, personal communication.
14. K. Nakamoto, "Infrared and Raman Spectra of Inorganic and Coordination Compounds", Wiley Interscience, New York, New York, 234 (1978).
15. F. A. Cotton, R. M. Wing, and R. A. Zimmerman, Inorg. Chem. 6, (1), 11 (1967).
16. Von Mattes, R. and G. Lux, Z. Anorg. Allg. Chem. 424, 173-182 (1976).
17. W. E. Newton and J. W. McDonald, J. Less Common Metals 54, 51-62 (1977).
18. Op. cit., Nakamoto, 324.

Part B

X-ray Absorption Edge and EXAFS Spectroscopic Studies of
Molybdenum Ions in Aqueous Solution

Stephen P. Cramer

Exxon Research and Engineering Company

Linden, New Jersey 07036

Penny Slusser and Harry B. Gray

Arthur Amos Noyes Laboratory

California Institute of Technology

Pasadena, California 91125

Introduction

Molybdenum compounds play an important role in both biological and industrial catalysis,¹ owing in part to their rich oxidation-reduction chemistry in aqueous solution.² It is now well established that all oxidation levels between II and VI are represented by stable species in the aqueous chemistry of molybdenum,²⁻²⁷ although in certain cases the structures of these species are not known. Our recent interest in this area has centered on the structure of the red species that is present in acidic aqueous solutions of Mo(IV).^{3-7,25} Several different proposals have been put forward in regards the structure of this species, but it appears from the elegant study by Murmann⁷ that a trinuclear formation is correct.

We have now completed extensive investigation of the X-ray absorption edge and EXAFS spectra of aqueous Mo(IV) solutions with variations in pH and added anions. We have also examined the edge and EXAFS spectra of aqueous solutions containing Mo(II), Mo(III), and Mo(V). The results and principal structural conclusions drawn from these studies are reported herein.

Experimental Section

Sample Preparation and Characterization

Aqueous Mo(II) was prepared in trifluoromethanesulfonic acid by the method of Bowen and Taube.²⁶ The Mo(III) samples were prepared in 3 M methanesulfonic acid using a Jones reductor and purified by column chromatography.²⁷ Mo(IV) in 4 M methanesulfonic acid was prepared by the method of Ardon and Pernick,⁶ and lower acid concentrations were achieved by addition of solid NaOH. Solid NaCl or NaBr was added to the 4 M sample until saturation for the anion experiments. Finally, aqueous Mo(V) was prepared by reduction over mercury.²⁸ All of the samples were characterized by optical absorption spectroscopy, and oxidation states were verified by ceric ion titration.

Data Collection

The solutions were loaded into lucite cuvettes with 1 mm thick lucite windows and 5 or 10 mm path lengths. The air-sensitive Mo(II) and Mo(III) samples were stored over zinc amalgam and loaded into the cuvettes in an anaerobic glove box just prior to data collection. Spectra were recorded at the Stanford Synchrotron Radiation Laboratory.

Data Analysis

The spectra were calibrated using the Mo foil edge inflection as 20003.9 eV, and the EXAFS was processed using standard procedures of pre-edge subtraction, spline removal, and Fourier filtering.²⁹ The curve-fitting analysis of the

EXAFS data depends upon the assumption of phase shift and amplitude transferability between compounds of similar chemical structure.²⁹⁻³⁰ The molybdate ion MoO_4^{2-} was used as the standard for Mo-O interactions, while the compound $\text{K}_2[\text{Mo}_3\text{O}_4(\text{ox})_3(\text{H}_2\text{O})_3]$ ³¹ was used for Mo-Mo functions. K_3MoCl_6 ³² and $(\text{NH}_4)\text{MoOBr}_4 \cdot \text{H}_2\text{O}$ ³³ were used for the Mo-Cl and Mo-Br functions.

The curve-fitting program simulated the EXAFS as:

$$\chi(k) \cong \frac{1}{k} \sum_s \frac{N_s A_s(k) e^{-2\sigma_s^2 k^2}}{R_s^2} \sin(2kR_s + \alpha_s(k))$$

where k is the photoelectron wave number, R_s is the distance of a group of N_s scatterers to molybdenum, σ_s is the mean deviation of R_s , and $\alpha_s(k)$ is the total phase shift. The amplitude function A_s depends not only on the electron-atom backscattering amplitude for the particular scattering atom, but also on the properties of the particular X-ray absorbing species.³⁴

Definition of $A_s(k)$ for a given Mo-X pair requires knowledge of the appropriate Debye-Waller factor for a simple standard compound. For the Mo-O amplitude we used the σ of 0.0411 Å for MoO_4^{2-} calculated from the vibrational spectrum.³⁵ The Mo-Mo amplitude was calibrated by using the Mo-Mo stretching frequency of aqueous Mo(II) of 355.7 cm^{-1} ,³⁶ and the formula:³⁷

$$\sigma_{\text{vib}} = \left| \frac{h}{8\pi^2 \mu c \omega} \coth \frac{hc\omega}{2kT} \right|^{1/2}$$

where μ is the reduced mass, and ν is the vibrational frequency in wave numbers, which yields a σ of 0.0377 Å. Since all of the calculated Debye-Waller factors were obtained through differences with respect to these standards, they should be recalculated in the future if more accurate values for MoO_4^{2-} and Mo(II)-Mo(II) become available.

The particular functional forms and parameters used for phase shifts and amplitudes are summarized in Table 1. Furthermore, a comparison of our amplitudes with theoretical backscattering amplitudes³⁸ is given in Figure 1. Since it is possible that the Fourier filtering and fitting procedure eliminated some of the low k structure in the Mo-Mo amplitude and phase shift, the fits were always begun at $k = 6 \text{ \AA}^{-1}$.

Results and Discussion

The aqueous molybdenum samples yielded a remarkable diversity of edge and EXAFS spectra, which reflect the profound electronic and atomic rearrangements that occur upon redox changes. The edge data (Figure 2) are treated first, then the general EXAFS Fourier transform results (Figure 3). Finally, the results of a curve-fitting analysis (Figure 4) of the EXAFS data for each particular oxidation state are presented.

Table 1. Fourier transform analysis.^a

Sample	Calculated Distance (Å)	Calculated Neighbor Number
$(\text{Mo}_3\text{O}_4(\text{C}_2\text{O}_4)_3(\text{H}_2\text{O})_3)^{2+}$	2.49 ^b	2 ^b
Mo(V) (aq)	2.51	0.89
Mo(IV) (aq)	2.48	2.0
Mo(IV) (aq) + Cl^-	2.48	2.1
Mo(IV) (aq) + Br^-	2.48	2.0
Mo(IV) (aq) pH 1.6	2.49	1.8
Mo(IV) (aq) pH 1.8	2.46	1.6
Mo(IV) (aq) 5M NaOH	2.51	1.5
Mo(III) (aq)	2.46	0.75
Mo(II) (aq)	2.17	0.79

^aused as standard

^btransform range: 4-15 Å⁻¹, k³ weighting

Figure 1

A comparison of theoretical and experimental amplitudes
for oxygen and molybdenum

COMPARISON OF THEORETICAL AND EXPERIMENTAL AMPLITUDES

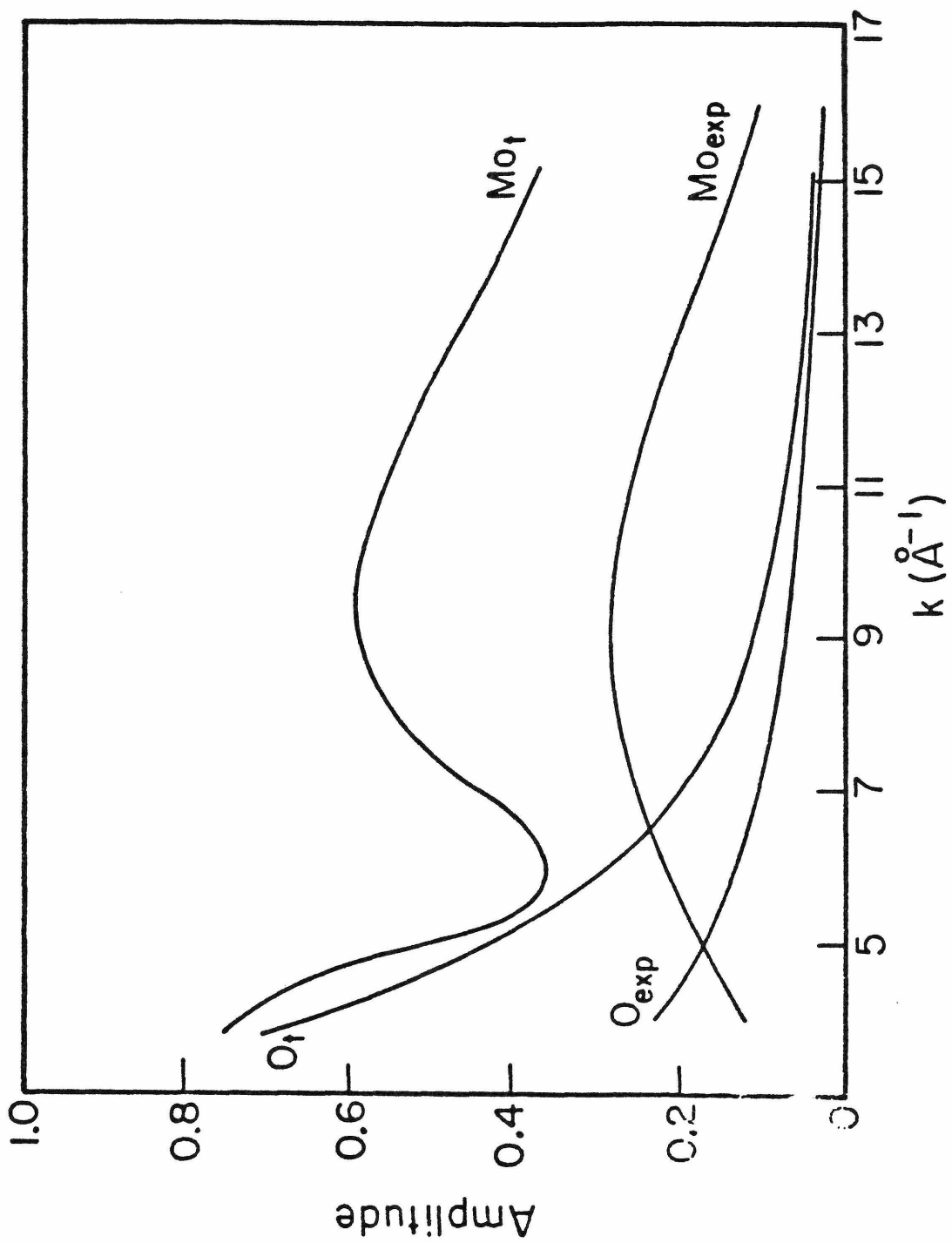


Figure 2

The absorption edge region for aqueous Mo(II), Mo(III), Mo(IV) and Mo(V). The spectra were scaled to yield the same amplitude at 20200 eV. Therefore, the differences in peak heights near the edge are significant.

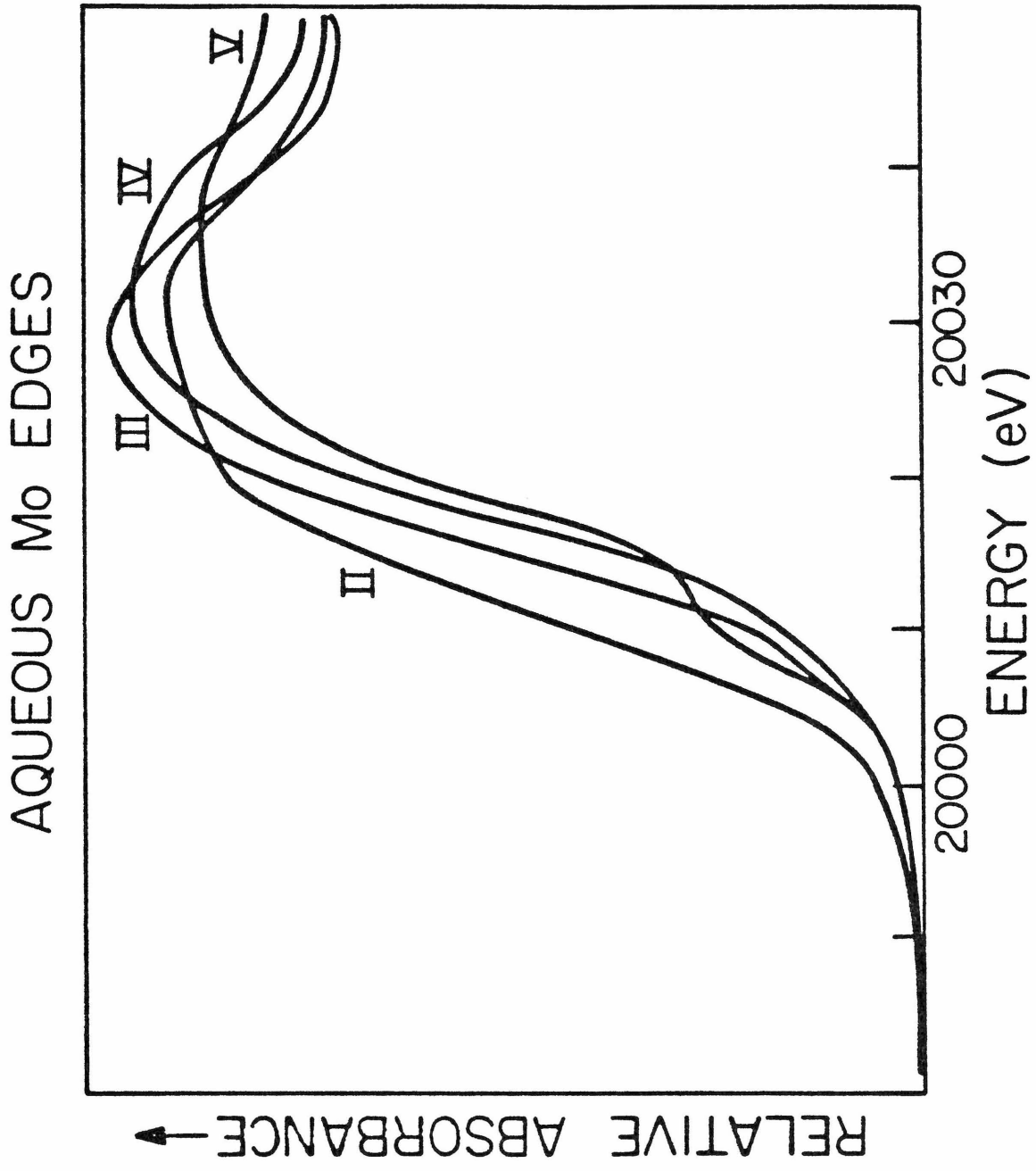


Figure 3

EXAFS Fourier transforms for aqueous Mo. Range: 4-15 \AA^{-1} ,
 k^3 weighting.

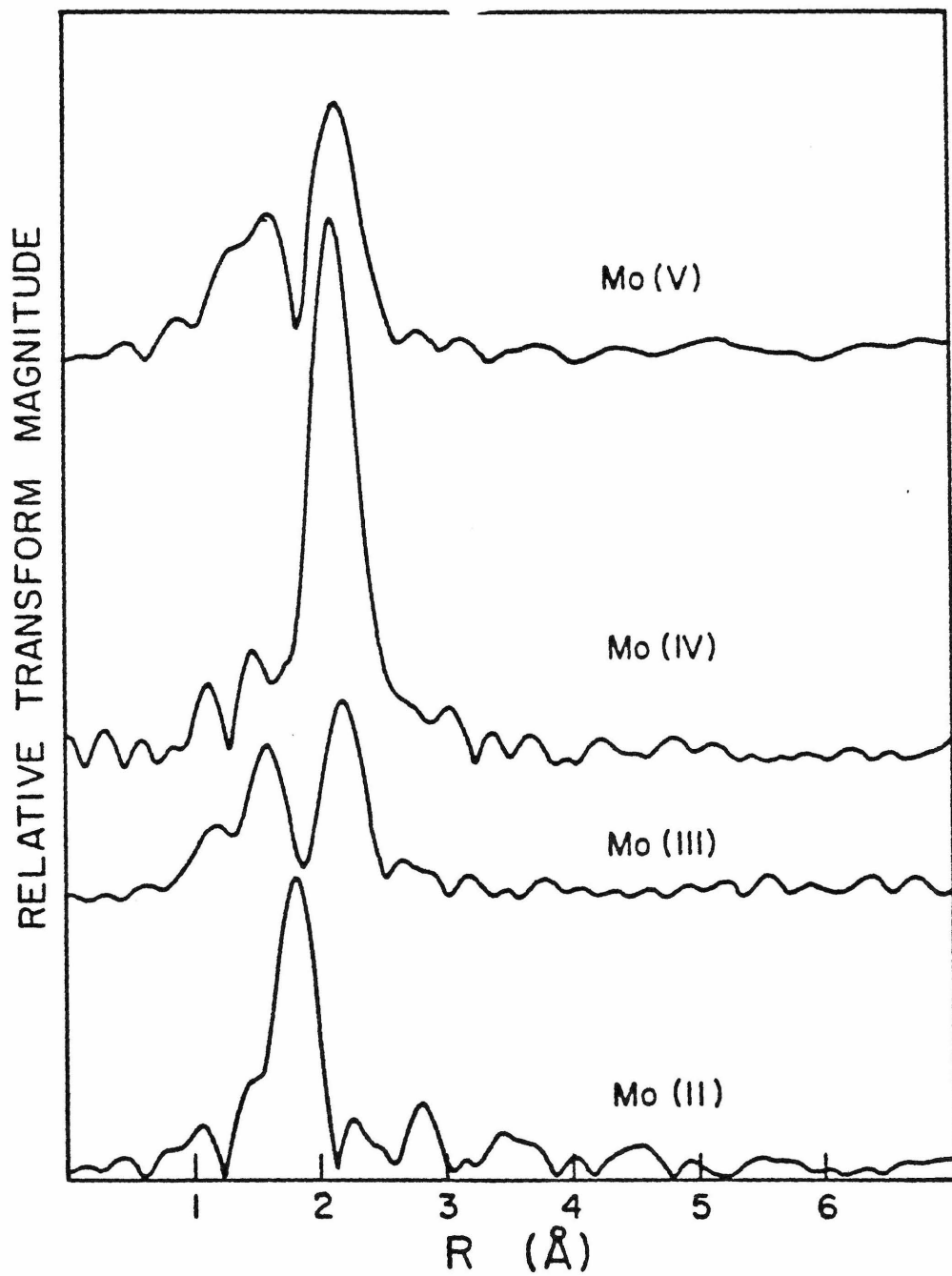
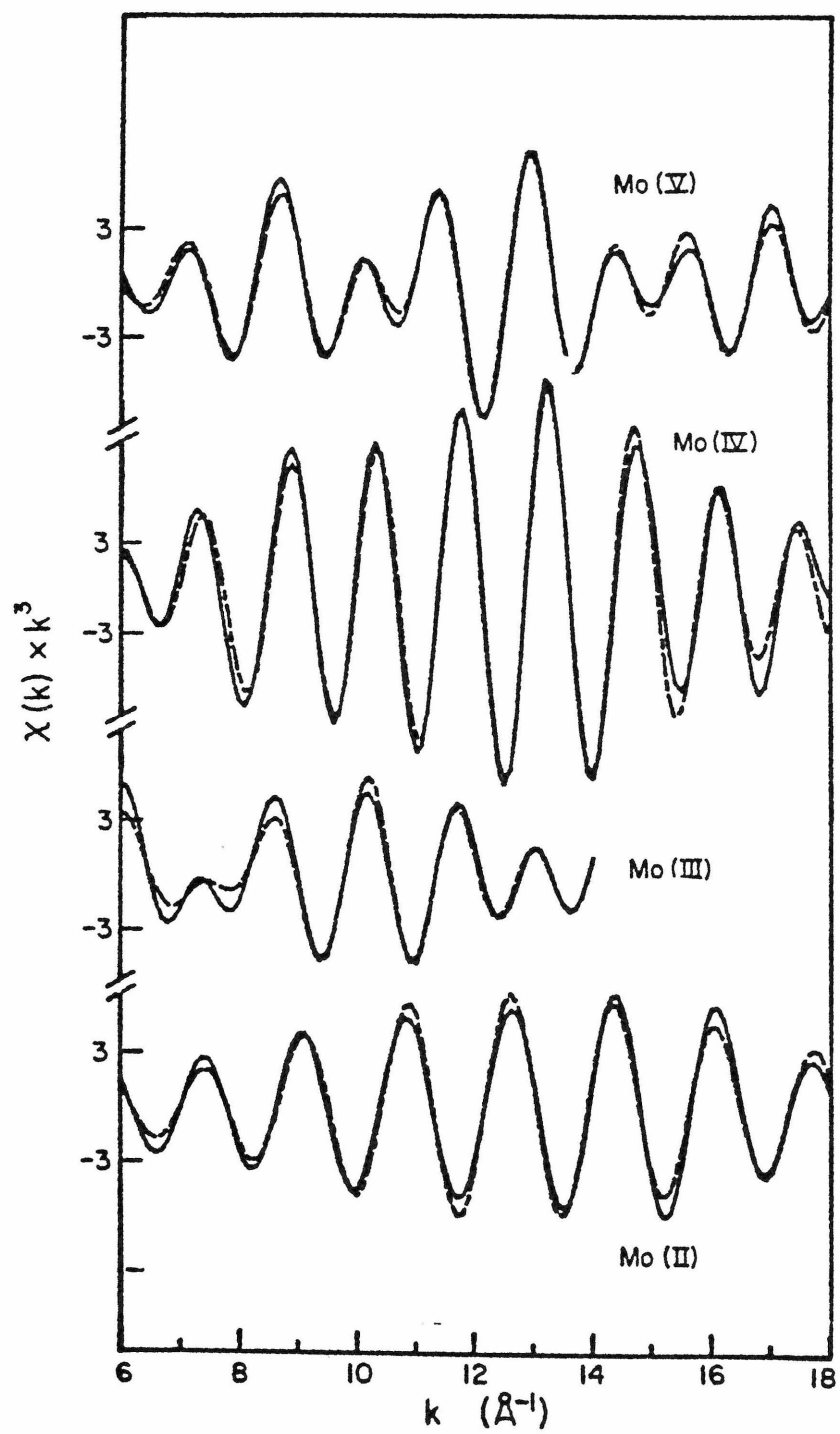


Fig. 2

Figure 4

Fourier-filtered EXAFS (solid line) and best fits (dashed line) for aqueous Mo.



Edges

The edge region can provide useful information about the electronic structure of the X-ray absorbing atom.³⁹ Because of lifetime broadening, molybdenum K edges have a natural linewidth of about 6 eV,⁴⁰ about equal to the spectrometer resolution, and one therefore does not observe the sharp structure associated with the edges of lower Z elements. Nevertheless, it is clear that the edges move progressively to higher energy as the oxidation state is raised. The biggest shift is between Mo(II) and Mo(III), and subsequent shifts are progressively smaller. If one accepts the edge position as a semi-quantitative indicator of the charge on the X-ray absorbing atom, then these data indicate an increasing amount of covalency as the formal oxidation state is raised. Finally, the Mo(V) sample has a low energy shoulder in its spectrum which is a characteristic feature of terminal oxo groups.^{39,41}

EXAFS Fourier Transforms

Fourier transformation of the EXAFS data yields a pattern which is qualitatively similar to a radial distribution function.⁴² The transforms for all samples are dominated by a peak corresponding to the Mo-Mo interaction. A quantitative analysis of peak heights and positions (Table 2), using the cluster $[\text{Mo}_3\text{O}_4(\text{ox})_3(\text{H}_2\text{O})_3]^{26-31}$ as a standard, suggests presence of a single Mo-Mo interaction in aqueous Mo(II), Mo(III), and Mo(V), but two Mo-Mo

Table 2. Aqueous Molybdenum Curve-Fitting Analysis.

Sample	Mo-M		Mo-O		Mo-O'		F ^a
	Number	R (Å)	Number	R (Å)	Number	R (Å)	
Mo(II)	0.77	2.117					0.502
	0.90	2.123	1.5	2.14			0.332
	1	2.119	4	2.14	0.10		0.327
Mo(III)	0.6	2.54					3.160
	0.7	2.54					0.858
	0.8	2.54	2.2	2.06	2.24		0.426
	1	2.54	3.6	2.05	2.20	0.76	0.365
Mo(IV)	1.9	2.493					1.612
	2.0	2.493	1.2	1.88			0.851
	2.0	2.493	2.1	1.89	2.05		0.192
[Mo ₃ O ₄ ox ₃] ²⁺	2	2.493	2	1.88	0.031	0.077	0.234
	2.0	2.488					1.653
	2.0	2.488	1.2	1.92			0.975
	2.0	2.488	2.1	1.92	2.07		0.510
Mo(V)	2	2.488	2	1.91	0.042	0.090	0.430
	0.87	2.56					2.983
	0.87	2.56	1.9	1.93			1.289
	0.88	2.56	1.8	1.93	1.68		0.289
	1	2.562	2	1.93	0.042	0.038	0.232

^a Calculated from $\nu M_O - M_O$.^b $(\sum(\chi_{\text{obs}} - \chi_{\text{calc}}) \cdot k^6) / N$.

interactions (per Mo) in Mo(IV). Furthermore, the Mo(II)-Mo(II) distance is significantly shorter than that found in the other oxidation states.

At distances shorter than the Mo-Mo bond lengths, the transforms of the Mo(III), Mo(IV), and Mo(V) EXAFS contain features due to Mo-O interactions. Relative to the Mo-Mo peak, these features are strongest for Mo(III), somewhat weaker for Mo(V) and smaller yet for Mo(IV). The consequence of this is evident in the curve-fitting analyses described below, where inclusion of Mo-O components significantly improves the fits for Mo(III) and Mo(V), but is less important for Mo(IV) and Mo(II). Because of the artifacts which can arise from peak overlap and truncation effects, a quantitative analysis of the Mo-O region was not attempted on the transforms themselves.

Curve Fitting

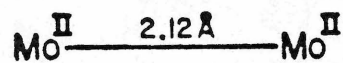
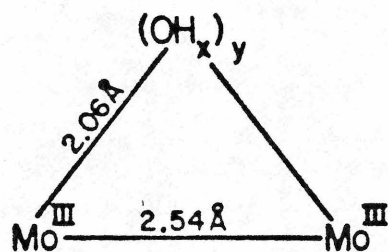
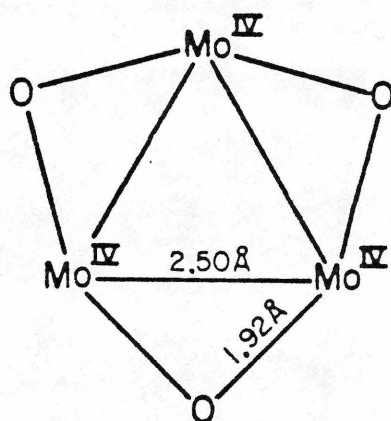
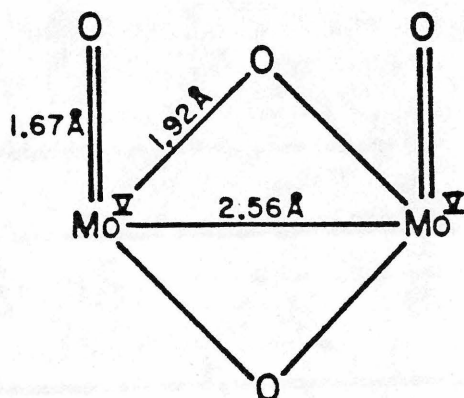
The curve fitting results of this investigation are summarized in Figure 5. The optimization procedure refined two variables per shell, one being the Mo-X distance and the other being either the scatterer number or the Mo-X Debye-Waller factor. In the fits using integral scatterer numbers we have used a number of ligands consistent with the known chemistry for that Mo oxidation state.

Mo(II) - An excellent fit was obtained with a single Mo-Mo interaction at 2.12 Å, and a slight improvement resulted from adding a Mo-O component at 2.13 Å. The short

Figure 5

Schematic representation of curve-fitting results for various oxidation states.

AQUO Mo CORE STRUCTURES



Mo-Mo distance is consistent with a quadruply bound dinuclear species. This Mo-Mo bond length is similar to the 2.11 Å value found for $\text{Mo}_2(\text{O}_2\text{CCH}_3)_4$ ⁴³ and $\text{K}_4\text{Mo}_2(\text{SO}_4)_4 \cdot 2\text{H}_2\text{O}$.⁴⁴ The predicted Mo-O distance of 2.13 Å is reasonable, and the large Debye-Waller factor probably indicates a relatively disordered coordination of water to this dinuclear species.

Mo(III) - Useful data were restricted to a maximum of $k = 14 \text{ \AA}^{-1}$. A good fit required not only a Mo-Mo component at 2.54 Å, but two different Mo-O components at 2.06 and 2.23 Å. The Mo-Mo distance is considerably longer than the 2.43 Å bond length in $\text{KMo}_2(\text{OH})_2(\text{ac})(\text{EDTA})$.⁴⁵ Thus, although Mo(III) is electronically capable of metal-metal triple bonding, it does not appear to have used multiple bonding in this aquo ion. The 2.06 Å Mo-O component is most reasonably assigned to bridging oxygens, and comparison with typical oxo bridge bond lengths (1.92 Å) suggests that protonation to form a hydroxide bridge has occurred. Finally, the longer Mo-O component is ascribable to a Mo-H₂O distance. In all other aquo species examined, Mo-H₂O interactions made negligible contributions to the EXAFS. The fact that water of solvation is seen in this case might be due to the relative substitutional inertness of d^3 Mo(III).

Mo(V) - Again, three components were required for a good fit. A 2.56 Å Mo-Mo distance was found, as well as 1.92 and 1.67 Å Mo-O distances. The Mo-Mo distance found

for the aquo ion is typical for oxo bridged dinuclear Mo(V) compounds.⁴⁶ Similarly, the Mo-O distances of 1.92 Å and 1.67 Å are normal for bridging and terminal oxo's respectively. The amplitudes are all consistent with a dinuclear Mo₂O₄ structure which has now been observed in a large number of Mo(V) compounds.

Mo(IV) - Because of controversy over the nature of this species, a variety of aqueous Mo(IV) samples was investigated. For the 4 M methanesulfonic acid sample, the calculations gave 2.0 Mo at 2.49 Å, an amplitude roughly twice as large as that found for Mo(II) and Mo(V). Further improvement was had by using Mo-O components at 1.88 and 2.04 Å, but the effect of these additions was small compared to their contribution to the Mo(III) and Mo(V) fits.

Although the 2.49 Å Mo-Mo distance was originally compared³ to dinuclear species such as MoO₂⁴⁷ and Mo₂O₂(i-pro)₄,⁴⁸ it is also very close to the Mo-Mo distances found in recently discovered trinuclear clusters Mo₃O₄(ox)₃(H₂O)₃]²⁻ (2.49 Å)³¹ and Mo₃O₄(EDTA)²⁻ (2.50 Å).⁴⁹ Thus, the Mo-Mo distance is of no value in determining the core structure. In the original work on aquo Mo(IV) a Mo-Mo amplitude of 1.5 was reported. However, reinspection of earlier results³⁰ showed a consistent tendency to underestimate oxo-bridged Mo amplitudes by about 20%. Use of the new Mo-Mo functions based on [Mo₃O₄(ox)₃(H₂)₃]²⁻ yielded a Mo-Mo amplitude very close to 2. In fact, visual comparison

Figure 6

EXAFS Fourier transforms for some Mo(IV) samples. Top to bottom: 5M NaOH; pH 1.8; pH 1.6, 4M HMSF + NaCl; 4M HMSF; $\text{Mo}_3\text{O}_4(\text{ox})_3$ Range: 4-15 \AA^{-1} , k^3 weighting.

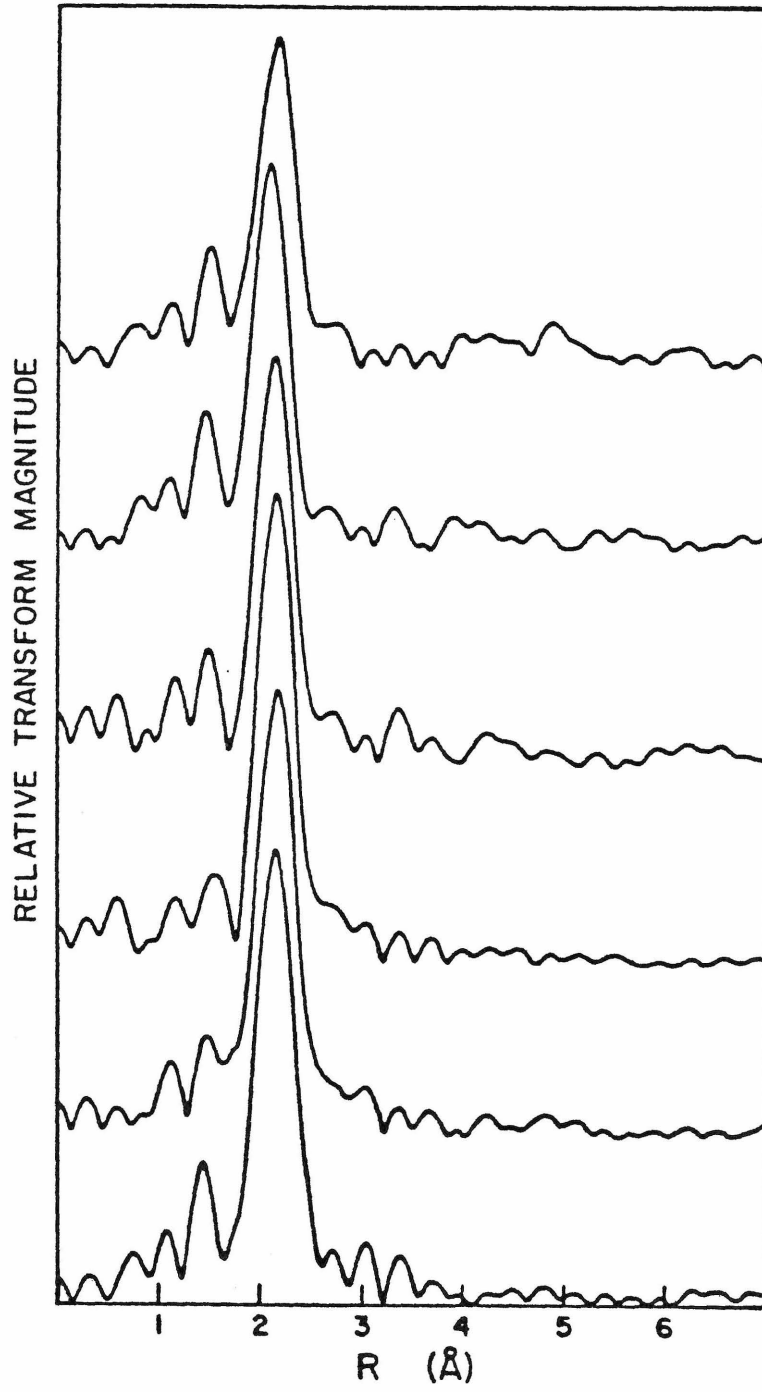
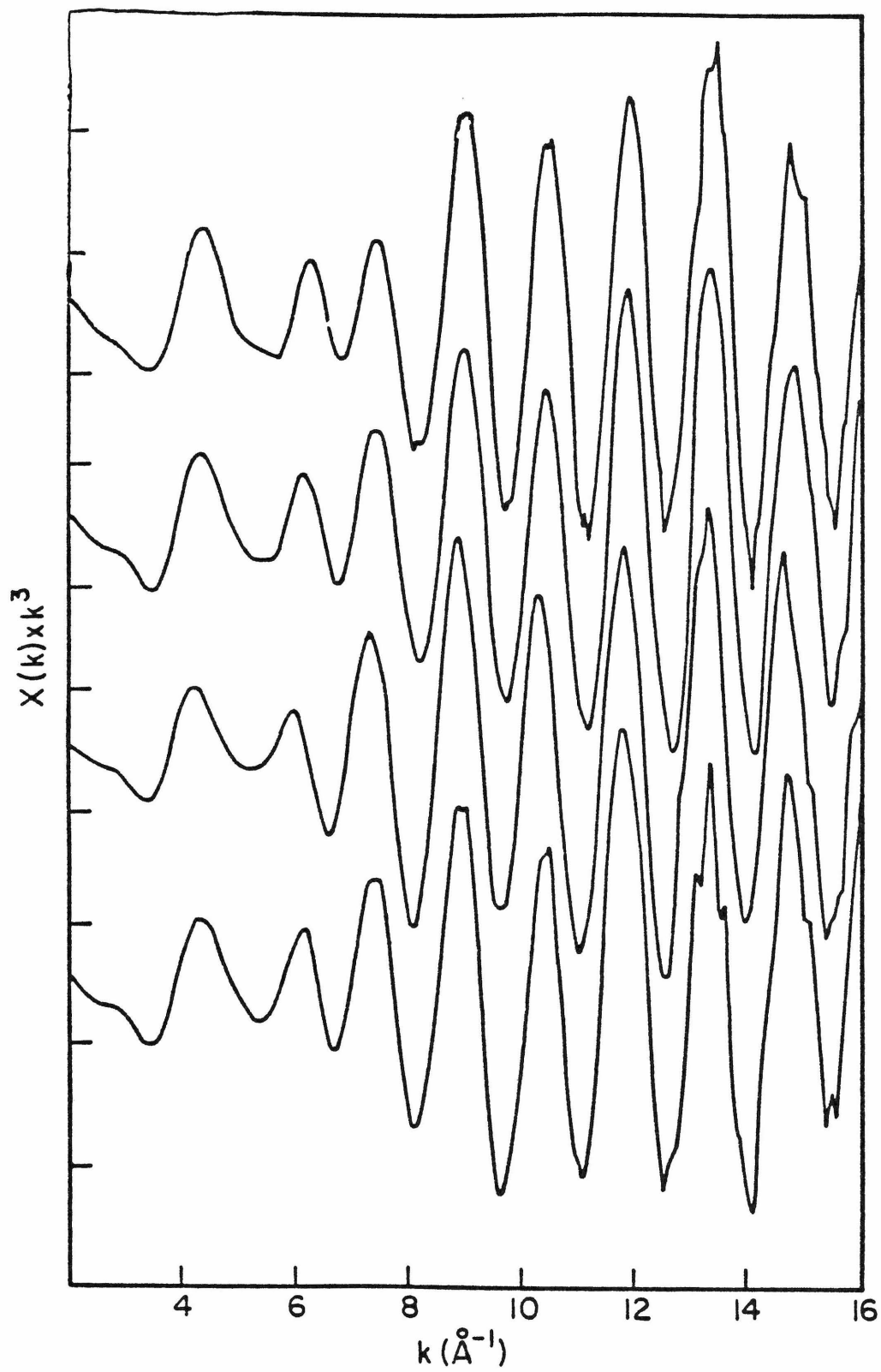


Figure 7

EXAFS data for some Mo(IV) samples. Top to bottom:

$K_2(Mo_3O_4(ox)_3(H_2O)_3)$, Mo(IV)-4M HMSF, Mo(IV)-4M HMSF + NaCl,

Mo(IV)-4M HMSF + NaBr.



of the solid state and solution data shows that the spectra are nearly identical (Figures 6 and 7). In 4 M methane-sulfonic acid therefore, Mo(IV) undoubtedly exists predominantly as a trinuclear species.

It is also useful to compare the calculated Mo-O distance of aquo Mo(IV) with the values obtained for $K_2Mo_3O_4(ox)_3(H_2O)_3$. In the cesium salt of the latter compound each molybdenum is connected to two bridging oxygens with an average distance of 1.921 Å, and the EXAFS fit gave 1.91 Å for the same distance. However, the trimer also has a capping oxygen at 2.019 Å, two oxalate oxygens per molybdenum at 2.091 Å, and a single water oxygen at 2.154 Å. For this second shell of oxygens the fit gave a 2.05 Å distance with a deviation of 0.09 Å, as opposed to the true mean of 2.09 Å. Thus, in interpreting the aquo Mo(IV) fits, it appears reasonable to assign the 1.88 Å Mo-O component to doubly bridging oxygens, and the 2.04 Å component to a weighted average of triply bridging oxygen and water of solvation. A similar conclusion as to the nature of Mo(IV) (aq) was reached recently by Murmann,⁷ who demonstrated the trinuclear nature of this ion by isotope exchange experiments with $(Mo_3O_4(NCS)_9)^{5-}$.

As the pH of the medium was increased, the Mo-Mo amplitude decreased. The same phenomenon was observed in the Fourier transforms (Figure 3 and Table 2). This amplitude decrease could have two different origins, either

a partial conversion of a trinuclear structure to a bi- or mononuclear one, and/or an increase in the appropriate Debye-Waller factor.

The largest changes observed were for Mo(IV) in basic solution. Both Fourier transform and curve-fitting analysis yielded a Mo-Mo amplitude of 1.5, as opposed to 2.0 for a symmetric trinuclear species. The best fit predicted a Mo-Mo distance of 2.545 Å, and Mo-O components at 1.96 and 2.10 Å. Clearly, a major structural change has occurred in basic solution, and one possibility would be some type of trinuclear ion in which a central Mo is oxo-bridged to two Mo neighbors. The stages between strong acid and strong base may represent intermediates in the breakup of the original triangular trimer.

Finally, the effects of the presence of halide ions on the spectrum were investigated by saturating the 4 M HMS Mo(IV) solutions with NaCl or NaBr (Figure 7). The chloride data could accommodate a Mo-Cl distance of 2.48 Å. However, no new peaks occurred in the Fourier transform, and an alternative explanation for the data would be a correlation with the Mo-Mo component. Because the Mo-Mo and Mo-Cl phase shifts are similar modulo 2, a better test was had with the Br⁻ ion. Again, no new peaks were observed in the Fourier transform, and the data were virtually identical to the original methanesulfonic acid sample.

Summary

This study has shown X-ray absorption spectroscopy to be a valuable tool for the elucidation of ionic structure in solution. Characterization of metal-ligand and metal-metal distances was straightforward with experimental phase shifts, and accuracy on the order of $\pm 0.012 \text{ \AA}$ is to be expected. This accuracy is less when unresolved EXAFS components have markedly different Debye-Waller factors.

Determination of coordination numbers and Debye-Waller factors, however, is complicated by the close correlation between these two quantities. Despite these difficulties, the calculated Debye-Waller factors for Mo-O and Mo-Mo interactions show reasonable systematic trends. For example, trinuclear Mo(IV) was shown to have the most rigid Mo-Mo distance ($\sigma = 0.031 \text{ \AA}$, followed by oxo-bridged Mo(V) (0.037 \AA), quadruply-bound Mo(II) (0.038 \AA), and hydroxo-bridged Mo(III) (0.044 \AA). Trends in the mean deviations of Mo-O distances were also as expected. The capacity for calculating Debye-Waller factors from experimental amplitude functions is clearly a significant improvement for EXAFS analysis.

The structural results are consistent with the known chemistry of molybdenum. Binuclear species dominate the aqueous chemistry of Mo(II), Mo(III), and Mo(V), whereas Mo(IV) in strong acid appears to be trinuclear. Some evidence for a lowering of symmetry in the latter species was observed at

higher pH values, but no clear evidence for halide coordination could be seen in strong acid solution. We expect that both the structural information and the improvements in analysis techniques obtained in this study should be useful for characterization of molybdenum in materials such as supported catalysts and amorphous materials.

Acknowledgment. Research at California Institute of Technology was supported by the National Science Foundation.

References

1. Ardon, M.; Pernick, A. J. Less Common Met. 1977, 54 233.
2. Chalilpoyil, P.; Anson, F. C. Inorg. Chem. 1978 17 2418.
3. Haight, G. P.; Sager, W. F. J. Am. Chem. Soc. 1952 74 6056.
4. Haight, G. P. J. Inorg. Nucl. Chem. 1962 24, 673.
5. Bergh, A. A.; Haight, G. P. Inorg. Chem. 1962 1 688.
6. Ardon, M.; Pernick, A. J. Am. Chem. Soc. 1973 95 6871.
7. Murmann, R. K. J. Am. Chem. Soc. 1980 102 3984.
8. Krumenacher, L.; Bye, R. J. Bull. Soc. Chim. Fr. 1968 3099 3103.
9. Ojo, J. Folorunso; Taylor, R. S.; Sykes, A. G. J. Chem. Soc. Dalton Trans. 1975 500.
10. Aveston, J.; Anacher, E. W.; Johnson, J. S. Inorg. Chem. 1964 3 755.
11. Simon, J. P.; Souchay, P. Bull. Soc. Chem. Fr. 1956 1402.

12. Lamache-Duhameaux, M. Rea. Chim. Minek. 1968 5 1001.
13. Viossat, B.; Lamache, M. Bull. Soc. Chim. Fr. 1975 1570.
14. Cotton, F. A.; Wilkinson, G. "Advanced Inorganic Chemistry", 3rd ed., Interscience: New York, 1972; pp. 944-972.
15. Cotton, R.; Rose, G. Aust. J. Chem. 1968 21 1883.
16. Jezowska-Trzebiatowska, B.; Rudolph, M. Rocs. Chem. 1967 41 453.
17. Ardon, M.; Pernick, A. Inorg. Chem. 1973 13 2484.
18. Bowen, A. R.; Taube, H. J. Am. Chem. Soc. 1971 93 3287.
19. Bowen, A. R.; Taube, H. Inorg. Chem. 1974 13 2245.
20. Someya, K. Z. Anorg. Allegem. Chem. 1928 175 349.
21. Hartman, H.; Schmidt, H. J. Z. Phys. Chem. (Frankfurt am Main) 1957 11 234.
22. Forster, F.; Fricke, E. Angew Chem. 1923 36 458.
23. Wandlaw, W.; Wormwell, R. L. J. Chem. Soc. 1927 1087.
24. Ardon, M.; Pernick, A. Inorg. Chem. 1974 13 2275.
25. Cramer, S. P.; Gray, H. B.; Dori, Z.; Bino, A. J. Am. Chem. Soc. 1979 101 2770.
26. Bowen, A. R.; Taube, H. Inorg. Chem. 1974 13 2245.
27. Pernick, A.; Ph.D. Thesis, Heb. U. of Jerusalem 1974.
28. Kolthoff, I. M. Vol. Analysis 1957 3 92.
29. Cramer, S. P.; Hodgson, K. O. Prog. Inorg. Chem. 1979 25 1.
30. Cramer, S. P.; Hodgson, K. O.; Stiefel, E. I.; Newton, W. E. J. Am. Chem. Soc. 1978 100 2748.

31. Bino, A.; Cotton, F. A.; Dori, Z. J. Am. Chem. Soc.
1978 100 5252.
32. Anilius, Z.; van Laar, B.; Rietveld, H. M. Acta Crys.
1969 B25 400.
33. Scane, J. G. Acta Crys. 1967 23 85.
34. Lee, P. A.; Beni, G. Phys. Rev. 1977 B15 2862.
35. Muller, A.; Nagarajan, G. Z. Naturforschg. 1966 21b 508.
36. Clark, R. J. H.; Franks, M. L. J. C. S. Chem. Comm. 1974
316.
37. James, R. W. Z. Phys. 1932 33 737.
38. Teo, B. K.; Lee, P. A. J. Am. Chem. Soc. 1979 101 2815.
39. Kutzler, F. W.; Natoli, C. R.; Miesmer, D. K.; Doniach,
S.; Hodgson, K. O. J. Chem. Phys.
40. Krause, M. O.; Oliver, J. H. J. Phys. Chem. Ref. Data
1979 8 329.
41. Cramer, S. P.; Hodgson, K. O.; Gillum, W. O.; Mortensen,
L. E. J. Am. Chem. Soc. 1978 100 3398.
42. Sayers, D. E.; Stern, E. A.; Lytle, F. W. Phys. Rev.
Lett. 1971 27 1204.
43. Lawton, D.; Mason, R. J. Am. Chem. Soc. 1965 87 921.
44. Angell, C. L.; Cotton, F. A.; Frenz, B. A.; Webb, T. R.
J. Chem. Commun. 1973 339.
45. Kreale, G. G.; Geddes, A. J.; Sasaki, Y.; Shibahara, T.;
Sykes, A. G. J. C. S. Chem. Comm. 1975 356.
46. Stiefel, E. I. Prog. Inorg. Chem. 1976 22 1.
47. Brandt, B. G.; Skapslci Acta Chem. Scand. 1967 21 661.

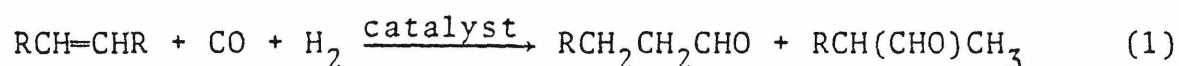
48. Chisholm, M. H.; Cotton, F. A.; Extine, M. W.; Riechert, W. W. Inorg. Chem. 1978 17 2944.
49. Bino, A.; Cotton, F. A.; Dori, Z. J. Am. Chem. Soc. 1979 79 3842.

Chapter 3

Photochemical Hydroformylation Using
Trirutheniumdodecacarbonyl as a
Homogeneous and a Heterogeneous Catalyst

Abstract: $\text{Ru}_3(\text{CO})_{12}$ reacts photochemically in the presence of olefins, CO, and H_2 to catalyze the hydroformylation reaction. Typical yields are 1.5×10^{-3} moles of aldehydes in a 2:1 linear to branched chain ratio. A heterogeneous catalyst can also be effected by photoinduced fragmentation of the cluster in the presence of polyvinyl-4-pyridine. Attachment of a Ru-CO moiety was confirmed by IR and elemental analysis. The first step in catalyst activation was shown to be formation of $\text{Ru}(\text{CO})_4$ olefin with a quantum yield of 0.03 for 1-pentene. Subsequent steps involved formation of a hydrido-olefin complex, rearrangement to a hydrido-alkyl, "CO insertion," and reductive elimination of an aldehyde. Olefin isomerization and alkane production are also seen under reaction conditions. Formation of larger ruthenium carbonyl clusters led to catalyst deactivation. Photolysis of $\text{Ru}_3(\text{CO})_{12}$ in the presence of H_2 led to the formation of $\alpha\text{-H}_4\text{Ru}_4(\text{CO})_{12}$. This molecule can also effect catalysis of the hydroformylation reaction, although yields are an order of magnitude less than for the parent cluster. Photolysis of $\text{Ru}_3(\text{CO})_{12}$ in the presence of various substrates showed formation of $\text{Ru}(\text{CO})_4\text{L}$ as the initial product. No spectroscopic evidence for an intermediate substituted cluster is seen. This can be ascribed to the electronic excited state being a $\sigma \rightarrow \sigma^*$ (metal-metal bonding to metal-metal antibonding) transition. Population of this state should lead to metal-metal bond cleavage and fragmentation.

Since its discovery in 1938,¹ the oxo reaction has become a major industrial process resulting in the production of over five billion pounds of chemicals in 1969.² The reaction is so named as it yields oxygenated products from hydrocarbons: the elements of formaldehyde (H-CHO) are added across the double bond of an olefin. Catalysis has been affected by a variety of metal carbonyls and other complexes, such as cobalt,³ rhodium,⁴ iron,⁴ and manganese⁵ carbonyls, bis(triphenylphosphine)ruthenium(II),⁶ bis(triphenylphosphine)rhodium(I)^{7,8} and hydridocarbonyltris(triphenylphosphine)rhodium(I).^{9,10} Schematically, the reaction may be represented as in equation (1)

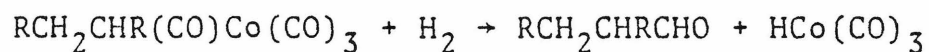
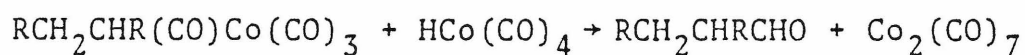
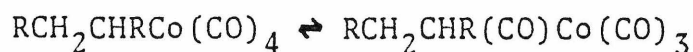
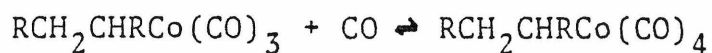
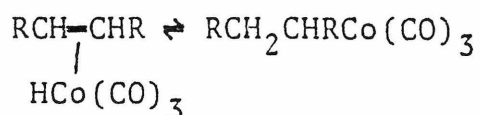
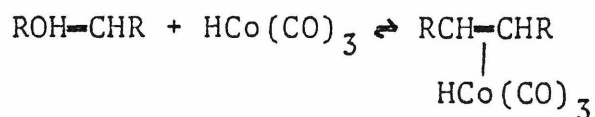
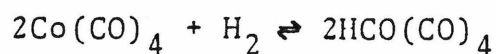


The primary and especially the secondary reaction products (aldehydes and alcohols, respectively) have invaluable industrial applications.¹¹ The lion's share of production capacity is directed toward the synthesis of C₈, C₁₀, and C₁₃ alcohols important to plasticizers, lubricants, and detergents.¹² The formation of long chain monoaldehydes¹³ and dialdehydes¹⁴ also have extensive industrial applications. Thus, the process is both commercially important and academically interesting.

The raw materials for the reaction are readily and economically available,^{15,16} however, reaction conditions are severe (100°-200°C, 200-400 atmospheres). If it were

possible to generate active catalysts at lower temperatures and pressures, considerable savings in valuable fuel sources could be effected. Realizations of this sort could be made by the development of efficient photochemically induced catalysts bound to a polymeric support. Harnessing solar energy has obvious economic benefits, and "heterogenizing" homogeneous catalysts optimizes the best features of the homogeneous species (e.g., increased selectivity, mild reaction conditions, well defined active sites, and variable steric and electronic control at the metal site)¹⁷ while eliminating the undesirable aspects (e.g., reactor corrosion, difficulty of product separation, and catalyst destruction pathways).¹⁸ In addition further benefits might be derived from increases in substrate size selectivity,¹⁹ catalytic activity,^{20,21} protection from water,^{22,23} and generation of catalysts inoperative homogeneously.²⁴

Concomitant to the synthesis and study of a polymerically bound catalyst, an elucidation of the primary processes operative in the homogeneous catalytic system should be made. Although hydroformylation has been studied extensively since its discovery, the details of the reaction have yet to be unequivocally determined. The most thoroughly investigated system is that of $\text{Co}_2(\text{CO})_8$ for which Heck and Breslow postulate the following mechanism:^{25,26}



Although this reaction scheme empirically accounts for all observations, concrete evidence in the form of isolable intermediates has proven elusive. Similarly, a study of the photochemically induced hydroformylation by Frazier²⁴ netted no real insight into the mechanics of this analogous reaction, and complications due to air sensitivity and catalyst deactivation by tetramer formation were prohibitive. Therefore, further research on this system seemed fruitless, and attention was turned to other metal carbonyls. In particular, the generation of multiple low valent reactive species from the decomposition of metal carbonyl cluster compounds seemed promising. For these reasons and the fact that it is a known thermal oxo catalyst,²⁷⁻²⁹ the study of the photo-catalytic homogeneous and heterogeneous

hydroformylation properties of $\text{Ru}_3(\text{CO})_{12}$ was instigated.

Experimental Section

$\text{Ru}_3(\text{CO})_{12}$ was purchased from ROC-RIC and recrystallized from toluene. Freeze dried polyvinyl-4-pyridine was prepared by Dr. Alan Rembaum of the Jet Propulsion Laboratory. All substituted silanes were purchased from PCR Chemicals, aldehydes from Aldrich, 99.5 atom % pure, and triphenyl phosphine from MCB. Carbon monoxide, hydrogen, and ethylene, 99% purity, were obtained from Matheson Gas Products. Spectroquality solvents from MCB Chemical Company and olefins from Chemical Samples were dried by standard procedures.³⁰ Deuterated benzene used for NMR experiments was from Aldrich, 99.5 atom % pure. Analyses of photoproducts were performed by Galbraeth Laboratories, Inc., Knoxville, Tennessee.

Electronic absorption spectra and spectral changes were recorded with a Cary 17 spectrophotometer; quantum yield data on a Beckman IR-12 spectrometer. Infrared spectra were recorded on a Perkin-Elmer 225 instrument. NMR measurements were made on Varian T-60, A-60A, and 220 nuclear magnetic resonance spectrometers. Aldehyde production was measured on a Hewlett-Packard 5750 gas chromatograph with a flame detector using a 20' x 1/8" 25% STAP column (60°). Olefins and alkanes were measured with a 25' β, β' ODPN on carbowax column at 40° on a Perkin-Elmer 3920 gas chromatograph.

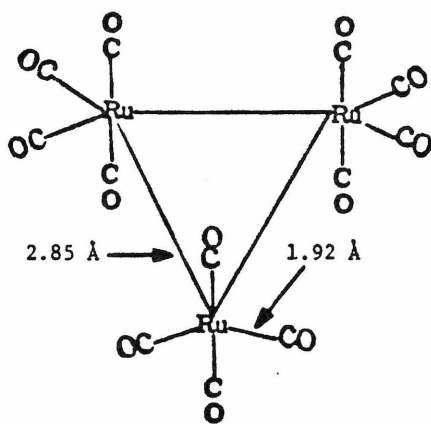
Light sources for photolyses (200, 250, and 1,000 watt Hg-Xe lamps) were used in conjunction with Corning cut-off filters to obtain the desired wavelength. Samples were cooled either with a compressed air stream or a constant temperature bath. Ferrioxalate actinometry³¹⁻³³ was used for quantum yield determinations. The procedure was modified to adopt the precautions of Bowman and Demas.³⁴ The quantum yields for reactions of $\text{Ru}_3(\text{CO})_{12}$ with various substrates was determined by monitoring the disappearance of the 390 band. Typical photon flux was 1.03×10^{-6} Einsteins/minute at 366 nm.

Photolyses were conducted in two-arm evacuable quartz cells with a spectrophotometer cell and a Kontes quick release valve. For experiments with gaseous reagents a calibrated volume was added to act as a gas reservoir so measured pressures of gases could be added. For batch homogeneous and heterogeneous hydroformylation experiments, one atmosphere of synthesis gas was reacted; the relative amounts of H_2 and CO were varied to study gas ratio dependencies. Typical ratios were 80:20 H_2 :CO. Pentenes were dried separately over lithium aluminum hydride and vacuum transferred into the cell. A thousandfold excess of pentene, i.e., $[\text{pentene}] = 1 \text{ M}$, $[\text{Ru}_3(\text{CO})_{12}] = 10^{-3} \text{ M}$ was used for homogeneous reactions. For heterogeneous experiments, ca. 100 mgs of freeze-dried polyvinyl-4-pyridine was pumped-on and heated for at least one hour prior to reaction to remove air and water. Experiments

with variously substituted silanes, i.e., Me_3SiH , Me_3SiCl , Et_3SiH , Ph_3SiH , and Cl_3SiH were done with 1:1 $\text{R}_3\text{SiH}:\text{Ru}$ ratios.

Results and Discussion

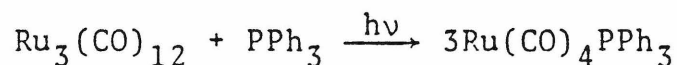
Trirutheniumdodecacarbonyl $\text{Ru}_3(\text{CO})_{12}$ was first prepared by Heiber and Fischer.³⁵ Although a crystal structure has not been done for this complex, Corey and Dahl³⁶⁻³⁸ have shown that it is isomorphous to the osmium analogue $\text{Os}(\text{CO})_{12}$ and that the latter has approximately D_{3h} molecular symmetry in the crystalline state. The triangular cluster is held together by metal metal bonds only, all carbonyl groups are terminal as confirmed by mass spectral data:³⁹⁻⁴²



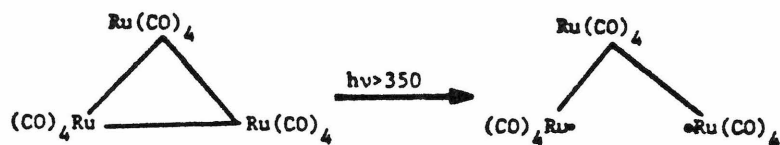
Two of the carbonyls attached to each metal are essentially in the plane of the metal atoms, the other two are perpendicular. The mean bond lengths are 2.85 Å between the metal

atoms, 1.92 Å for the Ru-C bond, and 1.15 Å for C-O.⁴³

The electronic spectrum (Figure 1) has been measured and the lowest energy absorption (391 nm) has been ascribed to metal-metal interactions.⁴⁴ A calculation of the electronic structure by Tyler has confirmed this to be a metal localized transition from a sigma bonding to a sigma antibonding orbital, as indicated in the MO scheme in Figure 2.⁴⁵ Depopulation of the bonding level results in cluster fragmentation as is the case for the photochemical bond scission in dimeric species.⁴⁶ The thermally inert Ru-Ru bond⁴⁷ undergoes facile cleavage upon photoexcitation, yielding the coordinately unsaturated Ru(CO)₄ moiety evidence by reactions of the type below:⁴⁸



If analogous to the dimeric systems, initial cleavage of the triangle would result in a metal diradical $\dot{\text{Ru}}(\text{CO})_4$, which would undergo further fragmentation as shown below. While



little evidence existed for this mechanism in Ru₃(CO)₁₂

142

Figure 1

The electronic spectra of $\text{Ru}_3(\text{CO})_{12}$ in 2-methylpentane
at 300 and 77°K.

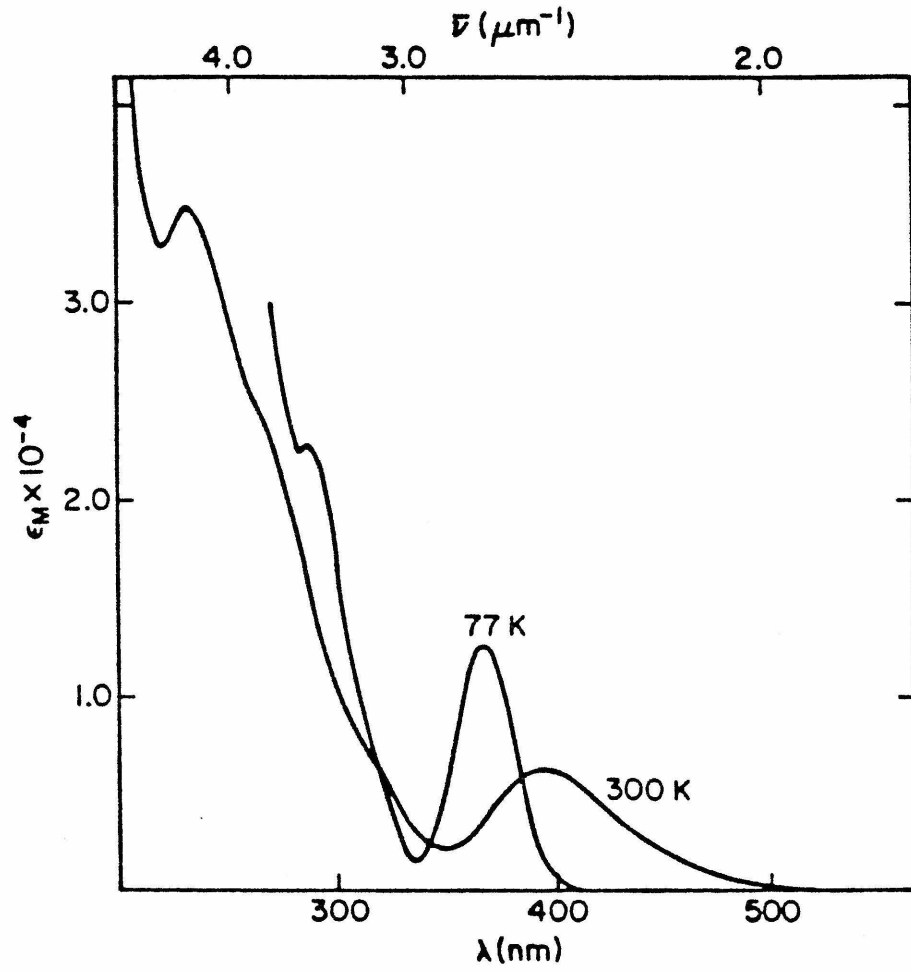
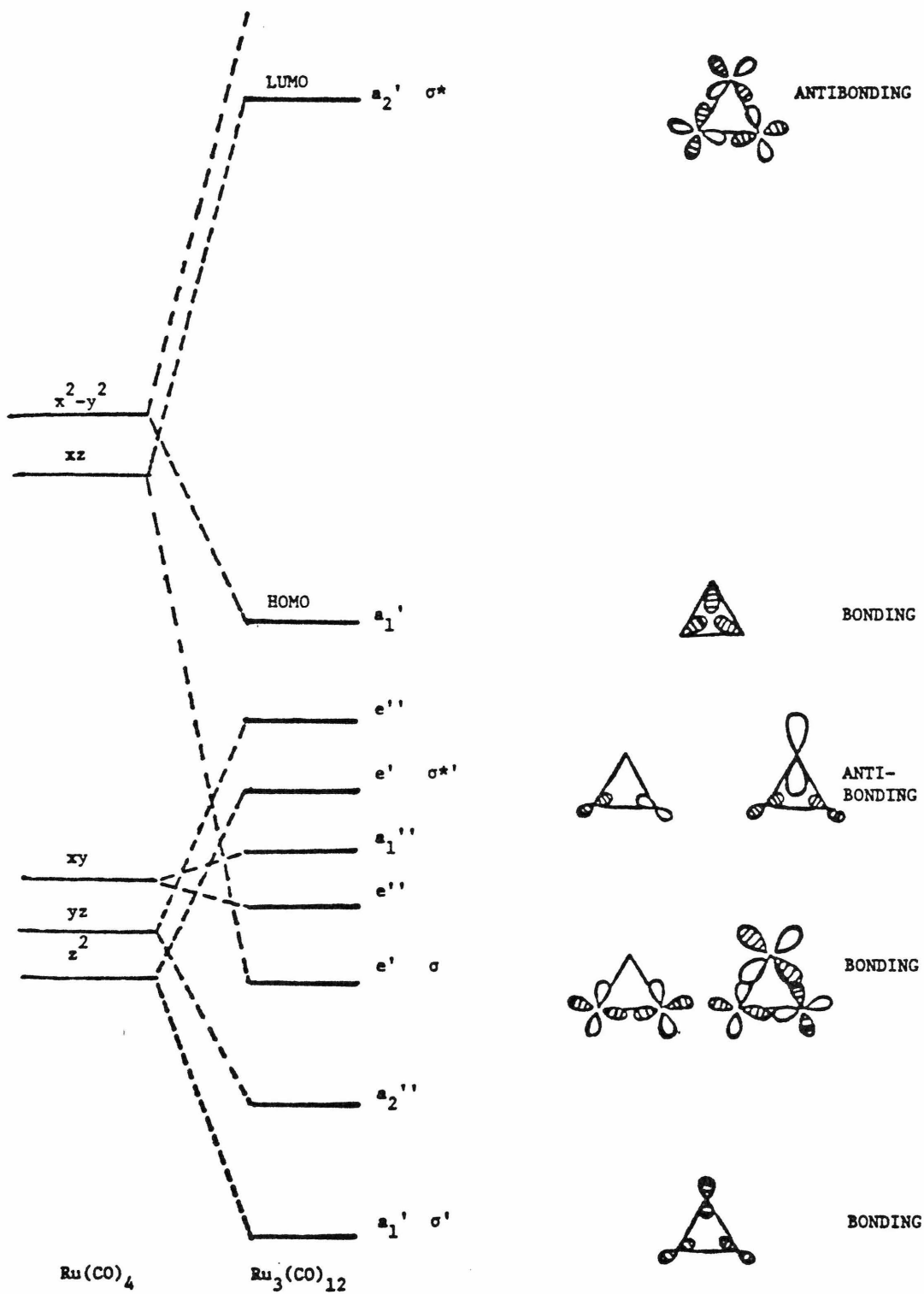


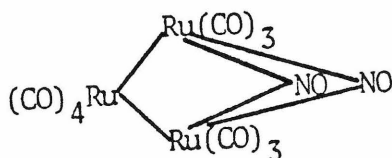
Figure 2

MO scheme for $\text{Ru}_3(\text{CO})_{12}$ showing the principal bonding and antibonding orbitals.



the reaction of $\text{Os}(\text{CO})_{12}$ with halogens give rise to the linear compounds $\text{Os}_3(\text{CO})_{12}\text{X}_2$.⁴⁹ In contrast, the corresponding reaction with the ruthenium triangle yields predominantly $\text{Ru}_3(\text{CO})_{12}\text{X}_6$,⁵⁰ although the nature and distribution of products is dependent upon the experimental conditions. The compounds $\text{Ru}(\text{CO})_4\text{X}_2$, $\text{Ru}_2(\text{CO})_6\text{X}_4$, and/or $\text{Ru}_3(\text{CO})_{12}\text{X}_6$ may be formed, but $\text{Ru}(\text{CO})_4\text{X}_2$ is the initial, identifiable species in each case. Several other reactions result in dimeric complexes,^{51,52} but these may again be due to recombination of monomers as in the halogen reaction. In no instance has the 1,3-disubstituted trimer been reported.

To elucidate the mechanism for declusterification, an experiment was performed in an attempt to trap 1 with nitric oxide. A novel nitrosyl substituted carbonyl cluster has been reported by the thermal reaction of $\text{Ru}_3(\text{CO})_{12}$ and NO :⁵³⁻⁵⁵



It was hoped that formation of this substituted cluster would be seen if photolysis under NO induced formation of 1. Irradiation into the 390 nm band ($\sigma\text{-}\sigma^*$ Ru-Ru transition) resulted in the disappearance of $\text{Ru}_3(\text{CO})_{12}$ and appearance,

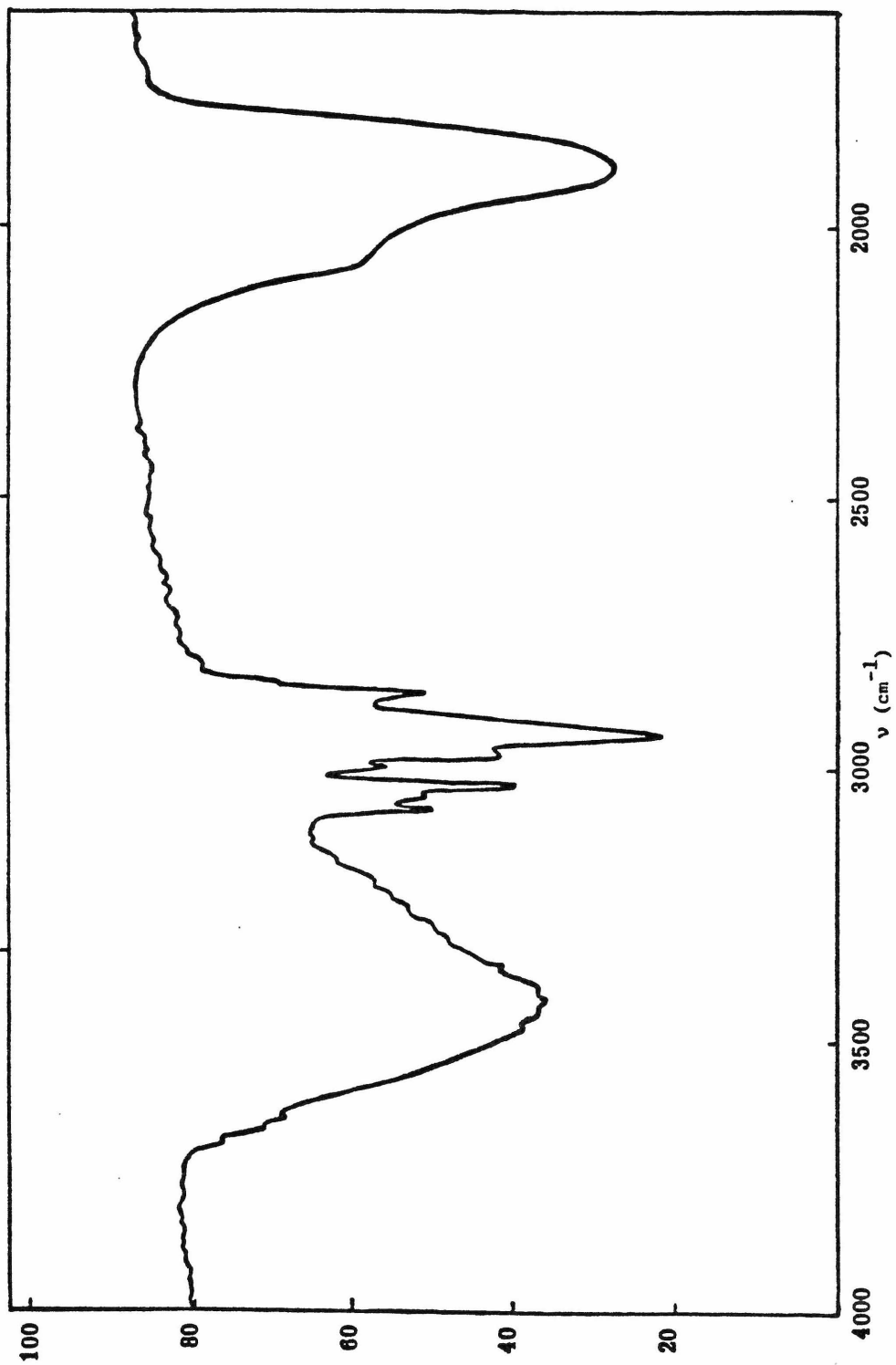
initially, of a species that absorbed at higher wavelengths. This is consistent with the formation of a nitrosyl complex, although it was not possible to determine whether $\text{Ru}_3(\text{CO})_{10}(\text{NO})_2$ or one of the known polymeric species⁵⁵ or some new complex was formed. Whatever its identity, the product began absorbing light at low concentrations and quickly decomposed. It was not possible, therefore, to obtain spectral evidence for product identification and thereby support for the proposed $\text{Ru}_3(\text{CO})_{12}$ fragmentation mechanism.

To determine if the photo-induced unsaturated ruthenium-carbonyl species might act as an oxo catalyst, a solution of $\text{Ru}_3(\text{CO})_{12}$, polyvinyl-4-pyridine (PV-4-P) and 1-pentene was irradiated in the presence of synthesis gas. Hydroformylation of the olefin was observed, with aldehydes being formed in a 2:1 (linear to branched chain) ratio. Typical yields were between the order of 5×10^{-5} and 1×10^{-3} moles total production, a turnover of between 100 and 5. Control experiments carried out in the absence of light resulted in no yield, indicating that the process is, indeed, a photocatalytic phenomenon. Another set of control experiments was run in the presence and absence of polymeric support; total aldehyde production was almost an order of magnitude greater for the former. That a true heterogeneous catalyst existed was confirmed by IR analysis of the reacted polymer. The spectrum in Figure 3 shows a broad absorption in the

Figure 3

IR spectrum of polyvinyl-4-pyridine reacted with $\text{Ru}_3(\text{CO})_{12}$.

Transmittance (%)



metal-carbonyl region, indicative of the attachment of a Ru-CO moiety. Unfortunately, the lack of spectral resolution precludes any structural determination. Elemental analysis showed 1% ruthenium/polymer by weight.

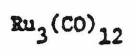
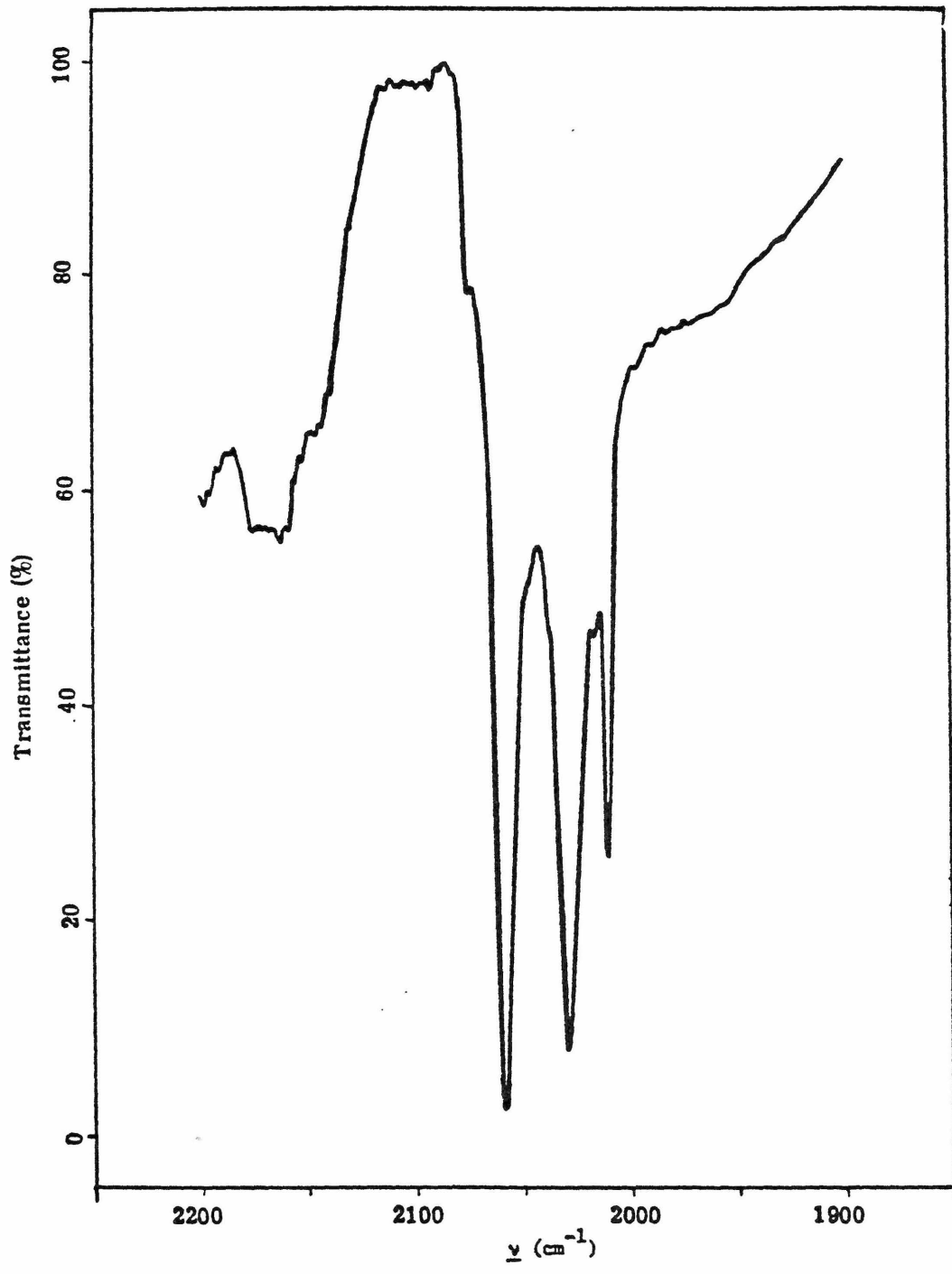
To complete characterization of the polymer system, a concomitant investigation of the homogeneous reaction was begun. An understanding of this mechanism would, hopefully, elucidate behavior of the heterogeneous system where low concentrations of the active species make spectral evaluation and identification impossible. Preliminary investigations were begun on the photochemistry of $\text{Ru}_3(\text{CO})_{12}$ and pyridine and the methyl-substituted pyridine derivatives (2- and 4- picoline). These substrates served as good models for the polymer, and attachment of the ruthenium-carbonyl moiety to PV-4-P was thought to be the initial step in catalyst formation. This supposition, however, was proven erroneous by a subsequent heterogeneous experiment: $\text{Ru}_3(\text{CO})_{12}$ solutions were irradiated in the presence of polyvinylpyridine and the reacted polymer was washed and isolated. Subsequently, the polymer was reacted with 1-pentene and synthesis gas (both thermally and photochemically), but there was no aldehyde formation. Obviously, then, polymeric attachment was not the primary step in the catalytic process. However, when $\text{Ru}_3(\text{CO})_{12}$ solutions were irradiated in the presence of PV-4-P and 1-pentene, the polymer isolated and reacted with olefin, H_2 , and CO, aldehydes were formed in a

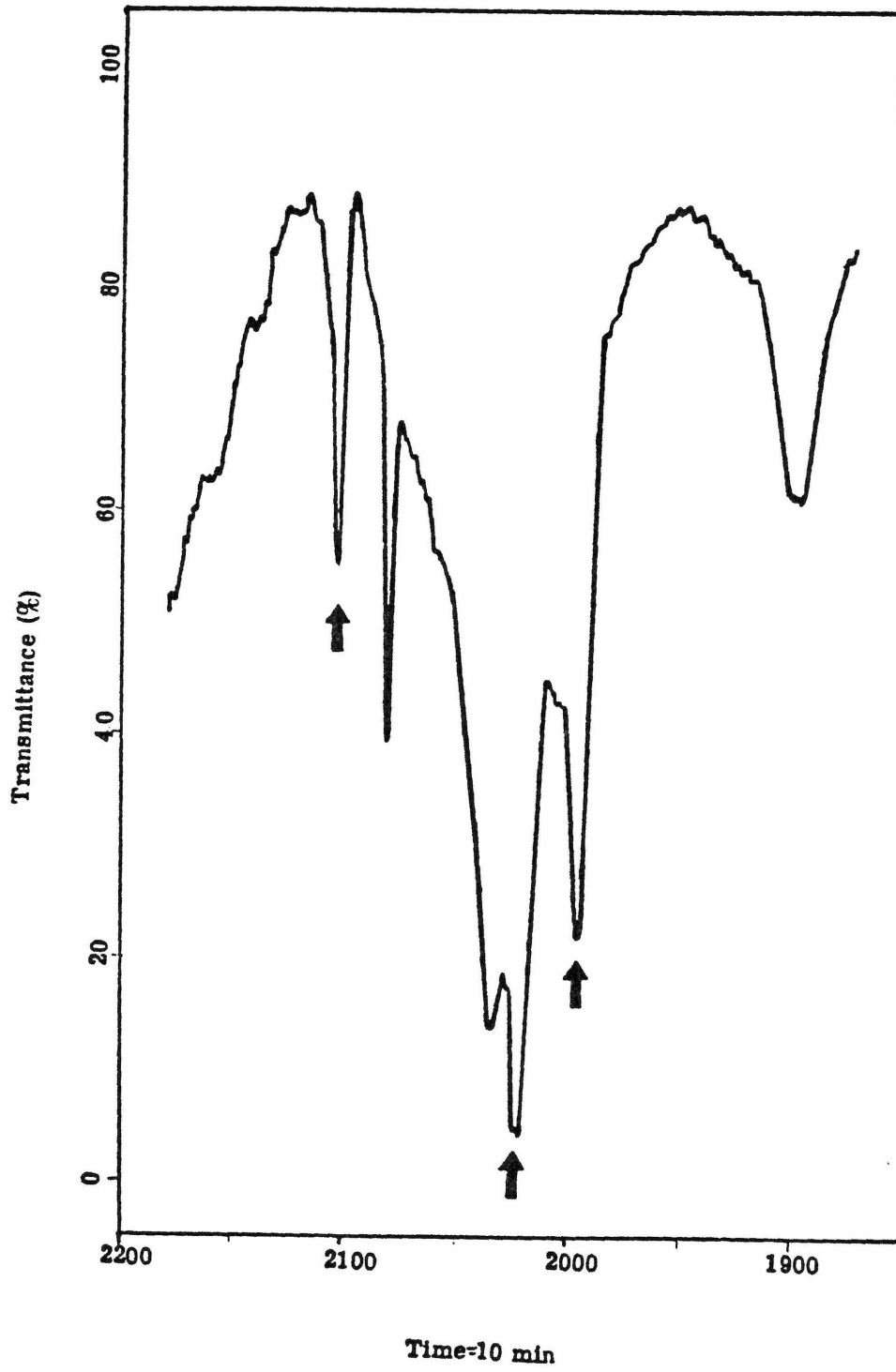
2:1 (linear to branched chain) ratio. Total yields after 18 hours thermal reaction were comparable to those of initial reactions run in the presence of all elements of the heterogeneous system.

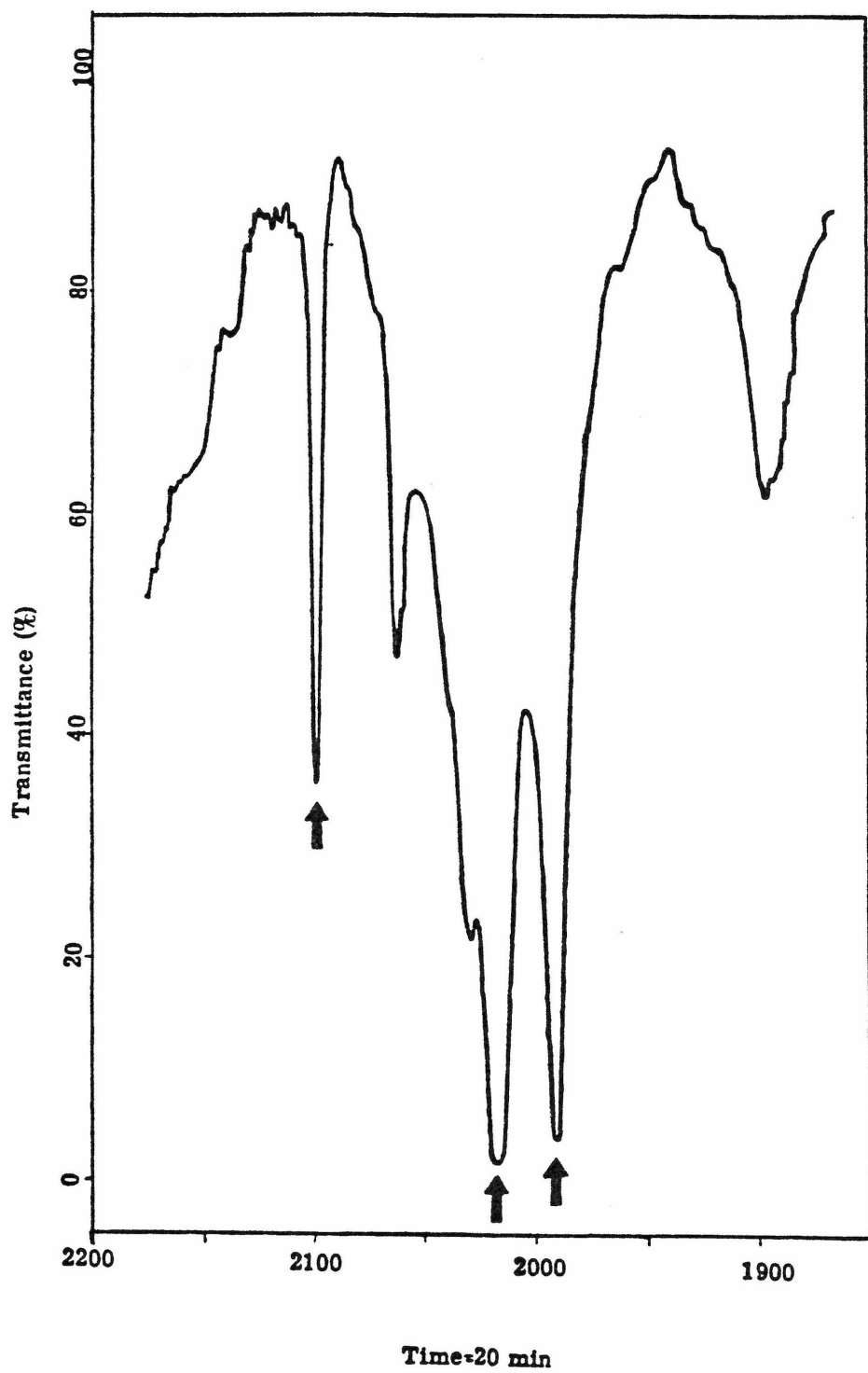
It is obvious from these results that the reaction of $\text{Ru}_3(\text{CO})_{12}$ with 1-pentene is critical to formation of a catalytically active species. Therefore, a photochemical investigation of this reaction was begun. Solutions of the trimer and olefin were irradiated at wavelengths greater than 355 nm and followed by UV-VIS and IR spectra as a function of time (Figure 4). Photolysis resulted in the formation of a single product, $\text{Ru}(\text{CO})_4\text{pentene}$, as evidence by comparison of the IR spectrum with those for $\text{Ru}(\text{CO})_4\text{ethylene}$ ³⁴ and $\text{Fe}(\text{CO})_4\text{pentene}$.⁵⁶ Upon addition of PPh_3 to the $\text{Ru}(\text{CO})_4\text{pentene}$ solution, a displacement reaction occurred yielding $\text{Ru}(\text{CO})_4\text{PPh}_3$ and also some $\text{Ru}_3(\text{CO})_9(\text{PPh}_3)_3$. Since there was no evidence for $\text{Ru}_3(\text{CO})_9(\text{pentene})_3$, the $\text{Ru}_3(\text{CO})_{12}(\text{PPh}_3)_3$ might have been formed due to increased CO lability and pentene loss. Another possible explanation is substitution on the bis-olefin complex postulated to be present in $\text{Fe}(\text{CO})_4$ olefin systems (see the mechanism for isomerization). A reaction scheme such as that below could account for the formation of the substituted triangle from the bis-olefin:

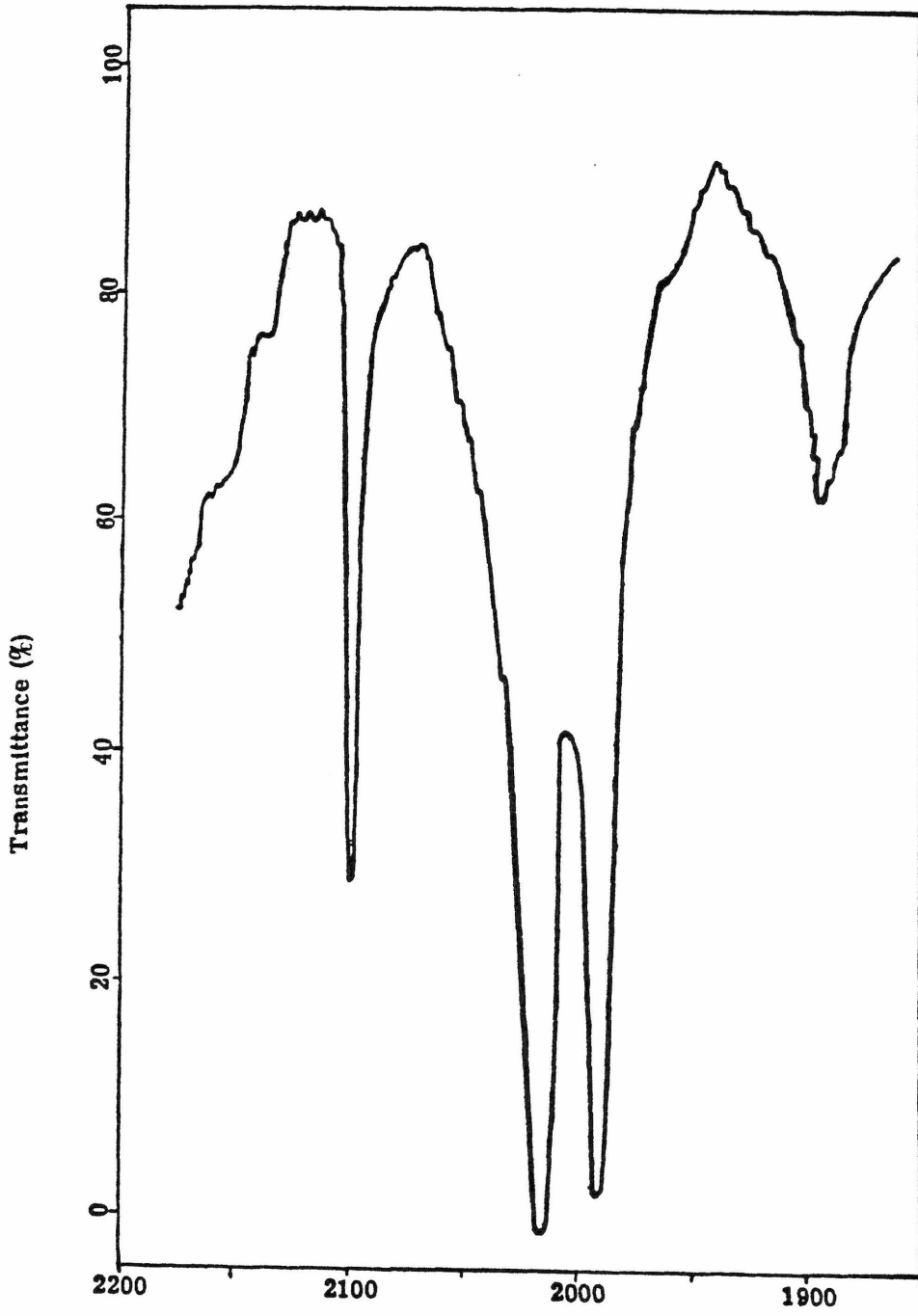
Figure 4

IR spectra as function of time for the photochemical
reaction of $\text{Ru}_3(\text{CO})_{12}$ and 1-pentene to form
 $\text{Ru}(\text{CO})_4$ pentene.

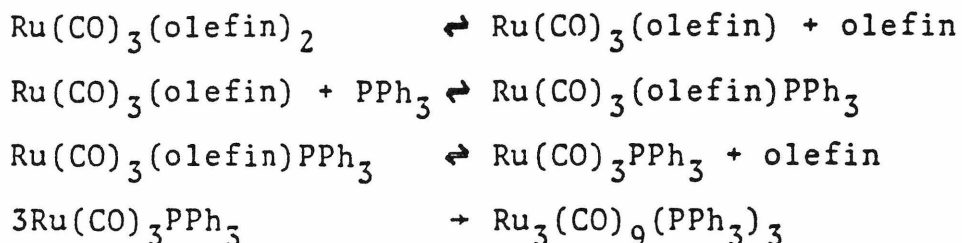




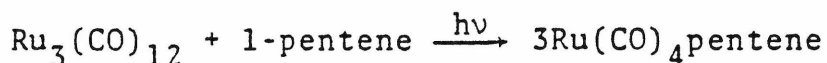




Time 30 min
 $\text{Ru(CO)}_4 \cdot \text{pentene}$



The coordinated olefin is obviously quite labile, and the reaction



is an equilibrium driven to the right photochemically. Cessation of irradiation results in the reappearance of the pale yellow color indicative of the triangle and bands for such in the IR. Similarly, removal of excess pentene drives the reaction back to the left, and one can isolate only $\text{Ru}_3(\text{CO})_{12}$ from such an endeavor. This type of substituted-monomer-trimer equilibrium has been seen in other $\text{Ru}_3(\text{CO})_2$ substrate reactions.⁴⁹

Because of the equilibrium conditions, it was not possible to obtain NMR evidence for pentene coordination--interference by the excess olefin necessarily present obscured other signals in this region. All NMR experiments were further plagued by concentration problems: the low solubility of $\text{Ru}_3(\text{CO})_{12}$ (ca. 10^{-3} M for any solvent) and the competing reaction to form larger metal clusters for photochemical reactions at maximum concentrations. In hopes of attaining greater yields of the mono-olefin species, synthesis was planned via the pentacarbonyl Ru(CO)_5 .

Unfortunately, irradiation of solutions with excess $\text{Ru}_3(\text{CO})_{12}$ under CO resulted not only in the formation of $\text{Ru}(\text{CO})_5$ but also a larger, unidentifiable metal cluster. Thus, this route had no advantage over that of direct triangle fragmentation and substitution.

Using $\text{Ru}_3(\text{CO})_{12}$ with ethylene as the substrate, it was possible to verify olefin coordination and to determine the chemical shift (8.2τ) for this complex (Figure 5). This is consistent with reported changes in NMR resonances for metal-coordinated species.⁵⁷⁻⁶⁰ The larger values of τ indicate greater electron density on the olefin π orbitals resulting in increased magnetic shielding. This is in accordance with the popular model proposed by Dewar⁶¹ and Chatt and Duncanson⁶² for olefin-metal bonding. This model (Figure 6) involves formation of a σ bond by donation of π electrons to the metal atom and a π bond by back donation from the d orbitals of the metal to olefin π^* orbital.

Coordination and subsequent olefin displacement are evidenced by conversion of the 1-pentene initially present to its isomers. That this is truly a photocatalytic phenomenon is indicated by the continued substrate interactions after cessation of irradiation. Table III shows the relative percentages of 1-pentene, trans-2-pentene, and cis-2-pentene subsequent to irradiation as a function of time. After one hour in the dark the equilibrium value found for the pentenes is essentially that of the expected

Figure 5

NMR spectrum of the photochemical reaction of $\text{Ru}_3(\text{CO})_{12}$
and ethylene to form $\text{Ru}(\text{CO})_4$ ethylene.

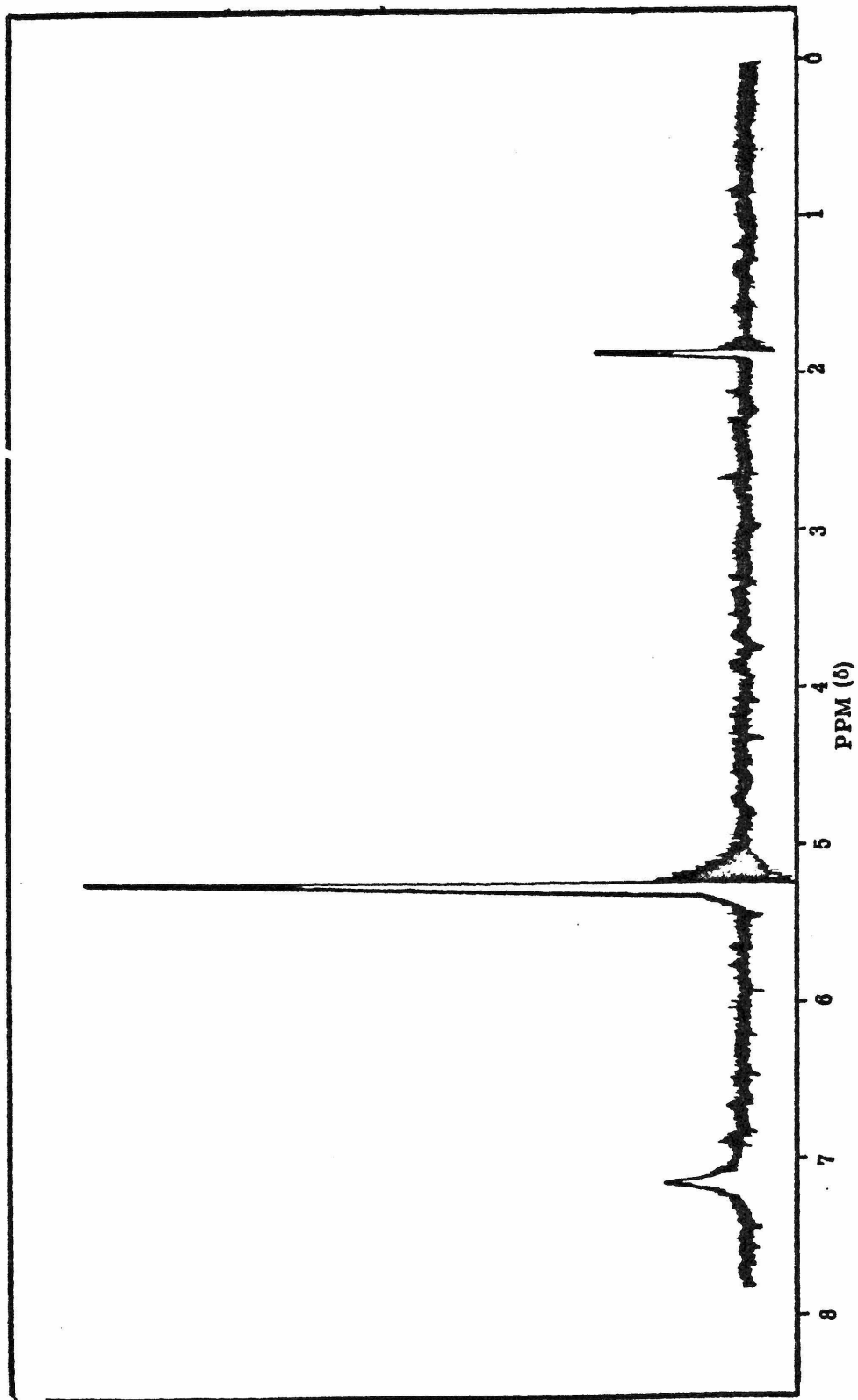


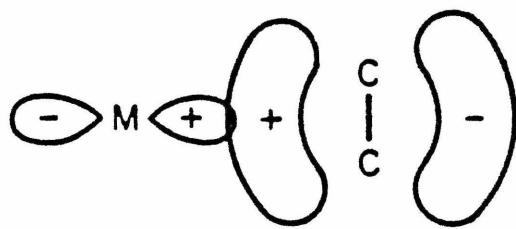
Figure 6

The Dewar-Chatt Duncanson model for olefin metal bonding.

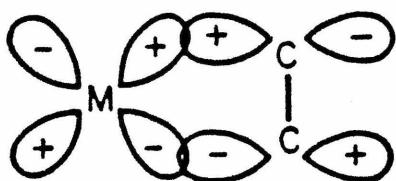
A) Sigma forward bonds.

B) Pi back bonds.

THE DEWAR AND CHATT AND DUNCANSON
MODEL FOR METAL-OLEFIN BONDING



$\underline{\sigma}$ -bond



$\underline{\pi}$ -bond

thermodynamic ratio.⁶³ After four hours, the photocatalyst has converted the pentenes past the point of equilibrium, which is reattained thermally after catalyst deactivation.

Although $\text{Ru}_3(\text{CO})_{12}$ is known to thermally isomerize 1-pentene,⁶⁴ it is doubtful that the same species is responsible for the photochemical process. Data from the thermal reaction indicate that dissociation of the Ru-CO bond is the rate-determining step, and other evidence indicates the reactive species is a substituted triangle. Since a monomeric species is generated photochemically, this catalyst is more likely analogous to the iron-pentacarbonyl system,⁶⁵ although less efficient. After 30 minutes irradiation, catalysis by $\text{Fe}(\text{CO})_5$ results in 70% conversion of 1-pentene, while the figure is less than 54% for the ruthenium complex. The greater reactivity of $\text{Fe}(\text{CO})_5$ has also been confirmed by a comparison in quantum yields for the initial formation of $\text{M}(\text{CO})_4$ pentene, with $\phi = .05$ for $\text{Fe}(\text{CO})_5$ ⁶⁶ and $\phi = .03$ for $\text{Ru}_3(\text{CO})_{12}$.

For the subsequent isomerization step, Wrighton has proposed the following mechanism for the $\text{Fe}(\text{CO})_5$ system:⁶⁵

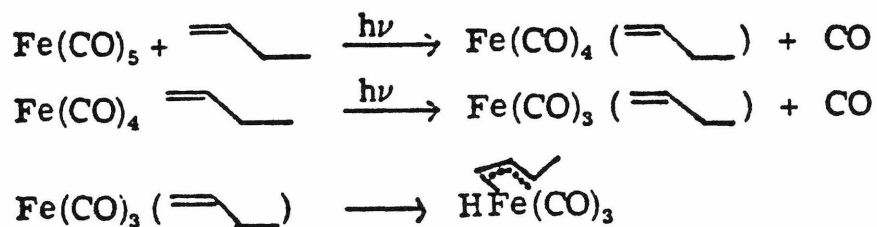
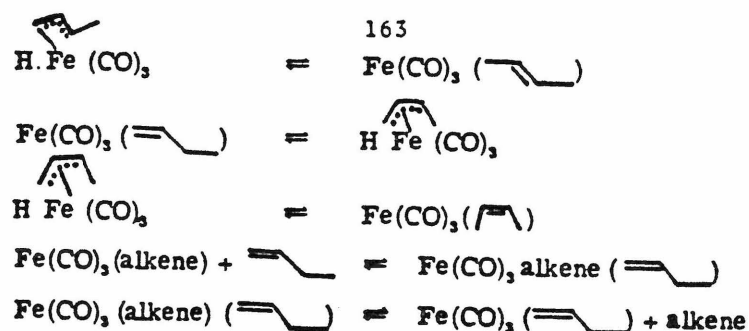


Table 1. Relative Percentages for the Isomerization of
1-Pentene after Cessation of Irradiation (time=
minutes)

Time	%1-Pentene	% <u>trans</u> -2-Pentene	% <u>cis</u> -2-Pentene
5	46	40	14
10	43	50	17
15	15	67	18
30	8	73	19
60	3	79	19
90	3	78	19
120	4	78	18
240	1	80	19
1250	2	80	18
1810	4.5	78	18
3700	3	79.5	18

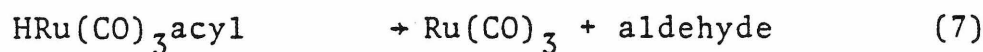
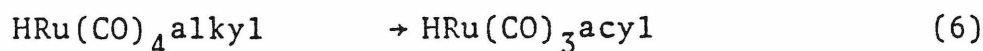
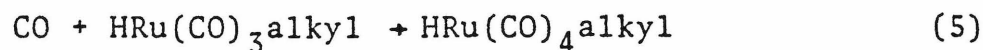
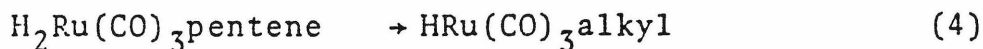
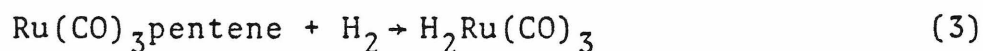
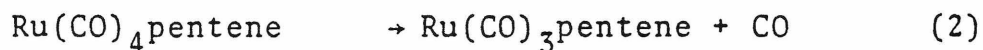


The available data indicate that this mechanism is also operative in the ruthenium system with generation of π -allylic and bis-olefin substituted intermediates. Numerous reports of the former have been described in the literature. For example, RuCl_3 reacts with 1,3-butadiene^{67,68} to give dichloro-(dodeca-2,6,10-triene-1,12-diyl)ruthenium and with isoprene to give $\text{RuCl}_2(\text{C}_{10}\text{H}_{16})$, a bridged chloro-complex containing the 2,7-dimethylocta-2,6-diene-1,8-diyl ligand coordinated onto ruthenium.⁶⁹ The reactions of $\text{Ru}_3(\text{CO})_{12}$ with allylic halides⁷⁰ or Grignard reagents also result in stable π -allylic complexes.⁷¹ A π -allylic-hydrido-Ru complex would be expected to be quite reactive and, therefore, reversible due to the well documented instability of monomeric ruthenium carbonyl hydride.⁷²

Unfortunately, direct evidence for a bis-olefin intermediate is nonexistent--although its formation is consistent with all the facts. Infrared analysis of the $\text{Ru}_3(\text{CO})_{12}$ and olefin reaction indicates the formation of $\text{Ru}(\text{CO})_4$ olefin

as the sole photoproduct; however, the analogous reaction using PPh_3 as the substrate produced a mixture of monomers: $\text{Ru}(\text{CO})_4\text{PPh}_3$ and $\text{Ru}(\text{CO})_3(\text{PPh}_3)_2$. The fact that no $\text{Ru}(\text{CO})_3(\text{olefin})_2$ is observed here or has been reported may be explained by the facility of olefin exchange. That numerous stable complexes are formed between the tricarbonyl and dienes⁷³⁻⁷⁶ indicates that a bis-olefin species should be possible.

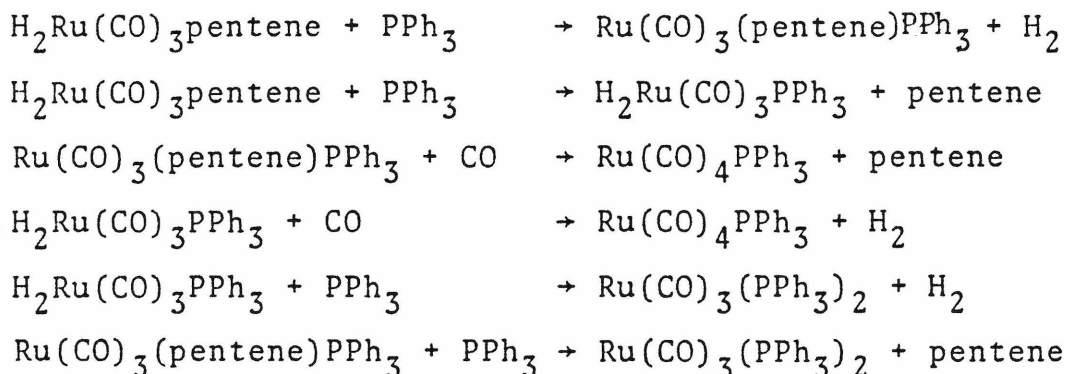
Upon identification of the $\text{Ru}(\text{CO})_4$ pentene complex, further experimentation was directed toward the determination of subsequent steps in the pathway to hydroformylation. Solutions of $\text{Ru}(\text{CO})_4$ pentene were prepared photochemically and allowed to react thermally with synthesis gas. Aldehydes were formed in a 2:1 (linear to branched chain) ratio with a total yield of 1.5×10^{-3} moles. Analogous experiments done in the absence of CO resulted not only in aldehyde formation but in even greater yields. Thus, it seemed the addition of CO inhibited hydroformylation by competing for a vacant coordination site. This could be explained by the scheme below:



Examples of σ -alkyl^{77,78} and σ -acyl⁷⁹ monomeric ruthenium complexes may be found in the literature and "CO insertion" is a common phenomenon for transition metal-alkyl-carbonyl complexes. Step 5 of the reaction scheme would seem to indicate that reductive elimination to form the alkane is possible, and this is indeed the case. Up to 20% pentene to pentane conversion has been observed under typical reaction conditions.⁸⁰ While being a deleterious route alternate to hydroformylation, this alkane production does substantiate the mechanism outlined above. After aldehyde (or alkane) extrusion, the $\text{Ru}(\text{CO})_3$ fragments react with each other and excess H_2 to yield larger hydride clusters. The IR analysis is inconclusive as to whether $\beta\text{-H}_4\text{Ru}_4(\text{CO})_{12}$ or $\text{H}_2\text{Ru}_4(\text{CO})_{13}$ is the product, and elemental analyses are complicated by the presence of some $\text{Ru}_3(\text{CO})_{12}$.

Attempts to isolate or obtain spectral evidence for the proposed hydride, $\text{H}_2\text{Ru}(\text{CO})_3\text{pentene}$, proved fruitless. The reaction to form aldehydes is extremely rapid, even at low temperatures, as evidenced by immediate changes in the IR upon H_2 addition. The concentration of the transient hydride, therefore, is necessarily low at any time during the reaction and, therefore, unobservable; analogous experiments using D_2 and H_2 resulted in identical spectra. Also, monomeric ruthenium carbonyl hydrides are notorious for their thermal instability; the only stable and isolable complexes under ambient conditions are $\text{H}_2\text{Ru}(\text{CO})_2(\text{PPh}_3)_2$ and

$\text{H}_2\text{Ru}(\text{CO})_2(\text{PEt}_3)_2$, formed from the reaction of $\text{H}_2\text{Ru}(\text{CO})_4$ at -63° .⁸¹ The lack of any stable monophosphine substituted monomeric hydride explains the failure of experiments to trap the intermediate by phosphine displacement of the olefin--even if $\text{H}_2\text{Ru}(\text{CO})_3\text{PPh}_3$ were formed, it would rapidly decompose. This intermediate could also explain the formation of $\text{Ru}(\text{CO})_9(\text{PPh}_3)_3$, although it does not eliminate the pathway via the bis-olefin complex. Other displacement reaction products were $\text{Ru}(\text{CO})_4\text{PPh}_3$ and $\text{Ru}(\text{CO})_3(\text{PPh}_3)_2$, which can be explained by hydrogen and olefin displacement reactions:



An NMR experiment to look at spectral changes after hydrogen addition to $\text{Ru}(\text{CO})_4$ ethylene was unsuccessful. It was hoped that a disappearance in the metal-olefin signal and concomitant appearance of a metal-alkyl or oxygenated product could be observed. But again equilibrium and concentration effects made this impossible; removal of excess ethylene and addition of H_2 yielded a spectrum of free ethylene.

Due to the elusive nature of the dihydride, experiments were run using trialkyl silanes as hydrogen analogues. $\text{Ru}(\text{CO})_4$ pentene was prepared and reacted with a variety of trialkyl silanes (Me_3SiH , Et_3SiH , Ph_3SiH , and Cl_3SiH) and two trialkylchlorosilanes (Me_3SiCl and Ph_3SiCl). In every case the reaction began almost instantaneously as evidenced by changes in the UV-VIS and IR spectra. Several low temperature experiments (0°) were run using Ph_3SiH in an attempt to isolate the adduct. Removal of the solvent, however, invariably resulted in spectral changes, presumably due to loss of pentene and/or hydrogen with aggregation of the Ru-CO moieties. Low temperature NMRs were impossible as the hydride resonance would be too weak under the reaction conditions, even if all the $\text{Ru}(\text{CO})_4$ pentene had been converted and trapped as $\text{HRu}(\text{SiPh}_3)(\text{CO})_3$ pentene. The trialkylchloro- and trichloro- silanes were used in hopes that the halogen- or Cl_3Si - metal bond would be stronger and thus prevent migration, but again, the reaction was extremely fast. While analyses of the supposed hydrosilation products were not made, gc data indicated a loss of pentene--evidence that the observed reaction was not a simple displacement of the labile olefin.

An alternate route to verification of the hydride-olefin intermediate would be to start the reaction from the other direction. Thus, if $\text{HRu}(\text{CO})_4(\text{SiR}_3)$ could be synthesized, reacted with olefin, and the reaction yielded

products identical to those with the $\text{Ru}(\text{CO})_4$ pentene catalyst, evidence for common intermediates and mechanisms would be gained. Identification of similar ruthenium carbonyl species formed upon reaction completion would also be informative for mechanistic considerations. With these thoughts in mind, the synthesis of $\text{HRu}(\text{CO})_4\text{SiPh}_3$ was attempted. Previous work on the photochemistry of these reactions done by Knox and Stone⁸² had led to the formation of $(\text{R}_3\text{Si})_2\text{Ru}(\text{CO})_4$ and $(\text{R}_3\text{Si})_2\text{Ru}_2(\text{CO})_6$, however, at low temperatures (less than 25°) photolysis of $\text{Fe}(\text{CO})_5$ and R_3SiH has successfully yielded the hydride species $\text{HFe}(\text{CO})_4(\text{SiR}_3)$.⁸³ As the temperature of the reaction is critical, a 3:1 $\text{Ph}_3\text{SiH}/\text{Ru}_3(\text{CO})_{12}$ solution was irradiated at 0° . Analyses by IR, however, indicated that $(\text{Ph}_3\text{Si})_2\text{Ru}_2(\text{CO})_6$ was the only product formed, and Toeppler pumping proved that hydrogen had been evolved. Evidently, $\text{HRu}(\text{CO})_3(\text{SiPh}_3)$ is simply too unstable to survive--even at fairly dilute concentrations (ca. 10^{-3} M) and low temperatures, the species combines to form dimers and H_2 .

Since isolation of the ruthenium-olefin-hydride complex seemed not possible, a synthesis of the corresponding osmium derivative was considered. This seemed promising as a number of monomeric osmium hydrides are known, including $\text{H}_2\text{Os}(\text{CO})_3\text{PPh}_3$.⁸⁴ Unfortunately, attempts to synthesize the $\text{Os}(\text{CO})_4$ pentene precursor from $\text{Os}(\text{CO})_{12}$ were not successful, obviating the subsequent reaction with H_2 . An IR of the

reaction was complex, with no indication that the mono-olefin complex was formed. Subsequent work by Tyler has indicated that CO substitution, rather than triangle fragmentation is the predominate reaction for the osmium system.⁸⁶ In view of such further investigation of the $\text{Os}(\text{CO})_{12}$ system was not pursued.

While investigating the mechanism for $\text{Ru}(\text{CO})_4$ pentene catalyzed hydroformylation, the possibility of an alternate route to aldehyde formation was considered. Initial hydroformylation reactions had been done in the presence of both olefin and synthesis gas, so a ruthenium carbonyl hydride might also have been formed that subsequently acted as an oxo catalyst. Activation of molecular hydrogen by the reaction of photochemically generated 16-electron metal carbonyl species is known,⁸⁷ so this supposition is not unlikely. Irradiation of $\text{Ru}_3(\text{CO})_{12}$ solutions under an atmosphere of H_2 resulted in the formation of a single product, $\alpha\text{-H}_4\text{Ru}_4(\text{CO})_{12}$, as evidenced by UV-VIS (Figure 7) and IR analyses (Figure 8). Bridging positions for the hydrogen atoms have been confirmed by a laser raman spectrum but the exact structure of the complex has yet to be ascertained.⁸⁸ Of the several possibilities, two are considered especially likely (Figure 9). Formation of this larger cluster could be envisioned as follows:

Figure 7

UV-VIS spectra of the photochemical reaction of $\text{Ru}_3(\text{CO})_{12}$
and H_2 to form $\alpha\text{H}_4\text{Ru}_4(\text{CO})_{12}$.

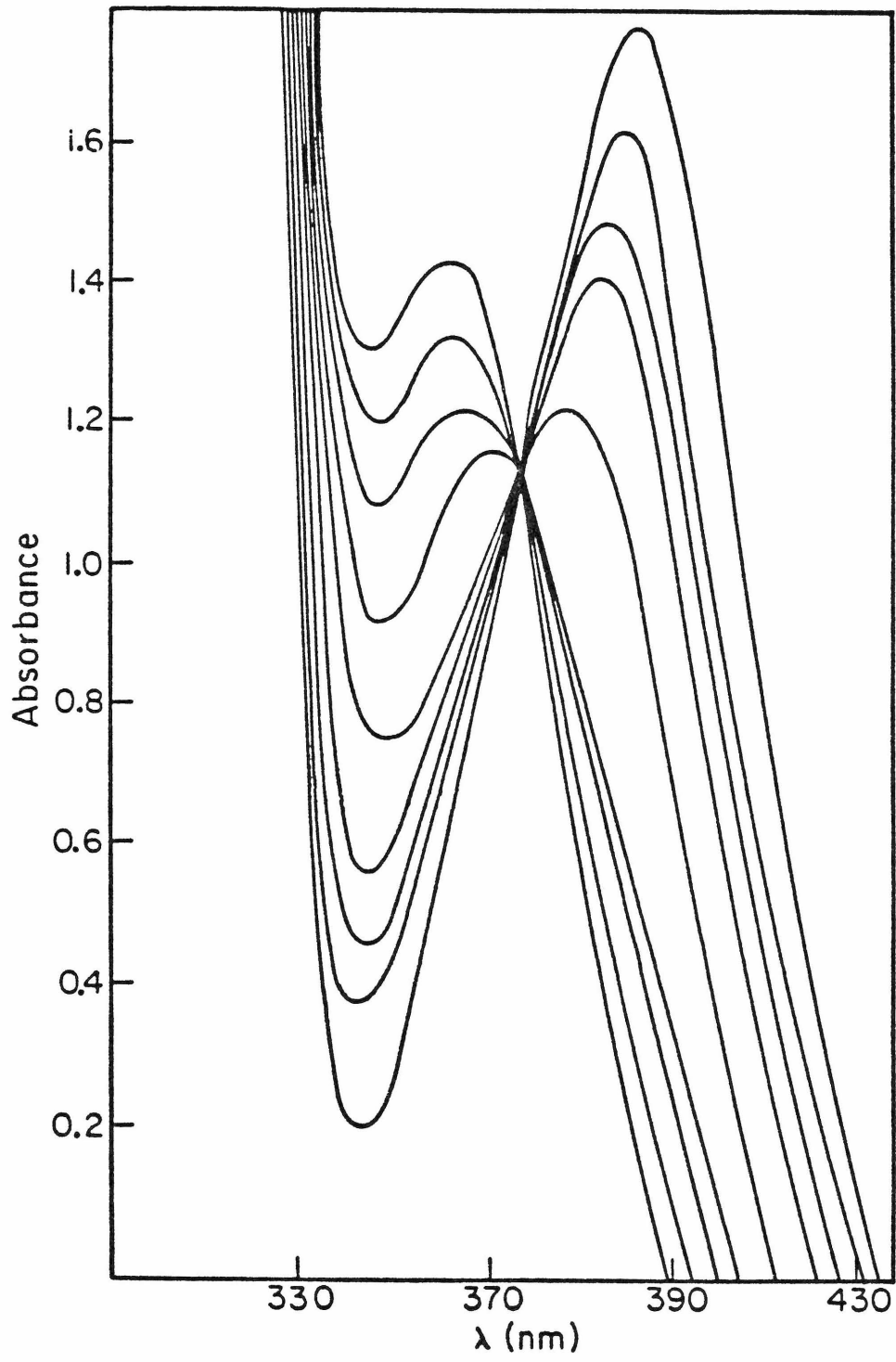
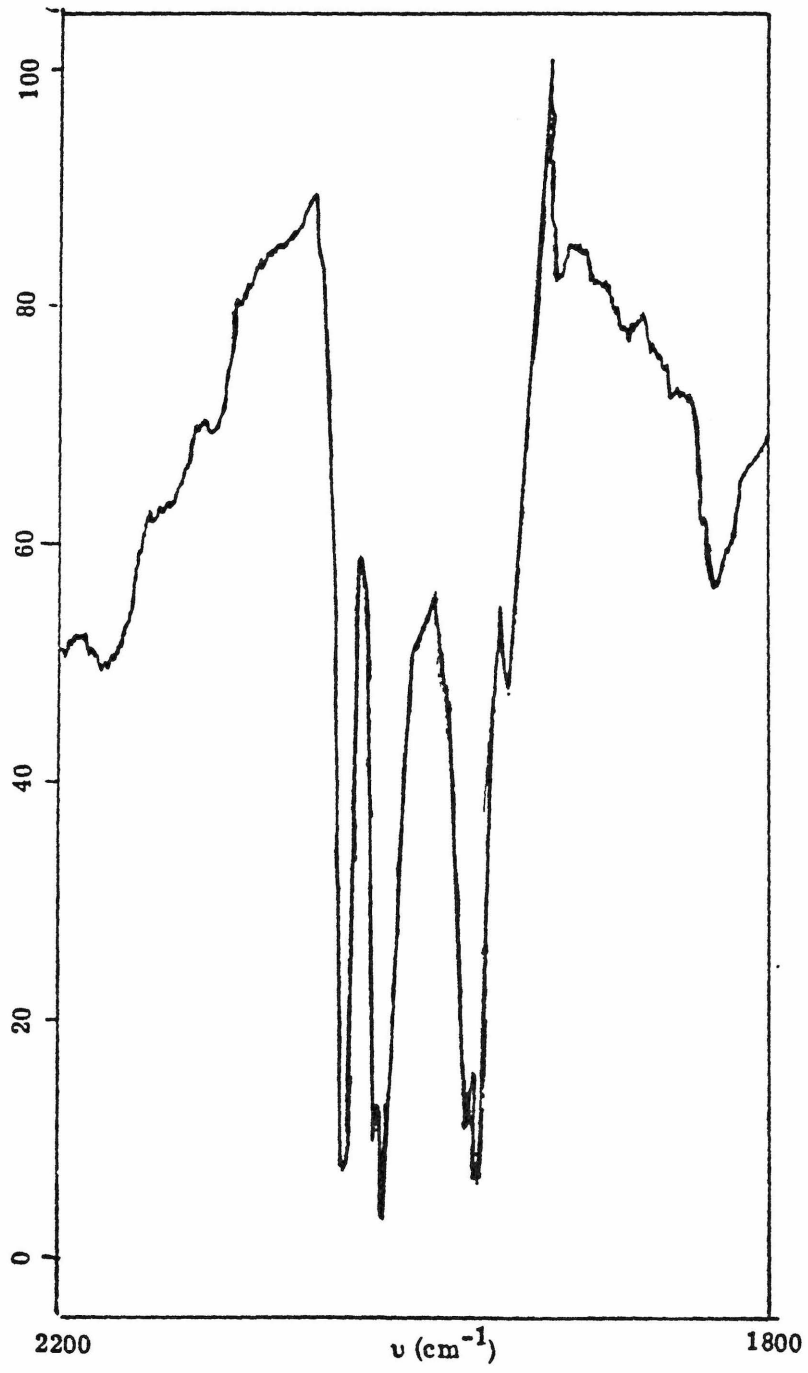


Figure 8

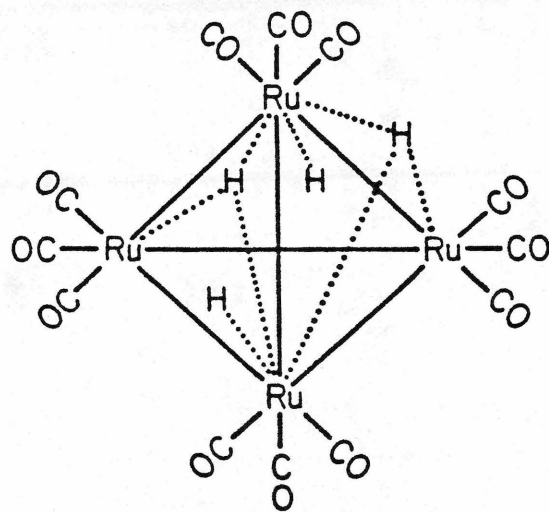
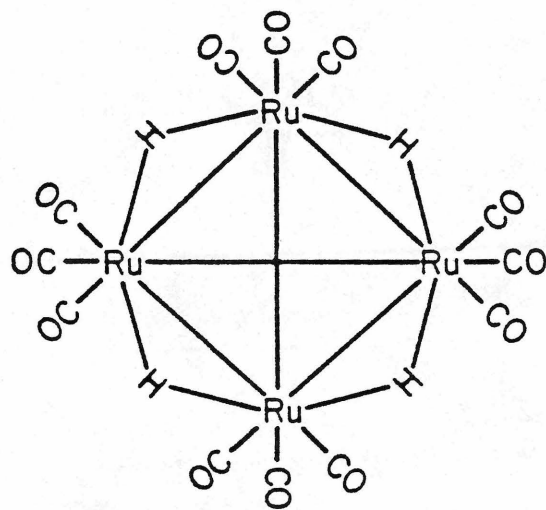
IR spectrum of $\alpha\text{H}_4\text{Ru}_4(\text{CO})_{12}$.

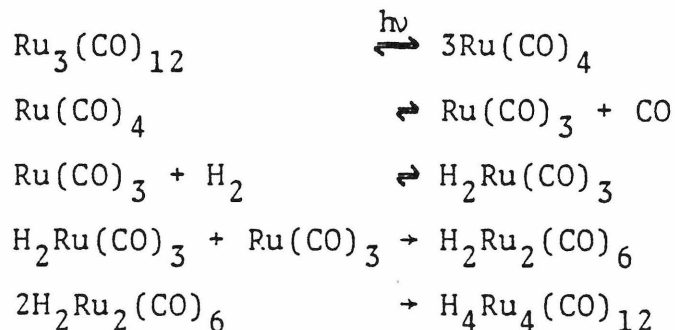


176

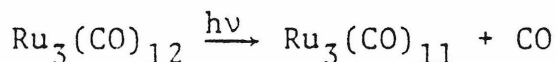
Figure 9

Proposed structures for $\alpha\text{H}_4\text{Ru}_4(\text{CO})_{12}$.





Since photodissociation of CO is probably not occurring under the reaction conditions ($\lambda > 355 \text{ nm}$), this reaction



is not a likely pathway to oxidative addition of H_2 .

Addition of 1-pentene to $\alpha\text{H}_4\text{Ru}_4(\text{CO})_{12}$ and subsequent thermal reaction resulted in hydroformylation of the olefin. The cluster is known to catalyze both the isomerization of pentenes⁸⁹ and the hydrogenation of unsaturated compounds,⁹⁰ so it is not surprising that it can serve as an oxo catalyst as well. Data for the isomerization reaction indicate that the mechanism involves α -alkyl intermediates formed by addition of the olefin to $\text{H}_4\text{Ru}_4(\text{CO})_{11}$. Redistribution of the hydrogen isotopes for the reaction of trans- $\text{C}_2\text{H}_2\text{D}_2$ with $\text{H}_4\text{Ru}_4(\text{CO})_{12}$ to yield $\text{C}_2\text{H}_3\text{D}$ and C_2HD_3 prove that the metal bound hydrogens are transferred to the olefin. This reaction followed by "CO insertion" and subsequent elimination could account for the observed hydroformylation.

To compare the photochemical and thermal yields for the two catalysts, identical solutions of $\text{Ru}_3(\text{CO})_{12}$ were prepared, two were photolyzed in the presence of 1-pentene until conversion to $\text{Ru}(\text{CO})_4$ pentene was evidenced and two with H_2 to form $\underline{\alpha}\text{H}_4\text{Ru}_4(\text{CO})_{12}$. Hydrogen was added to the $\text{Ru}(\text{CO})_4$ pentene solutions, 1-pentene to the $\underline{\alpha}\text{H}_4\text{Ru}_4(\text{CO})_{12}$ solutions, and analogous thermal and photochemical reactions were carried out for each system. The results are given numerically in Tables 2 and 3 and graphically in Figures 10-13. Several conclusions may be made from these data. First of all, the photochemical reactions for both systems result in higher yields and faster rates of formation. In each case then, a true photocatalyst is operative. For the $\text{Ru}(\text{CO})_4$ pentene system irradiation prevents reclusterification and subsequent catalyst deactivation. For the $\underline{\alpha}\text{H}_4\text{Ru}_4(\text{CO})_{12}$ system, the role played by light is not as obvious: its function may be to prevent destruction of the active species or to facilitate its formation and/or reaction.

Another interesting similarity of the photochemical catalysis is that peak yields are reached within the first 1-2 hours of the reaction, followed by a disappearance of the aldehydes already formed. Possibly these are being reduced to alcohols, a secondary product common to the hydroformylation process. That 1-hexanal will complex with $\text{Ru}(\text{CO})_4$ moieties was confirmed by a photochemical reaction

Table 2. Thermal and Photochemical Yields (10^{-4} Moles) for $\alpha\text{-H}_4\text{Ru}_4(\text{CO})_{12}$ Reactions as a Function of Time (min).

Time	Thermal Yield of 1-Hexanal	Thermal Yield of 2-me-Pentanal	Total Thermal Aldehyde Yield	Photochemical Yield of 1-Hexanal	Photochemical Yield of 2-me-Pentanal	Total Photochemical Yield
20	.95	.14	1.09	1.60	1.22	2.82
30	1.19	.38	1.57	1.80	1.73	3.53
60	1.40	.50	1.90	2.20	1.90	4.10
120	2.00	1.10	3.10	2.50	2.30	4.80
180	2.20	1.20	3.40	2.30	1.60	3.90
240	2.30	1.40	3.70	2.00	1.30	3.30
	2.35	1.40	3.75	1.80	1.00	3.20

Table 3. Thermal and Photochemical Yields (10^{-4} Moles) for $\text{Ru}(\text{CO})_4$ pentene Reactions as a Function of Time (min).

Time	Thermal Yield of 1-Hexanal	Thermal Yield of 2-me-Pentanal	Total Thermal Aldehyde Yield	Photochemical Yield of 1-Hexanal	Photochemical Yield of 2-me-Pentanal	Total Photochemical Yield
5	9.30	4.60	13.90	21.40	12.70	34.10
10	9.60	5.20	14.80	33.80	13.80	37.60
15	10.70	5.60	16.30	25.20	14.90	40.10
60	11.70	6.50	18.20	33.80	17.90	51.70
90	12.80	6.90	19.70	28.60	16.70	45.30
135	14.20	7.40	21.60	23.80	13.60	37.40
160	15.30	7.60	22.90	19.90	12.30	32.20
225	15.60	7.90	23.50	18.40	11.60	30.00
300	15.80	8.30	24.10	15.10	10.20	25.30

Figure 10

Thermal aldehyde production (10^{-4} moles) using
 $\alpha\text{H}_4\text{Ru}_4(\text{CO})_{12}$ as a function of time (min).

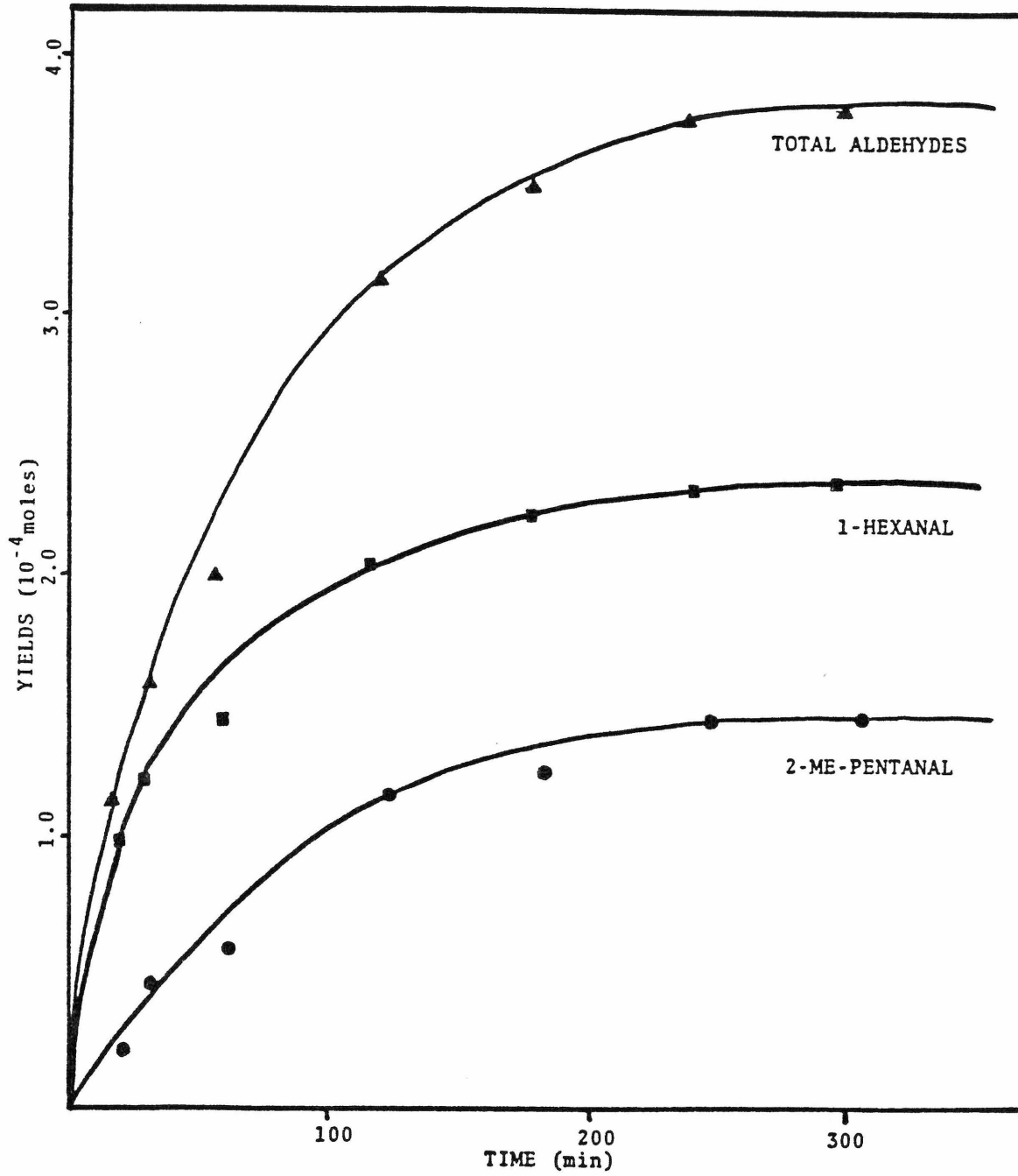


Figure 11

Photochemical aldehyde production (10^{-4} moles) using

$\alpha\text{-H}_4\text{Ru}_4(\text{CO})_{12}$ as a function of time (min).

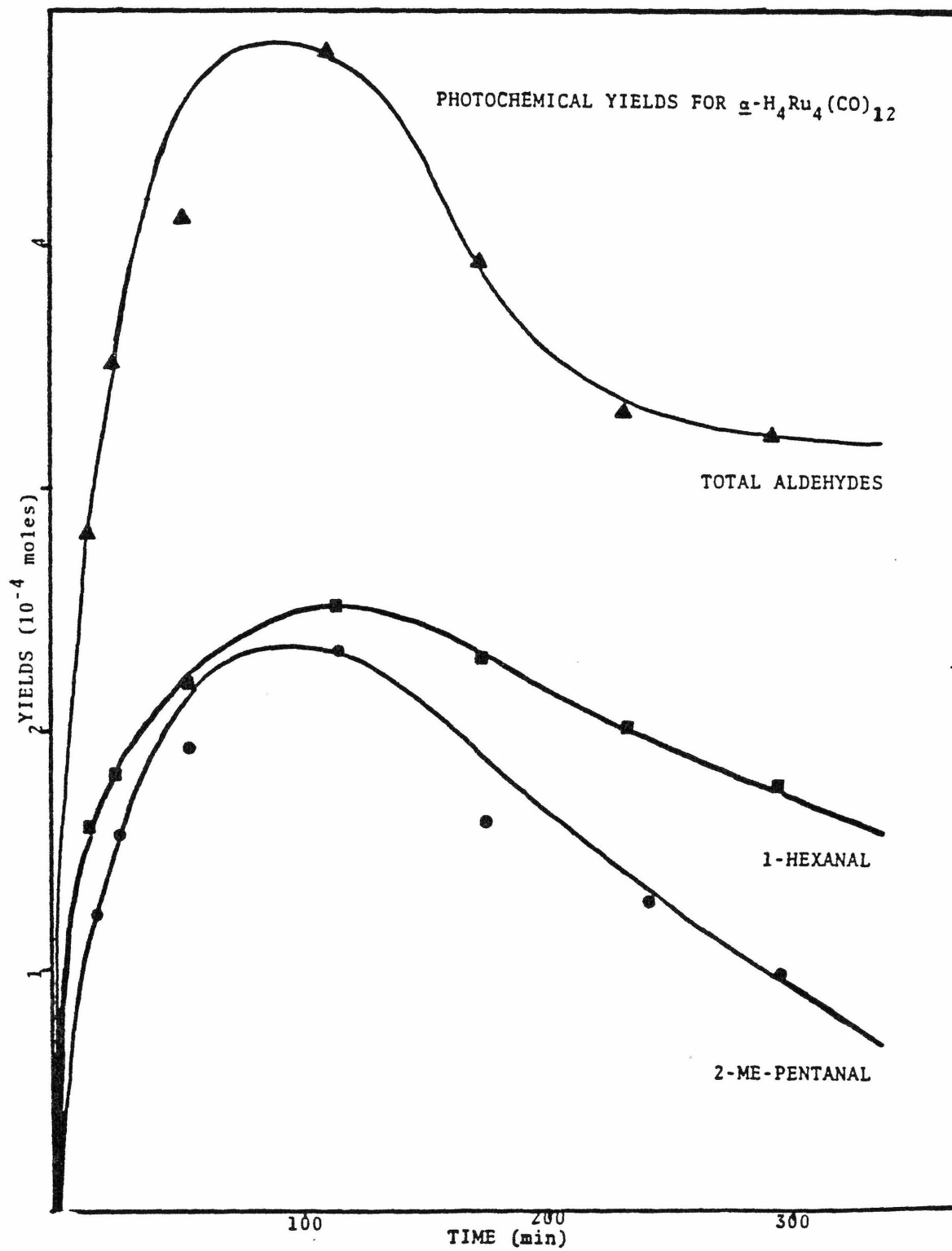


Figure 12

Thermal aldehyde production (10^{-4} moles) using
Ru(CO)₄pentene as a function of time (min).

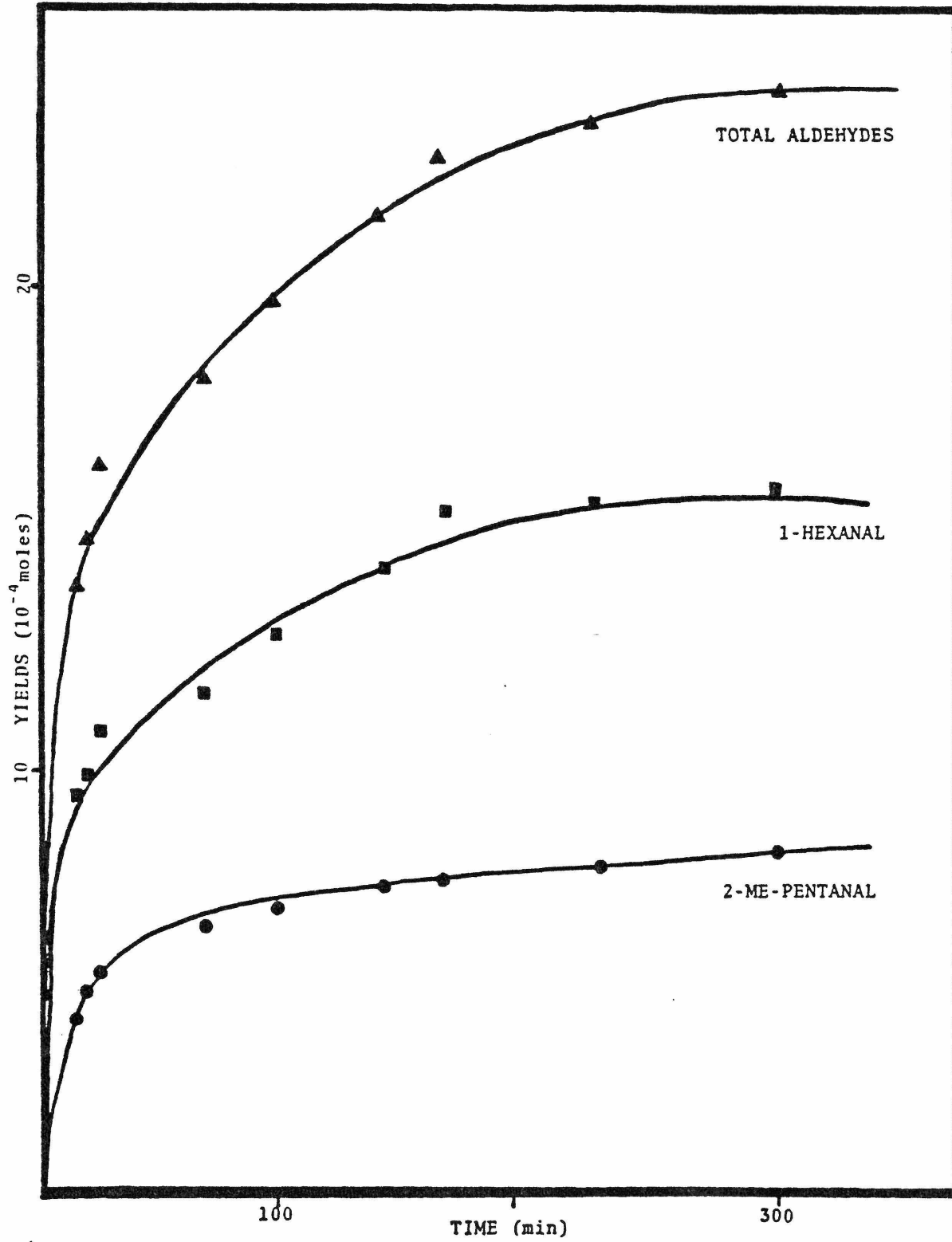
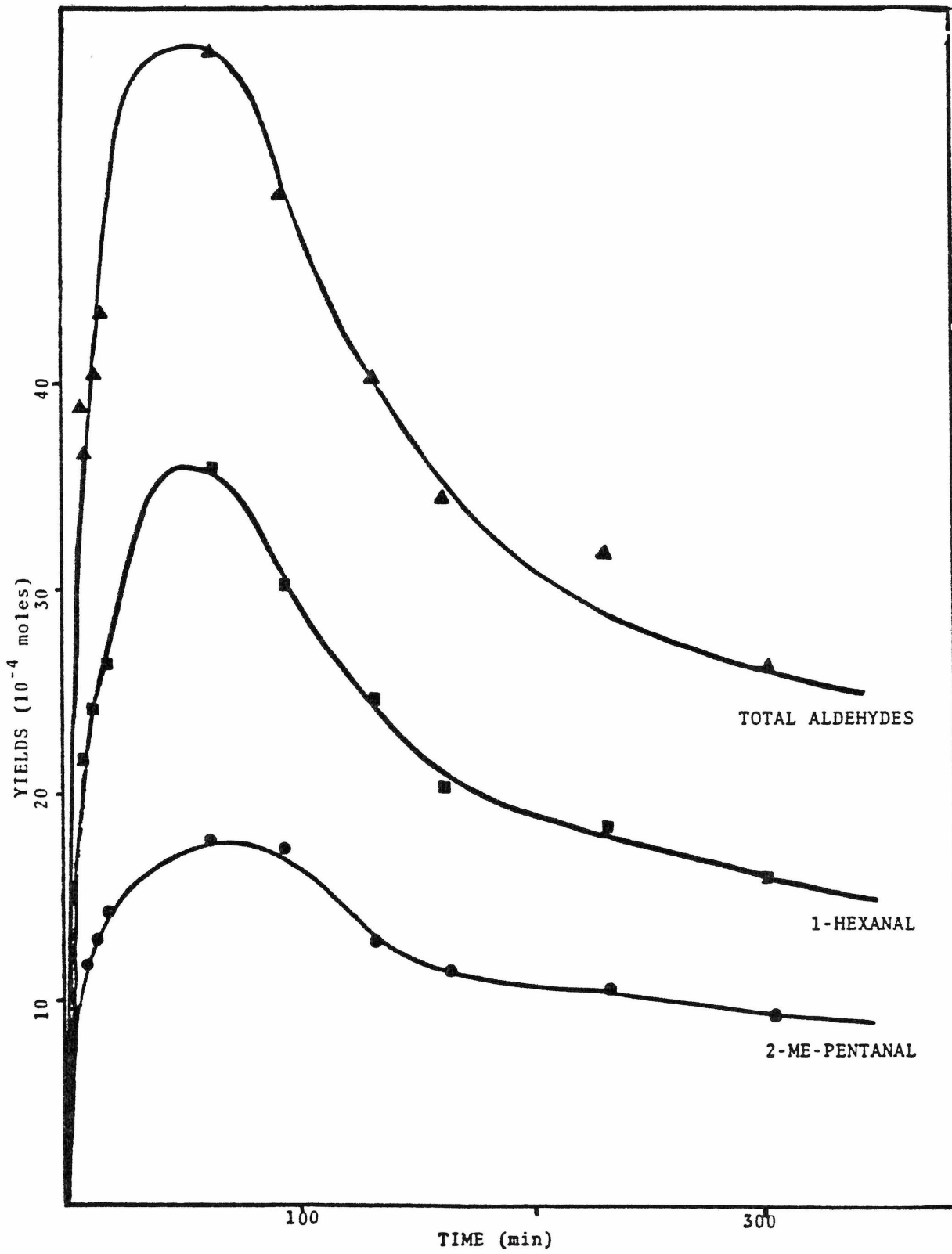


Figure 13

Photochemical aldehyde production (10^{-4} moles) using
Ru(CO)₄pentene as a function of time (min).

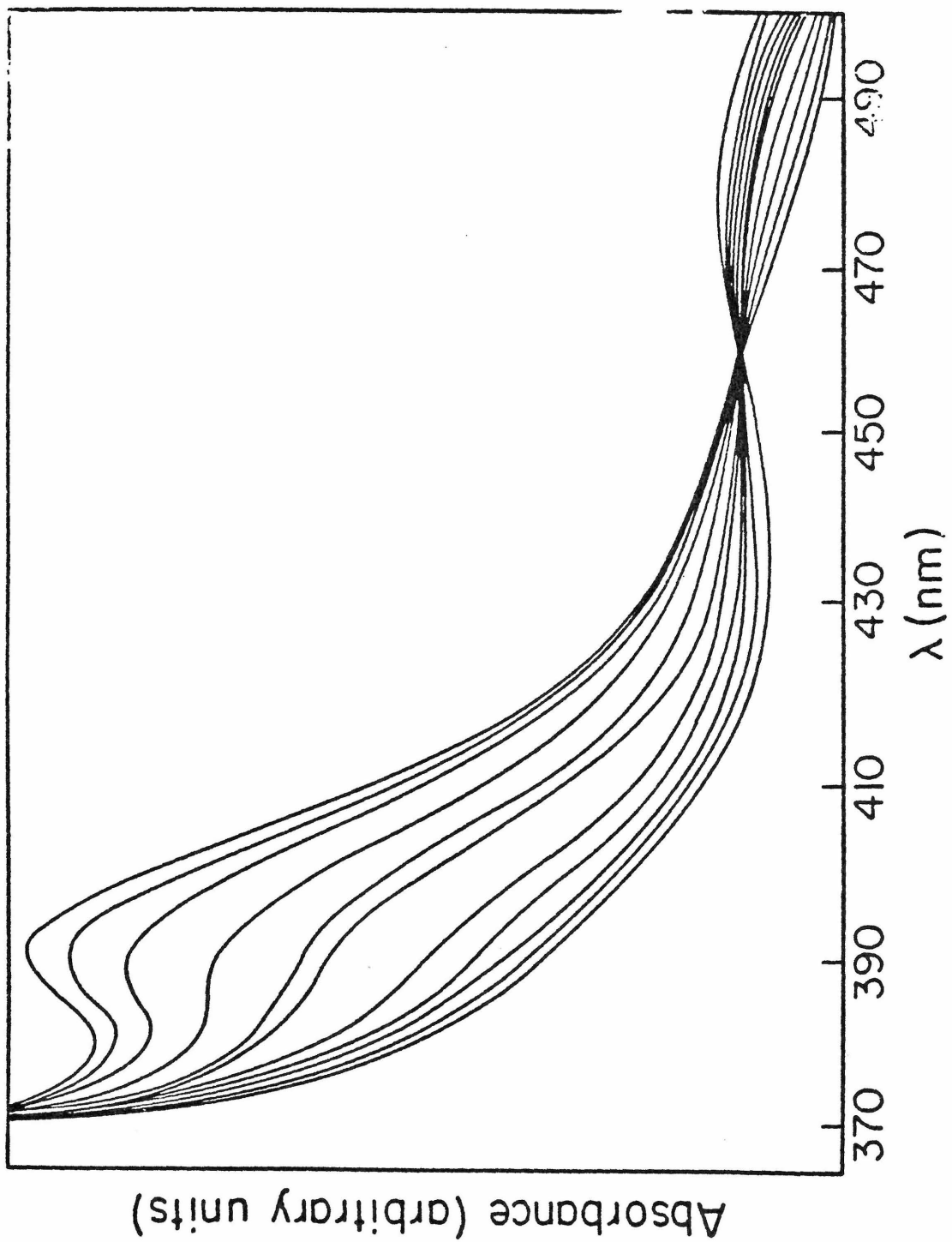


between $\text{Ru}_3(\text{CO})_{12}$ and the aldehyde (Figure 14). Although as yet unconfirmed, the complex probably involves bonding of the unsaturated acyl group or coordination via the lone pair of electrons on oxygen. The latter possibility seems particularly likely as the photochemical reactions of $\text{Ru}_3(\text{CO})_{12}$ with Et_2O and THF yield of monomeric adducts. Photolysis of an aldehyde- $\text{Ru}(\text{CO})_4$ pentene solution results in displacement of the olefin. This was confirmed by IR, although the complexity of the spectrum made it impossible to determine whether the ruthenium-aldehyde species and/or some larger cluster is formed.

Probably the most important aspect of the data is a comparison of the relative aldehyde production. The preponderance of 1-hexanal found for both systems is reasonable due to steric considerations. More significantly, the total yields are significantly greater for the $\text{Ru}(\text{CO})_4$ -pentene reactions: thermally they are about 6 times that of the corresponding $\alpha\text{-H}_4\text{Ru}_4(\text{CO})_{12}$ reaction, and photochemically this factor exceeds 10. Thus, although the $\alpha\text{-H}_4\text{Ru}_4(\text{CO})_{12}$ system contributes to the hydroformylation process, it seems that formation of the $\text{Ru}(\text{CO})_4$ pentene complex is the major pathway to homogeneous hydroformylation.

Figure 14

UV spectrum of $\text{Ru}_3(\text{CO})_{12}$ and 1-hexanal reaction.



References

1. O. Roelen, German Patent 849548 (1938); Z. Chem. 927 (1953).
2. H. Weber and J. Falke, Ind. Eng. Chem. 62, 33 (1970).
3. I. Wender, H. W. Sternberg, R. A. Freidel, J. Metlin, and R. Markby, U.S. Bur. Mines, Bull. 600 (1962).
4. H. Wakamatsu, J. Chem. Soc. Jap., Pure Chem. Sect. 85, 227 (1964).
5. J. B. Zachry, Ann. N.Y. Acad. Sci. 125, 154 (1965).
6. D. Evans, J. A. Osborn, F. H. Jardine, G. Wilkinson, Nature 206, 1203 (1965).
7. F. H. Jardine, J. A. Osborn, G. Wilkinson, and J. F. Young, Chem. Ind. (London) 560 (1965).
8. J. A. Osborn, F. H. Jardine, J. F. Young, and G. Wilkinson, J. Chem. Soc. A 1711 (1965).
9. G. Yagupsky, C. K. Brown, and G. Wilkinson, J. Chem. Soc. A 1392 (1970).
10. C. K. Brown and G. Wilkinson, J. Chem. Soc. A 2753 (1970).
11. G. O. Hatta, J. Amer. Chem. Soc. 86, 3903 (1964).
12. M. Hill, Petrol Refiner 43, 135 (1964).
13. T. G. Selin and R. West, J. Amer. Chem. Soc. 84, 1863 (1962).
14. J. Wender, S. Metlin, S. Ergun, H. W. Sternberg, and H. Greenfield, J. Amer. Chem. Soc. 78, 5401 (1956).

15. A. Roche, C. Paul, and J. Saralahors, Petrol Refiner 43, 161 (1964).
16. K. Ziegler, Chim. Ind. (Paris) 92, 631 (1964).
17. R. D. Sanner, N.S.F. Proposal, Studies of the Petrochemical Generation of Polymer-Bound Catalysts (1976).
18. W. D. Bonds, Jr., C. H. Brubaker, Jr., E. S. Chardrasekaran, C. Gibbons, R. H. Grubbs, and L. C. Kroll, J. Am. Chem. Soc. 97, 2128 (1975).
19. R. H. Grubbs, L. C. Kroll, and E. M. Sweet, J. Micromol. Sci. Chem. 7, 1047 (1973).
20. S. E. Jacobsen, W. Clements, H. Hiramoto, and C. U. Pittman, Jr., J. Mol. Catal. 1, 73 (1975).
21. C. U. Pittman, Jr., S. E. Jacobson, and H. Hiramoto, J. Am. Chem. Soc. 97, 4774 (1975).
22. C. U. Pittman, Jr., and R. M. Hanes, Ann. N.Y. Acad. Sci. 239, 76 (1974).
23. D. C. Meckers, D. A. Kooistra, and G. W. Green, J. Am. Chem. Soc. 94, 3984 (1972).
24. C. C. Frazier, Ph.D. Thesis, California Institute of Technology, 1975.
25. D. S. Breslow and R. F. Heck, Chem. Ind. (London) 83, 457 (1959).
26. R. F. Heck, Adv. Organometal Chem. 4, 243 (1966).
27. P. Pino, F. Piacenti, M. Bianchi and R. Lazzaroni, Chim. Ind. (Milan) 50, 106 (1968).
28. F. Piacenti, M. Bianchi, and R. Lazzaroni, Chim. Ind.

- (Milan) 50, 318 (1968).
29. G. Braca, G. Sbrana, F. Piacenti, and P. Pino, Chim. Ind. (Milan) 52, 1091 (1970).
30. E. C. Murray and R. N. Keller, J. Org. Chem. 34, 2234 (1969).
31. C. A. Parker, Proc. Roy. Soc. (London) A220, 104 (1953).
32. C. G. Hatchard and C. A. Parker, ibid, A235, 518 (1956).
33. J. G. Calvert and J. N. Pitts, "Photochemistry", John Wiley and Sons, Inc., New York, 1966, pp. 783-786.
34. W. D. Bowman and J. N. Demas, J. Phys. Chem. 80, 2434 (1976).
35. W. Hieber and H. Fischer, Ger. 695, 589 (1940).
36. E. R. Corey and L. F. Dahl, Inorg. Chem. 1, 521 (1962).
37. E. R. Corey and L. F. Dahl, Dissertation Abstr. 24, 1384 (1963).
38. E. R. Corey and L. F. Dahl, J. Am. Chem. Soc. 83, 2203 (1961).
39. J. Lewis, A. B. Manning, J. R. Miller, and J. M. Wilson, Chem. Comm. 391 (1966).
40. H. Albert, J. Organometal Chem. 28, 428 (1971).
41. B. F. G. Johnson, J. Lewis, I. G. Williamson, and J. Wilson, Chem. Comm. 391 (1966).
42. B. F. G. Johnson, J. Lewis, I. G. Williamson, and J. Wilson, J. Chem. Soc. (A) 341 (1967).
43. M. I. Bruce and F. G. A. Stone, Angew. Chem. Internat. Ed. 7, 427 (1968).

44. E. W. Abel and R. A. N. MacLean, unpublished results.
45. David R. Tyler, Candidacy Exam, California Institute of Technology, 1977.
46. M. S. Wrighton, Topics in Current Chemistry, 65, 37 (1975).
47. M. A. Schroeder and M. S. Wrighton, J. Am. Chem. Soc. 98, 551 (1976).
48. B. F. G. Johnson, R. D. Johnston, P. L. Josty, J. Lewis, and I. G. Williams, Nature 214, 901 (1967).
49. I. G. Williams, B. F. G. Johnson, R. D. Johnston, and J. Lewis, Chem. Comm. 861 (1968).
50. B. F. G. Johnson, R. D. Johnston, and J. Lewis J. Chem. Soc. (A) 792 (1969).
51. S. A. R. Knox and F. G. A. Stone, J. Chem. Soc. 2559 (1967).
52. S. A. R. Knox and F. G. A. Stone, J. Chem. Soc. 2874 (1971).
53. J. R. Norton and J. P. Collman, Inorg. Chem. 13, 476 (1973).
54. J. R. Norton, J. P. Collman, G. Dolcetti, and W. T. Robinson, Inorg. Chem. 11, 382 (1972).
55. J. R. Norton, J. P. Collman, and D. Valentine, Jr., J. Am. Chem. Soc. 91, 7537 (1972).
56. M. A. Schroeder and M. S. Wrighton, J. Am. Chem. Soc. 98, 551 (1976).
57. G. O. Schenck, E. K. von Gustorf, and M. J. Jung, Tet. Lett. 1059 (1962).

58. E. K. von Gustorf and J. C. Hogan, Tet. Lett. 3191 (1968).
59. A. J. P. Domingas, B. F. G. Johnson, and J. Lewis, J. Organometal Chem. 36, C43 (1972).
60. J. S. Ward and R. Pettit, Chem. Comm. 1419 (1970).
61. M. J. S. Dewar, Bull. Soc. Chim. Fr. 18, C71 (1951).
62. J. Chatt and L. A. Duncanson, J. Chem. Soc. 2939 (1953).
63. G. C. Bond and M. Hellier, J. Catal. 4, 1 (1965).
64. M. Castiglioni, L. Milone, D. Osella, G. A. Vaglio, and M. Valle, Inorg. Chem. 15, 395 (1976).
65. M. A. Schroeder and M. S. Wrighton, J. Am. Chem. Soc. 98, 551 (1976).
66. M. S. Wrighton, personal communication.
67. J. K. Nicholson and B. L. Shaw, J. Chem. Soc. (A) 807 (1966).
68. J. E. Lydon, J. K. Nicholson, B. L. Shaw, and M. R. Truter, Proc. Chem. Soc. 421 (1964).
69. R. Burt, M. Cooke, and M. Green, J. Chem. Soc. (A) 2975 (1970).
70. G. Sbrana, G. Bracca, F. Piacenti, and P. Pino, J. Organometal. Chem. 13, 240 (1968).
71. J. Powell and B. L. Shaw, J. Chem. Soc. (A) 159 (1968).
72. R. Wryman, J. Organometal. Chem. 56, 339 (1973).
73. C. T. Sears and F. G. A. Stone, J. Organometal. Chem. 11, 644 (1968).
74. R. J. H. Cowles, B. F. G. Johnson, P. L. Josty, and J. Lewis, Chem. Comm. 392 (1969).

75. J. Lewis, F. A. Cotton, A. J. Deeming, P. L. Josty, S. S. Ullah, A. J. P. Domingas, and B. F. G. Johnson, J. Am. Chem. Soc. 93, 4624 (1971).
76. A. J. Birch, P. E. Cross, J. Lewis, and P. A. White, Chem. and Ind. 838 (1964).
77. R. B. King, Advan. Organometal. Chem. 2, 157 (1964).
78. G. W. Parshall, J. J. Mrowca, Advan. Organometal. Chem. 9, 157 (1970).
79. M. L. Green, L. C. Mitchard, and M. G. Swanwick, J. Chem. Soc. (A) 794 (1971).
80. A. Gupta, personal communication.
81. J. D. Cotton, M. I. Bruce, and F. G. A. Stone, J. Chem. Soc. (A) 2162 (1968).
82. S. A. R. Knox and F. G. A. Stone, J. Chem. Soc. (A) 2559 (1969).
83. I. Jetz and W. A. G. Graham, Inorg. Chem. 10, 4 (1971).
84. F. L'Eplattenier and F. Calderazzo, Inorg. Chem. 11, 20921 (1962).
85. J. Nasielski, P. Kirsch, and L. Wilputte-Steinhart, J. Organometal. Chem. 27, C13 (1971).
86. D. R. Tyler, Ph.D. Thesis, California Institute of Technology, 1979.
87. S. C. Tripathi, S. C. Srivastara, R. P. Mani, and A. K. Shirmal, Inorganica Chim. Acta 15, 280 (1975).
88. M. Valli, D. Osella, G. A. Vaglio, Inorganica Chim. Acta 20, 213 (1976).

89. P. Frediani, M. Bianchi, and F. Piacenti, Chim. Ind.
(Milan) 53, 80 (1970).

PROPOSITION 1

The Photochemistry of Bridging Vinylidenes

Vinylidenes or methylene carbinos ($:C=CR_2$) are the valence tautomers of acetylenes. Although unstable in the free state, they have been shown to form stable complexes with a variety of transition metals.¹⁻⁷ The chemistry of this class of compounds is interesting in that it illustrates the conversion of metal to carbon single and multiple bonds (Figure 1).⁸ This scheme also illustrates the electrophilicity of the α position and the nucleophilicity of the β position in the isoelectronic series for a terminally bound carbonyl, acetylide, and vinylidene. The electrophilicity of a vinylidene complex varies with the metal, ancillary ligands, and the charge on the complex as a whole.

As two electron donors, the vinylidene ligand is analogous to carbon monoxide and isonitriles and may be bound either in a terminal or a bridging position. Recently a number of binuclear complexes have been isolated as illustrated in Figure 2.^{3,9-13} Since it is known that bridging groups can have a marked influence on the photoreactivity of cluster compounds,¹⁴ it would be interesting to study the specific effect of vinylidene ligand acting in this capacity. In particular we propose to study the photoreactivity of $Fe_2(\mu-C-CPh_2)(CO)_8$, $Cp_2Re_2(\mu-C=CHPh)(CO)_4$, $Cp_2Mn_2(\mu-C=CHPh)(CO)_4$, and $Cp_2Ru(\mu-C=CH_2)(\mu-CO)(CO)_2$.

A cursory study of the photochemistry of $Cp_2Mn_2(\mu-C=CHPh)(CO)_2$ has shown it to be sensitive to ultraviolet irradiation:¹¹

Figure 1

Chemical transformations which relate metal to
carbon single, double, and triple bonds.

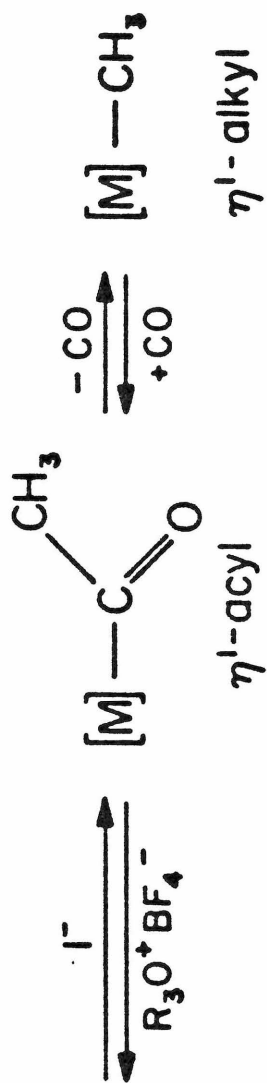
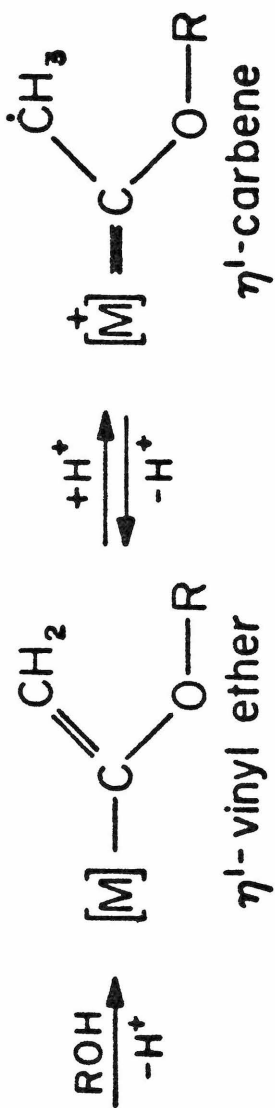
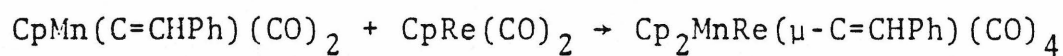
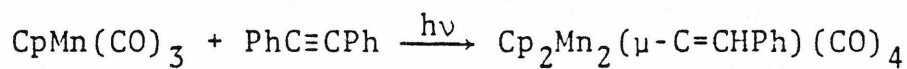
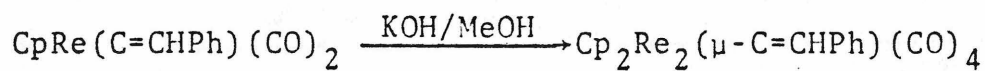
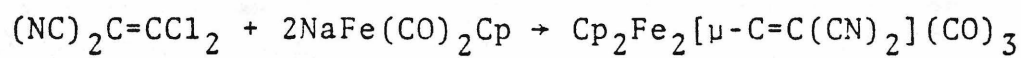
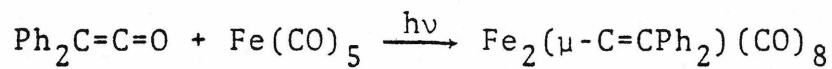
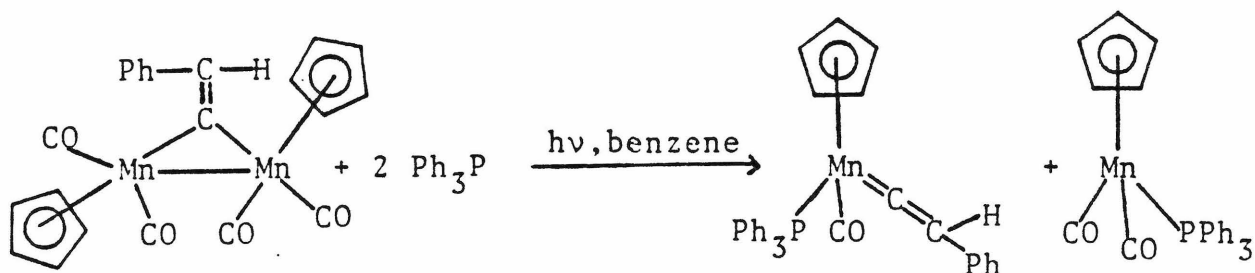


Figure 2

Synthetic routes to binuclear vinylidenes.





Although only a qualitative investigation was made, it was proposed that dissociation of the Mn-Mn bond was the first step in the photoprocess. This was followed by migration of a μ -C-Mn bond to form $\text{CpMn}(\text{C}=\text{CHPh})(\text{CO})_2$ and $\text{CpMn}(\text{CO})_2$ which react rapidly with PPh_3 present to form the indicated products.

That the manganese atom is more strongly bound to the $\text{C}=\text{CHPh}$ ligand than with CO was confirmed by mass spectral data.¹¹ Elimination of $\text{C}=\text{CHPh}$ was shown to occur from the completely decarbonylated ion $[\text{Cp}_2\text{Mn}_2(\text{C}=\text{CHPh})]^+$. This is explained by the increased electron withdrawing properties of the $\text{C}=\text{CHPh}$ ligand as compared to CO. In an infrared study of $\text{CpMn}(\text{C}=\text{CHPh})(\text{CO})_2$ and other $\text{CpMn}(\text{CO})_2\text{L}$ cymantrene

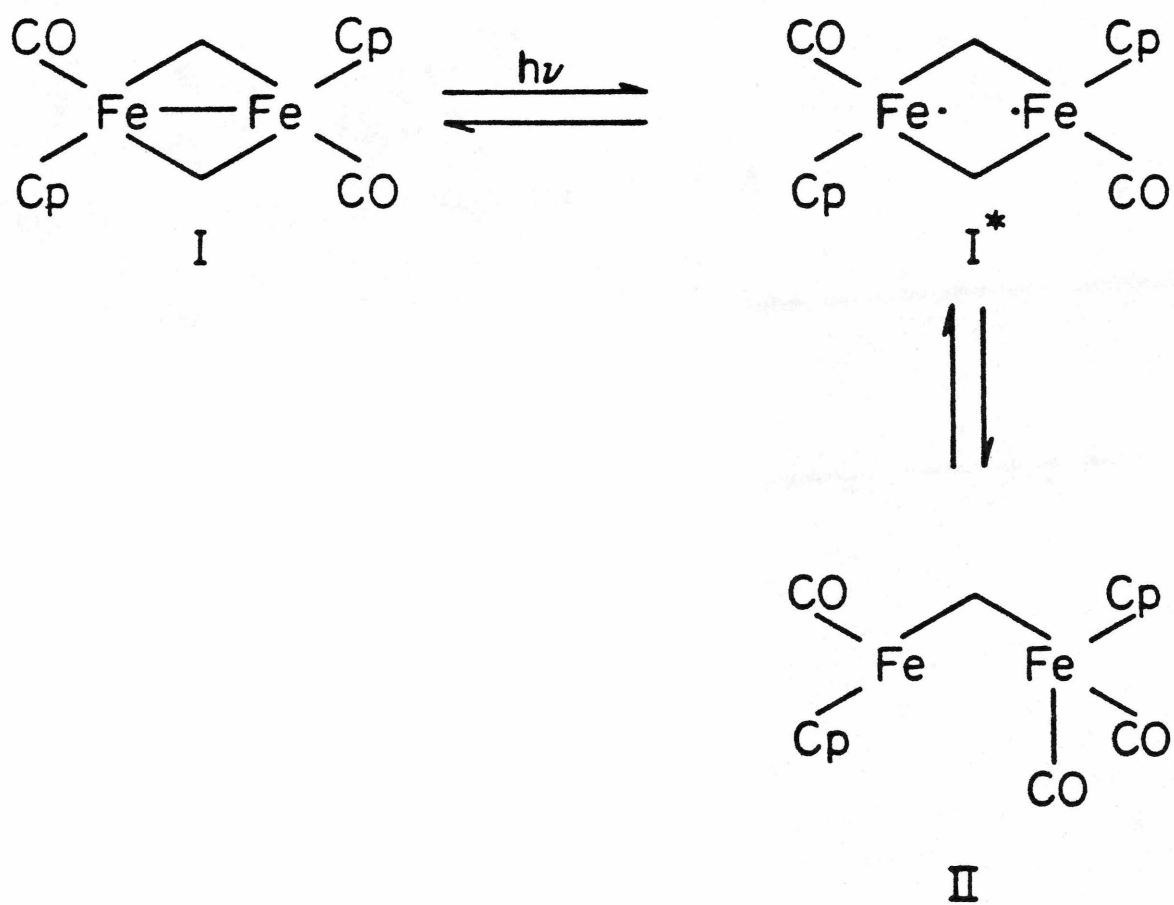
derivatives, Antonova et al., have estimated the electronic effect of C=CHPh as a ligand (Table 1).¹¹ On the basis of K_{CO} values, the order of decreasing electronic-withdrawing properties is seen to be



Thus, phenylvinylidene has an even greater π accepting capacity than CO.

It would be instructive to study the photofragmentation of this molecule and the related vinylidene dimers in more detail. In particular, low temperature photolyses should be especially informative. If the primary photoprocess is indeed scission of the metal-metal bond, then disappearance of the $\sigma - \sigma^*$ (metal-metal bonding to metal-metal antibonding) transition should be evidenced in the electronic absorption spectrum. Furthermore, infrared spectra would allow conclusions as to whether the bridging ligand remained intact and a CO is lost from such a binuclear intermediate or subsequently from a monomeric fragment.

Previous work on the photochemistry of $\text{Cp}_2\text{Fe}_2(\text{CO})_4$ (where two carbonyls bridge the Fe-Fe unit) has shown metal-metal bond fragmentation to be the primary photochemical step.¹⁴ Rearrangement yields a monobridged intermediate which can react with substrates present in the medium (Figure 3). It seems likely that intermediates similar to those of $\text{Cp}_2\text{Fe}_2(\text{CO})_4$ will be formed from the vinylidene



bridged complexes if homolysis of the metal-metal bond is, indeed, the primary photoreaction. While the monobridged complexes may decompose rapidly to yield fragmentation products, $\text{Cp}_2\text{Ru}_2(\mu\text{-C=CH}_2)(\mu\text{-CO})(\text{CO})_2$ may form substituted clusters.

Reactions involving cleavage of the metal-metal unit should produce radical fragments capable of abstracting chlorine from chlorocarbon solvents or cross coupling reactions. These photochemical reactions should be studied to elucidate the mechanism of reaction and provide synthetic routes to unique mixed metal clusters. For example photolysis of $\text{Cp}_2\text{Fe}_2(\mu\text{-C=CHPh})(\text{CO})_4$ and $\text{Cp}_2\text{Mn}_2(\mu\text{-C=CHPh})(\text{CO})_4$ might prove a convenient route to $\text{Cp}_2\text{FeMn}(\mu\text{-C=CHPh})(\text{CO})_4$ heretofore unknown.

Another interesting avenue for research would be to study the photoreactivity of these complexes in the presence of various substrates. For example, photolysis of a bridging vinylidene complex in the presence of phenylacetylene, ketenes, or diazomethane could result in doubly bridged complexes with no formal metal-metal bond. Also, the formation of larger metalocycles could be envisioned as a result of the photoinduced insertion reactions of carbon monoxide, olefins, or acetylenes.

The vinylidene dimers should provide a unique and interesting class of compounds for photochemical study. In particular they should prove to be exciting and informative

with regard to metal-alkyl photochemistry as a whole and the photoinduced fragmentation of metal cluster compounds.

References

1. C. E. Dykstra and C. E. Schaefer, J. Am. Chem. Soc. 100, 1378 (1978).
2. J. M. Bellerby and M. J. Mays, J. Organomet. Chem. 117, C21 (1976).
3. R. B. King and M. S. Saran, J. Am. Chem. Soc. 95, 1817 (1973).
4. R. M. Kirchner and R. M. Ibers, Inorg. Chem. 13, 1667 (1974).
5. A. N. Nesmeyanov, G. G. Aleksandrov, A. B. Antonova, K. N. Anisimov, N. E. Kolobova, and Yu T. Struchkov, J. Organomet. Chem. 110, C36 (1976).
6. A. N. Nesmeyanov, N. E. Kolobova, A. B. Antonova, and K. N. Anisimov, K. N. Dokl. Chem. (Engl. Trans.) 220, 12 (1975).
7. A. Davison and J. P. Solar, J. Organomet. Chem. 155, C-8 (1978).
8. T. S. Briggs, W. D. Gwinn, W. L. Jolly, and L. R. Thorne, J. Am. Chem. Soc. 100, 7764 (1978).
9. O. S. Mills and A. D. Redhouse, Chem. Commun. 444 (1966).
10. R. B. King and M. S. Saran, J. Am. Chem. Soc. 94, 1784 (1972).
11. A. B. Antonova, N. E. Kolobova, P. V. Petrovsky, B. V.

- Lokshim, and N. S. Obezylik, J. Organomet. Chem. 137, 55 (1977).
12. N. E. Kolobova, A. B. Antonova, O. M. Khetrova, M. Yu. Antipin, and Yu. T. Struchkov, J. Organomet. Chem. 137, 69 (1977).
13. D. L. Davies, A. F. Dyke, A. Endesfelder, S. A. R. Knox, P. J. Naish, A. G. Orpen, D. Plaas, and G. E. Taylor, J. Organomet. Chem. 198, C43 (1980).
14. D. R. Tyler, Ph.D. Thesis, California Institute of Technology, 1979.

PROPOSITION 2

Hydrogen and Halogen Gas Production by a Photochemical
Reductive-Elimination Catalyst

Due to current interest in systems of homogeneous catalysts, extensive studies have been made on oxidative-addition reactions of transition metal complexes.¹ One area of particular importance is that involving metals of a d^8 electronic configuration. These may be subdivided further into two classes:

- 1) Addition reactions of coordinately unsaturated, square planar complexes
- 2) Addition reactions of five coordinate complexes (usually having a trigonal bipyramidal configuration)

The former are perhaps the most thoroughly investigated²⁻¹⁴ due to initial interest in Vaska's¹⁴ and related complexes. Addition of small, covalent molecules (including oxygen, olefins, acetylenes, hydrogen, non-metal hydrides, hydrogen halides and other protonic acids, metal halides, alkyl halides, acyl halides, halogens, and pseudohalogens) to these complexes is well documented.^{16,17} In some cases the reactions are thermally reversible under mild conditions, and photochemical reductive elimination of thermally non-labile adducts has been shown by Geoffrey.¹⁵ Here, ultraviolet irradiation of the H_2 and O_2 adducts of $IrCl(CO)(PPh_3)_2$, $IrI(CO)(PPh_3)_2$, $Ir(2-phos)_2^+$, and $Ir(2=phos)_2^+$ induces reductive elimination of molecular hydrogen or oxygen and regeneration of the square planar complex.¹⁹ Reductive elimination of HCl from $IrH(Cl)(CO)(PPh_3)_2$ also occurs upon

irradiation of argon-purged systems.

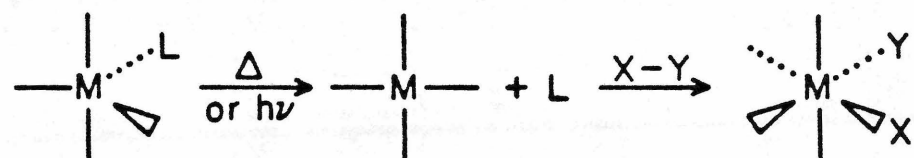
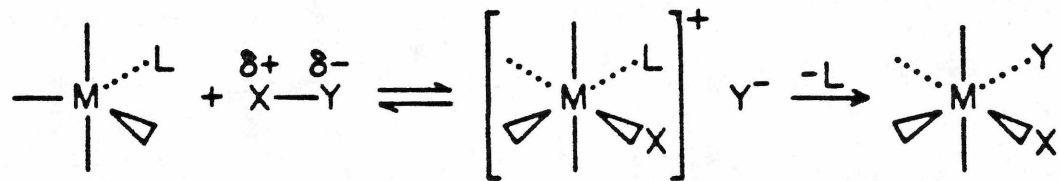
Less is known about the oxidative addition processes of d^8 complexes that are coordinately saturated. These reactions probably take place in two discrete steps, unlike their unsaturated counterparts, with loss of a neutral ligand. The reactions can be envisioned as proceeding by either of two pathways¹⁷ (Figure 1).

These compounds generally add only polar or electrophilic molecules, (e.g., hydrogen halides^{18,19} trifluoroacetic acid,²⁰ sulfonyl chloride,²⁰ strong acids, alkyl halides, tin halides,¹⁹ mercuric halides^{20,24,25} silicon hydrides,²¹ methyl iodide,^{20,22,23} halogens,^{4,18,22,26-28} and perfluoroalkyl halides) and do so in a consistently cis fashion. Obviously, unless either scheme 1 or 2 were reversible, simple reductive elimination would not result in the original complex. If it were possible to reductively eliminate the oxidative-addition adduct and reinsert the neutral ligand by photochemical techniques, then reversibility would be effected. This could provide methods for developing new homogeneous catalysts and/or enhancing the activity of known systems, since oxidative-addition and reductive-elimination reactions are important steps in the mechanisms by which catalysts for hydrogenation, hydrosilation, hydroformylation, and ethylene dimerization, etc., function.

Several systems are inherently interesting and might prove valuable to study. The relative reactivity of d^8

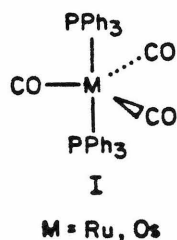
Figure 1

Oxidative addition of X-Y to coordinately
unsaturated d^8 complexes.



metals to undergo oxidative-addition reflects the stability of the corresponding d^6 configuration. This tendency increases in going from right to left and from top to bottom in the periodic table.¹ In an equivalent electron environment then, the relative order of reactivity would be $\text{Os}^0 > \text{Ru}^0 > \text{Fe}^0$, $\text{Ir}^{\text{I}} > \text{Rh}^{\text{I}} > \text{Co}^{\text{I}}, \text{Pt}^{\text{II}} \gg \text{Ni}^{\text{II}}, \text{Au}^{\text{II}}$.¹ Thus, complexes of Os^0 , Ru^0 , and Ir^{I} should be some of the most reactive species with regard to oxidative addition.

Reactions of bisphosphine complexes of $\text{Ru}(0)=\text{Ru}(\text{II})$ and $\text{Os}(0)=\text{Os}(\text{II})$ might be particularly interesting to study. The configurations of both have been established by infrared spectroscopy and the latter by X-ray diffraction²⁹ to be



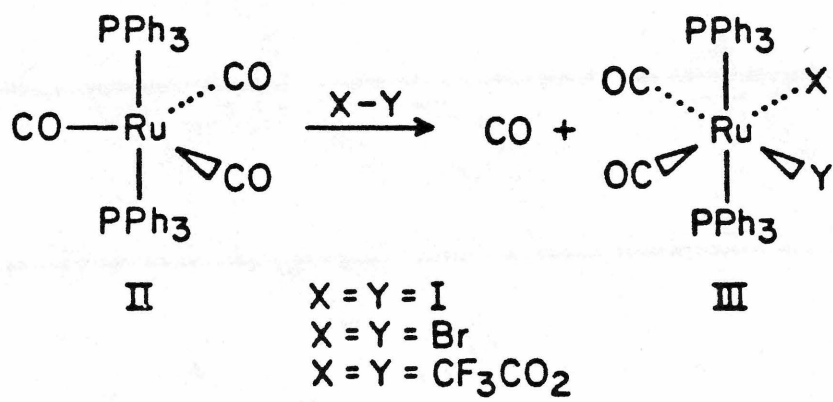
Both are known to undergo a series of oxidative-addition reactions for example, the ruthenium complex reacts with a variety of small molecules,³⁰ as depicted in Figure 2.

Addition of X-Y is cis, resulting in the stereochemistry indicated above for III. When X-Y is a hydrogen halide, the dihalide is formed and hydrogen gas is evolved. The dihalide is presumably formed via a hydride intermediate.

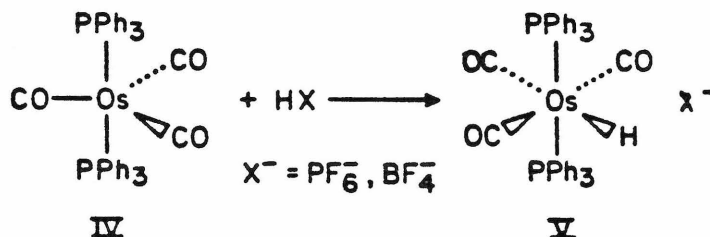
Similarly, hexafluorophosphoric and tetrafluoroboric acids react with $\text{Os}(\text{CO})_2(\text{PPh}_3)_2$ to form stable adducts^{31, 32}

Figure 2

Oxidative addition reactions of $\text{Ru}(\text{CO})_3(\text{PPh}_3)_2$.



as depicted in Figure 3:



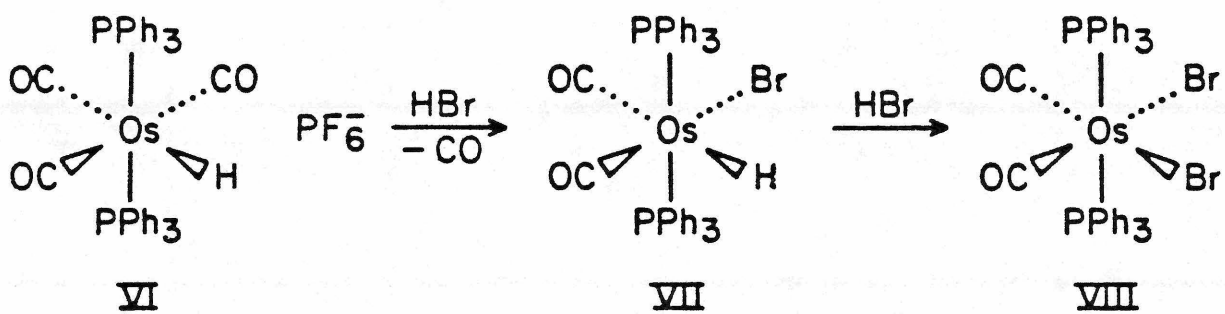
If a nucleophilic anion such as Br^- is present, one of the carbonyl groups is replaced, resulting in a neutral molecule. This, however, is unstable and reacts further with HBr, yielding H_2 and the dihalide (Figure 4).

In each of these cases, the initial step appears to be protonation, resulting in an octahedral d^6 configuration. The effectiveness of the trans-directory influence of ligands,³³ $\text{CO} > \text{PR}_3, \text{H}^-$, insures the loss of a mutually trans CO and thus formation of the cis oxidative-addition adduct. The stereochemistry has been proven by using dimethylphenylphosphine in place of triphenylphosphine in VIII in an NMR study. Furthermore, the infrared spectrum of the metal carbonyl region indicates a molecule of C_{2v} symmetry, consistent with VIII.

The reaction of $\text{M}(\text{CO})_3(\text{PPh}_3)_2$ and X-Y proceeds spontaneously with HCl, HBr, or HI and either the Ru or Os complex, yielding hydrogen gas and the dihalide. The reversibility of the reaction can be achieved in high yield by treatment of the latter with zinc dust in hot DMF under a CO

Figure 4

Reaction of $\text{OsH}(\text{CO})_3(\text{PPh}_3)_2$ with HBr.



atmosphere^{30,31} (Figure 5). Again, according to the trans-labilizing effect, the halide ligand would be expected to be the most labile:³⁴ $\text{CO} > \text{PR}_3 > \text{I}^- > \text{Br}^-, \text{Cl}^-$. The single IR stretching frequency for the metal carbonyl at 1895 cm^{-1} and 1890 cm^{-1} for the ruthenium and osmium complexes respectively, indicate that the reductive elimination and CO substitution yielded the starting trans-bistriphenylphosphine tricarbonyls.

Only one study has been done on the photochemical properties of the $\text{Ru}(\text{CO})_2\text{X}_2\text{L}_2$ series (L = a ligand with As or P donor atom, X = halogen). The work of Barnard³⁶ et al., indicated cis halogen and carbonyl complexes could be converted into their totally trans isomers by irradiation and that such was thermally reversible (Figure 6). Dissociation of a carbonyl ligand was postulated as the first step, as partial loss of CO resulted in the formation of $(\text{Ru}(\text{CO})\text{X}_2\text{L}_2)_2$ as a byproduct. So, although the carbonyl ligand is inert to thermal exchange (e.g., $\text{Ru}(\text{CO})_2(\text{PMe}_2\text{Ph})_2\text{Cl}_2$ can be heated to 80°C for several hours with no change³⁵), it can obviously be labilized by irradiation. This is to be expected as would a wavelength dependence on the type of elimination that prevails. No effort was made to isolate any wavelength of light, so this study provides no conclusive evidence against the possibilities of light initiated reductive elimination.

Figure 5

Reaction of $M(\text{CO})_3(\text{PPh}_3)_2$ to form $M(\text{CO})_3(\text{PPh}_3)_2$ ($M=\text{Ru,Os}$)

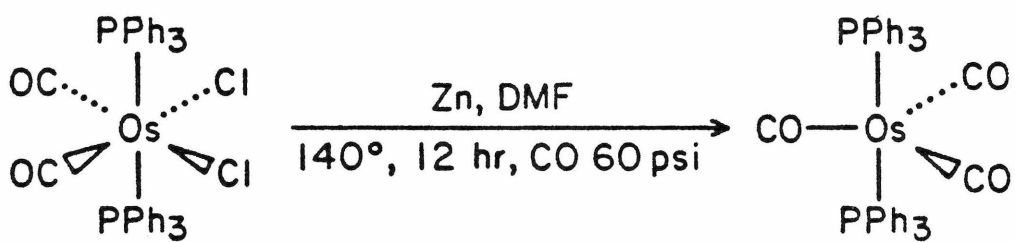
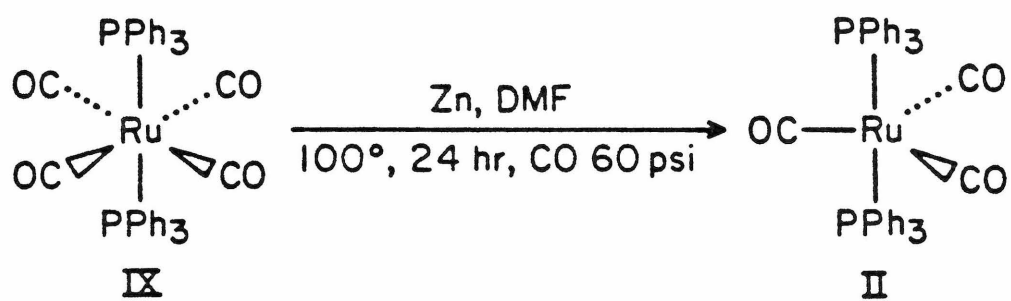
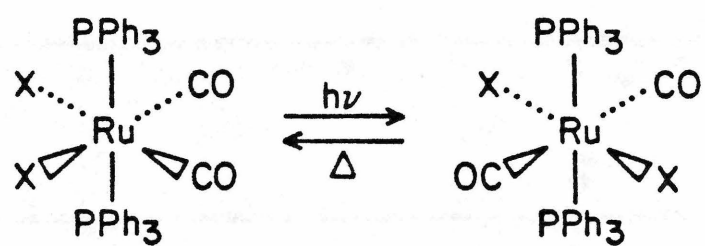


Figure 6

Photochemistry of $\text{Ru}(\text{CO})_3(\text{PPh}_3)_2$



The photochemical properties of these complexes depend on the electronic states, but there has been no attempt at any spectral analysis to date. If the system proved viable for reductive elimination, electronic absorption spectra would have to be measured in order to make definite band assignments and elucidate the nature of the excited states. Geoffrey's spectroscopic data for iridium complexes indicate that the lowest excited state of each is MLCT in nature.¹⁵ The photoelimination process could be attributed to this state; however, the mechanism of formation of the extruded covalent molecule is not clear. For the dihydride cases, Geoffrey also noted that both ligand field and LMCT states could be considered consistent with the observed photochemistry.¹⁶ Both of these were eliminated as there was only a very small shift in band position upon variation of the halogen in the complexes.³⁶ The energies of LF and LMCT transitions would be expected to be sensitive to changes in the halogen,³⁷ and such was not seen. The most probable mechanism was considered to be homolytic cleavage of the Ir-H bond producing H· and Ir(II). It would be interesting to study H₂ elimination, if such could be effected, in another system.

Both Ru(CO)₃(PPh₃)₂ and the osmium analogue³⁸ react with molecular hydrogen to produce H₂M(CO)₂(PPh₃)₂ at 120 atm and 130°C in THF. It would seem reasonable that these complexes could be synthesized thermally or perhaps photochemically and

reversibly so by the latter process. This would elucidate mechanistic aspects of elimination processes and the electronic states responsible.

Of primary interest, however, is the reaction with hydrogen halides. If it were possible to photochemically induce this reductive elimination, a neat and efficient homogeneous catalytic system for hydrogen and halogen gas production and energy storage could be achieved. Irradiation under a CO atmosphere or purge³⁹ at any time afterwards might reductively eliminate the halogen with regeneration of the initial catalyst. This cycle could conceivably be continued ad infinitum.

The ruthenium system is particularly interesting as it is important in the realm of catalysis: $\text{Ru}(\text{CO})_3(\text{PPh}_3)_2$ is one of the most effective ruthenium hydroformylation catalysts known.⁴⁰ Other five-coordinate complexes with catalytic activity could also be studied, and $\text{RuClH}(\text{PPh}_3)_3$,⁴⁰ $\text{RuCl}_2(\text{PPh}_3)_2$,⁴¹ and $\text{RhHCO}(\text{PPh}_3)_3$ ^{42,43} are likely candidates in this respect. If reductive elimination proved intractable for these saturated systems, investigation of square planar complexes such as $\text{RhCl}(\text{PPh}_3)_3$,⁴⁴⁻⁴⁸ $\text{RhH}(\text{CO})(\text{PPh}_3)_2$,⁴¹ $\text{RhCl}_2(\text{ethylene})_2$ ^{49,50} and $(\text{AsPh}_3)_2\text{Rh}(\text{CO})\text{Cl}$ ⁵¹ would be another possible avenue for research. They would provide attractive and interesting systems for spectroscopic and photochemical study in that they are catalytically important molecules. Such would elucidate both basic electronic states and

subsequent behavior and add to our understanding of the nature and reactions of an important class of compounds.

References

1. J. Halpern, Accts. Chem. Res. 3, 386 (1970).
2. L. Vaska, Accts. Chem. Res. 1, 335 (1968).
3. L. Vaska, J. Am. Chem. Soc. 83, 2784 (1961).
4. L. Vaska and J. W. Diluzio, J. Am. Chem. Soc. 94, 679 (1962).
5. L. Vaska and S. S. Bath, J. Am. Chem. Soc. 88, 1333 (1966).
6. L. Vaska, Science 140, 809 (1963).
7. L. Vaska and R. E. Rhodes, J. Am. Chem. Soc. 87, 4970 (1965).
8. L. Vaska, Science 152, 769 (1966).
9. L. Vaska and D. L. Eatone, J. Am. Chem. Soc. 88, 5324 (1966).
10. L. Vaska, L. S. Chen and W. V. Miller, J. Am. Chem. Soc. 93, 6671 (1971).
11. J. A. McGinnety, R. J. Doedens and J. A. Ibers, Inorg. Chem. 6, 2243 (1967).
12. L. Vaska, IXth International Conference on Coordination Chemistry, St. Moritz, 1966, Abstracts p. 332.
13. S. Doronzo and V. M. Bianco, Inorg. Chem. 11, 466 (1972).
14. L. Vaska, J. Am. Chem. Soc. 88, 5325 (1966).
15. G. L. Geoffrey, Ph. D. Thesis, CIT, 1974.
16. G. L. Geoffrey, G. S. Hammond and H. B. Gray, J. Am.

Chem. Soc. 97, 3933 (1975).

17. J. P. Collman and W. R. Roper, Adv. Organometal Chem. 7, 54 (1968).
18. L. Vaska and J. W. Diluzio, J. Am. Chem. Soc. 83, 2784 (1961).
19. J. Chatt and B. L. Shaw, J. Chem. Soc. 5075 (1962).
20. J. P. Collman and W. R. Roper, unpublished results.
21. A. J. Chalk and J. F. Harrod, J. Am. Chem. Soc. 87, 16 (1965).
22. V. Chatt and B. L. Shaw, J. Chem. Soc. 705, 4020 (1959).
23. R. Z. Heck, J. Am. Chem. Soc. 86, 2706 (1964).
24. R. S. Nyholm and K. Vrieze, Chem. Ind. (London) 318 (1964).
25. P. M. Adams, D. J. Cook and R. D. W. Kemmitt, Nature 205, 589 (1965).
26. L. Vallarino, J. Chem. Soc. 2287 (1957).
27. W. Hieber and E. Weiss, Z. Anorg. Allgem. Chem. 287, 223 (1956).
28. J. Chatt and B. L. Shaw, J. Chem. Soc. 2545 (1962).
29. J. A. Ibers and S. J. La Placa, Science 145, 920 (1964).
30. J. P. Collman and W. R. Roper, J. Am. Chem. Soc. 87, 4009 (1965).
31. J. P. Collman and W. R. Roper, J. Am. Chem. Soc. 88, 3504 (1966).
32. W. R. Roper, unpublished results.
33. L. Malatesta, M. Angoletta and F. Caglio, VIIIth

International Conference on Coordination Chemistry,
Vienna, 1964, Abstracts p. 210.

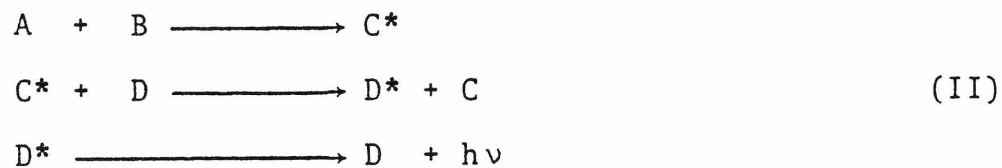
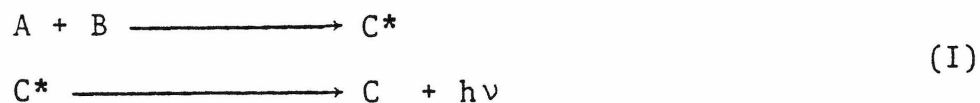
34. F. Basolo and R. G. Pearson, Mechanisms of Inorganic Reactions, A Study of Metal Complexes in Solution, John Wiley and Sons, Inc. New York, 1967, p. 355.
35. D. F. Shriver, "The Manipulation of Air Sensitive Compounds", McGraw-Hill, N.Y., 1969.
36. C. F. J. Barnard, J. A. Daniels, J. Jeffrey and R. J. Mawby, J. Chem. Soc. Dalton 953 (1976).
37. W. Strohmeier and F. J. Muller, Z. Naturforsch. 1324, 770 (1969).
38. G. L. Geoffrey, L. Vaska and H. B. Gray, unpublished results.
39. F. L. L'Eplattenier and F. Calderazzo, Inorg. Chem. 7 1290 (1965).
40. D. Evans, J. A. Osborn, F. H. Jardine, G. Wilkinson, Nature 208, 1290 (1965).
41. P. S. Hallman, D. Evans, J. A. Osborn and G. Wilkinson, Chem. Comm. 7, 305 (1967).
42. G. Yagupsky, C. K. Brown and G. Wilkinson, J. Chem. Soc. A, 1392 (1970).
43. C. K. Brown and G. Wilkinson, J. Chem. Soc. A, 2753 (1970).
44. F. H. Jardine, J. A. Osborn, G. Wilkinson and J. F. Young, Chem. and Inc. (London) 560 (1965).
45. J. A. Osborn, F. H. Jardine, J. F. Young and G.

- Wilkinson, J. Chem. Soc. A Inorg., Phys., Theoret. 1711 (1966).
46. J. Tsuji and K. Ohno, J. Am. Chem. Soc. 88, 3452 (1966).
47. J. Tsuji and K. Ohno, Tetrahedron Letters 4713 (1966).
48. J. Blum, E. Oppenheimer and E. D. Bergmann, J. Am. Chem. Soc. 89, 2338 (1967).
49. R. Cramer, J. Am. Chem. Soc. 87, 4717 (1965).
50. R. Cramer, J. Am. Chem. Soc. 89, 1633 (1967).
51. P. R. Rony and J. F. Roth, J. Mol. Catalysis 1, 13 (1975/6).

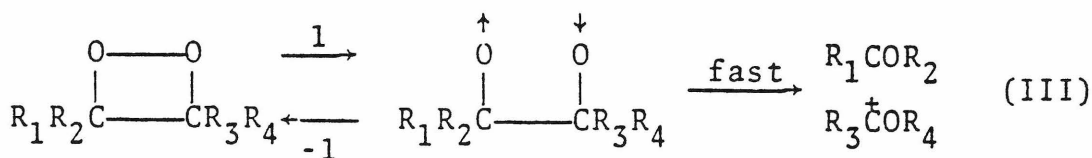
PROPOSITION 3

Synthesis and Reactivity of Silyldioxetanes

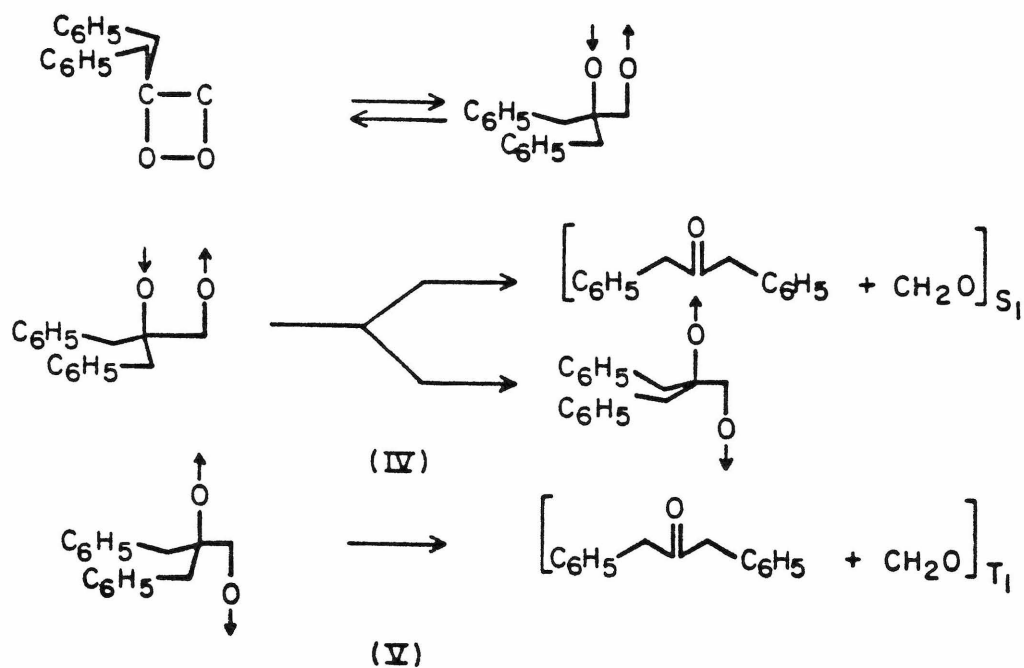
The cyclic four-membered peroxides known as dioxetanes comprise a unique and interesting class of compounds in that they produce electronically excited carbonyl moieties upon thermal decomposition.¹ This reaction is particularly important as it has been implicated in the bioluminescence of cyprindina hilygendorfi,^{2,3} the latia neritoides,⁴ and the firefly luciferin.⁵⁻⁸ Either of two processes is operative in these biological systems; the excited state intermediate produced is itself fluorescent or the excitation energy is transferred to an acceptor molecule that is fluorescent. These processes are indicated by Schemes I and II below, respectively:



Dioxetane sensitized chemiluminescence may be measured via Scheme II, with energy transfer from an excited state carbonyl species. Although there has been some controversy over the mode of decomposition, kinetic data and thermochemical calculations support a two-step, biradical mechanism:⁹



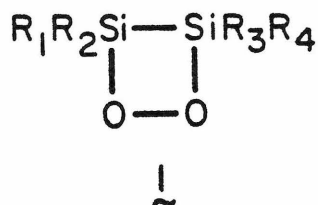
A modification of the above allows the originally formed singlet to undergo spin conversion, accounting for the observed production of triplet carbonyl species. For example in the case of 3,3-dibenzyl-1,2-dioxetane:¹⁰



Thermochemical calculations indicate and experimental evidence supports that only one excited state species is formed per dioxetane decomposition. The available energy is partitioned between the products, and this distribution can be calculated from the Boltzmann equation if the singlet pathway is not important.^{11,12} Thus it is possible to

produce discrete numbers of excited state molecules with known energies. These can be used to sensitize chemiluminescence or do "photochemistry without light".¹³

Although extensive studies have been made in the realm of organic peroxide chemistry, the analogous compounds of elements other than carbon have been virtually ignored. Very little, for example, is known about any peroxysilane, and no attempt has been made to even synthesize a silyl dioxetane. This species would be expected to show similar behavior to its carbon counterpart as an energy source and transfer agent. Also, the silyldioxetane and subsequent radicals produced might be expected to be more stable than their organic analogues due to a delocalization of electrons on to silicon through $d\pi - p\pi$ bonding not possible for carbon. This could elucidate mechanistic aspects of ring cleavage for both systems. If chemiluminescence is sensitized by the silyldioxetane in a manner similar to the carbon derivative, the existence of the elusive $Si = O$ species will be indicated. Furthermore, behavior of the $R-Si-O$ moiety is especially interesting as such is the fundamental linkage in the industrially important silicones. The silyldioxetane would provide a good model in this relation and possibly for a bonding calculation. For these reasons it is proposed to synthesize and study the cyclic inorganic peroxide 1



Part A. Primary Considerations: Contrasts in Carbon and Silicon Chemistry

In anticipation of the synthesis and study of silyl dioxetanes, it is necessary to consider the basic differences between carbon and silicon. Since both elements have similar electronic configurations ($C, 1s^2 2s^2 2p^2$; $Si, 1s^2 2s^2 2p^6 3s^2 3p^2$), similar physical and chemical properties would be expected. Within a broad framework this is true: silicon compounds are analogous in formula type while structure and behavior can be considerably different. Although silicon compounds are frequently more reactive than their carbon counterparts this tendency does not necessarily reflect less thermodynamic stability. In fact the bonds formed to silicon are often stronger than those to carbon as indicated below:¹⁴

Table 1. Bond Energies (kcal/mole)

<u>Silicon Bond</u>	<u>Bond Energy</u>	<u>Carbon Bond</u>	<u>Bond Energy</u>
Si-O	108	C-O	85.5
Si-F	135	C-F	116
Si-Cl	91	C-Cl	81
Si-Br	74	C-Br	68
Si-I	56	C-I	51
Si-C	76	C-C	82.6
Si-Si	53	C-Si	76

Another important difference between carbon and silicon is a reflection of the electronegativities of the two. Silicon is much more electropositive due to the increased shielding efficiency of the nuclear charge by filled orbitals. Therefore, ionic bond character and the possibility of heterolytic cleavage must be considered. Using Pauling's scale of electronegativity, the difference between silicon and other elements, percent ionic character for bonds, and ionic bond energies are tabulated below:^{15,16}

Table 2. Electronegativity, Ionic Character, and Ionic Bond Energy (kcal./mole) of Si-X Bonds

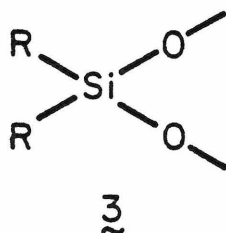
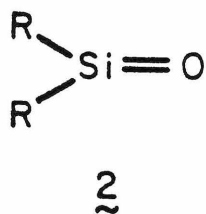
<u>Element</u>	<u>Electro- negativity</u>	<u>Δ Electro- negativity</u>	<u>% Ionic Character</u>	<u>Ionic Bond Energy</u>
Si	1.8	0	0	0
C	2.5	.7	12	222.9
H	2.1	.3	2	249.8
F	4.0	2.2	70	237.4
Cl	3.0	1.2	30	190.3
Br	2.8	1.0	22	179.0
I	2.4	.6	8	167.4
O	3.5	1.7	50	242.4
S	2.5	1.7	12	192.7

It is obvious that while the C-H bond would be expected to cleave yielding a proton, Si-H fragmentation would result in Si⁺ and a hydride ion. Thus, the difference in ionicity

will be reflected in bond strengths, and susceptibility and direction of attack.

Another reason for the increased reactivity of silicon derivatives is its larger size, 1.17 Å as opposed to .77 Å for carbon.¹⁷ Since silicon is about 50% larger, there is considerably less steric hindrance to attack. Many intermediates are postulated to be five-coordinate, so that considerable new bond making can be accomplished without prior loss of a coordinated group. In fact, many penta- and hexa-coordinated silyl compounds are known--the most familiar being SiF_6^{2-} .¹⁸ This increase in coordination number is possible due to the empty 3d orbitals available for bonding and stabilization of intermediates and transition states.^{19,20} The diffuseness of these orbitals makes them especially good at stabilization even at large internuclear distances. This participation by orbitals unavailable to carbon (due to the large energy gap between the 2p and 3d levels) is probably the most important reason for the increased reactivity of silicon. Another anomaly between carbon and silicon is the absence of any stable and characterized species containing formal multiple bonds for the latter. Several theories have been postulated to account for this incongruous behavior. First of all, this lack of multiply-banded species has been attributed to the formation of extremely strong σ bonds.²¹ For example, a silicon atom may combine with oxygen and alkyl groups in either of two

ways:

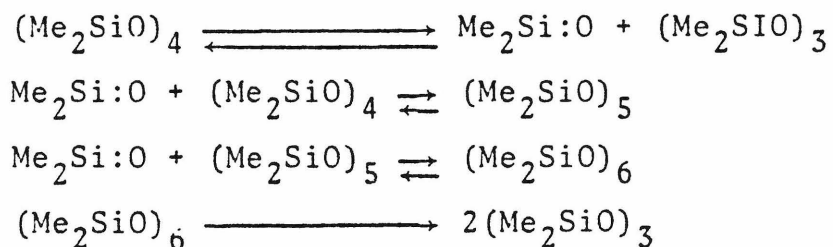


If the energy of the doubly bonded species is greater than twice the singly bonded one, the former will be thermodynamically more stable. However, the Si-O bond energy is known to be greater than that of C-O. So, even if Si=O and C=O are similar, it is conceivable that $2E(\text{Si-O})$ is larger than $E(\text{Si=O})$.

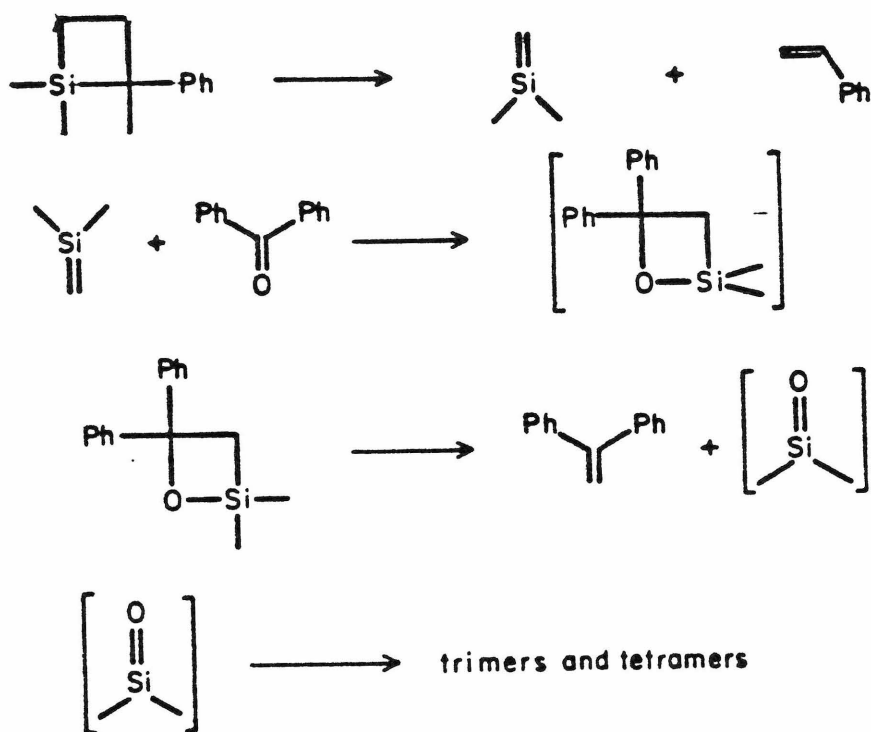
This argument loses credibility when considering π bonding for Si=Si and Si=C, as the singly bonded species are not inordinately strong. Here steric considerations are invoked¹⁷ --perhaps the greater bond length due to the size of the silicon atom makes $p\pi - p\pi$ overlap too small.^{21,22} Similarly, the 3p orbitals might be too diffuse,²³ although this is not supported by calculations using Slater orbitals.^{24,25} That interelectronic repulsions become important in the closer proximity requisite for multiple bonding has also been proposed,²² but the existence of P=O and S=O are contradictory to this argument. Another possible explanation is that the availability of the 3d orbitals facilitates conversion of double bonds²⁶ by increasing the number of σ bonds. The true explanation may be kinetic and/or a combination of all of these factors.

Recently data have been compiled evidencing that

silicon analogues to unsaturated compounds do exist²⁷ if only as short-lived intermediates during the formation of more stable products. Numerous examples in the literature support the formation of Si-C,²⁸⁻³³ Si=Si^{28,29,34,35} and Si=O^{30-33,36} moieties. The latter is of particular interest here, for silyldioxetane decomposition should initially yield a double bonded silicon-oxygen species if analogous to carbon chemistry. Reports of pyrolyses of cyclic-carbosiloxanes indicate that the products formed are consistent with loss of a silyl ketone group.³⁷⁻³⁹ Similar results were obtained for thermal decompositions of cyclo-siloxanes.^{36,40,41} For example dimethylsilanone is postulated as an intermediate in the gas phase pyrolysis of octamethylcyclotetrasiloxane yielding hexamethylcyclotrisiloxane and decamethylcyclopentasiloxane as the only products:³⁶

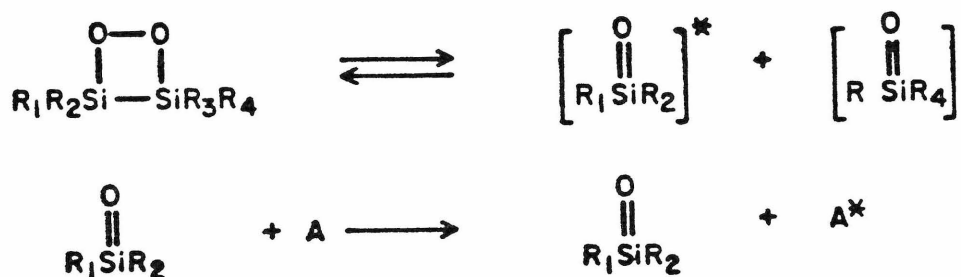


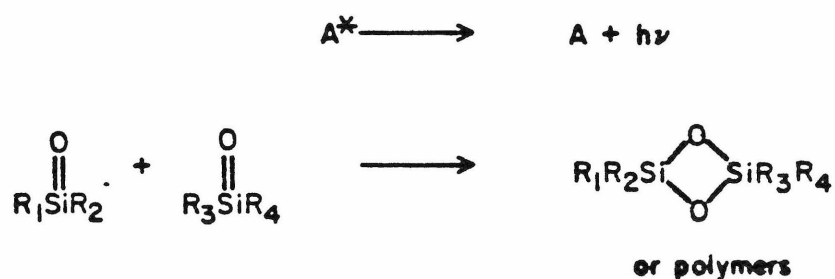
Similarly copyrolysis of 1,1-dimethyl-2-phenyl-1-silacyclobutane and benzophenone leads to products consistent with intermediate dimethylsilanone formation:³³



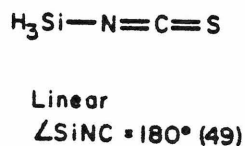
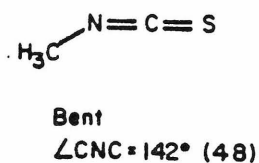
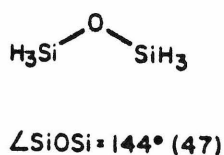
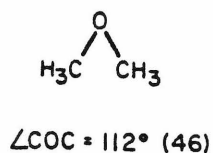
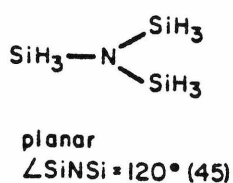
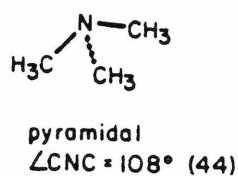
Results consistent with this mechanism are also obtained for silacyclobutane and a number of its derivatives with and without various trapping agents.³⁰

Thus, it seems very possible that silyldioxetane decomposition could lead to an excited-state silylcarbonyl moiety that might transfer its energy before rearrangement to a siloxane or silicone configuration. For example,





Dative $d\pi - p\pi$ bonding may also play a role in silyl-dioxetane chemistry, as there is ample evidence for this phenomenon in many silicon compounds. Differences in bond angles, bond strengths, and reactivity for silicon and carbon analogues indicate a bond order greater than one for the silyl derivatives.^{42,43} Structural differences, for example, are evidenced in the following compounds:



These differences have been rationalized in terms of maximum $p\pi - d\pi$ overlap.¹⁷ The configuration is altered upon going from carbon to silicon substitution so that the non-bonding electrons on nitrogen or oxygen have more p character and can delocalize onto silicon d orbitals. Intranuclear distances between Si-O and Si-N are also considerably shorter than would be expected for a single bond.¹⁷ Similarly, differences in the reactivity of alkyl and silyl-substituted amines⁵⁰⁻⁵⁴ implicate some degree of $p\pi - d\pi$ bonding. The latter exhibit reduced electron donor ability for nitrogen with concomitant loss of electron acceptor ability for silicon, consistent with nonbonding electron donation onto silicon. The implications for a silyldioxetane are obvious--some degree of dative Si-O multiple bonding should exist and conjugation throughout the ring is possible.

The π interactions between silicon and unsaturated substrates is also important. This results in electron delocalization onto the metal, strengthening of the Si-L bond, weakening of the substituent π bonding, and perturbation of the electronic spectrum. When the ligand π system is symmetrical around the molecular bond, interactions should be seen regardless of orientation. But for substituents such as phenyl, orientation of the nodal planes must coincide with the d orbitals in a certain way and rotation around the molecular axis must be minimal for interaction to

be important. Evidence for this type of bonding has been found in a detailed study of the UV spectra of $\text{Me}_3\text{SiC}_6\text{H}_5$ and its derivatives.⁵⁵ Similarly ESR^{56,57} studies of aromatic silicon compounds with an odd electron indicate delocalization from the ring to the silicon center, although there is little evidence for interaction between two or more aromatic substituents attached to the same silicon atom.⁵⁸ Thus, the data indicate that stabilization due to π interaction might be operative throughout the phenyl-silicon-oxygen system in an aromatic substituted silyldioxetane.

While the existence of $d\pi - p\pi$ interaction is obvious, how this is physically possible is not clear. Due to screening by s and p electrons, the d shells are considerably higher in energy and more diffuse than the s and p orbitals. Calculations for the ground state electronic configuration are hazardous at best, as it is not possible to meaningfully assess the value of the unoccupied d orbitals. However, an H-F calculation in Table 3 allows at least a qualitative evaluation.⁵⁹

Table 3. Calculated Values for the Orbital Energies and Mean Radii for the Outer Electrons in Some Configurations of Silicon, Obtained by the Hartree Fock Method

<u>Configuration</u>	<u>Term</u>	<u>Orbital</u>	<u>Mean Radius, Å</u>	<u>Orbital Energy, eV</u>
s^2p^2	3P	3s	1.17	-14.7
		3p	1.46	- 8.1
s^2pd	3F	3s	1.12	-18.2
		3p	1.37	-11.5
		3d	3.67 (max. at 2.9)	- 1.8
spd^2	5G	3s	1.06	-27.2
		3p	1.18	-19.9
		3d	2.44	- 2.9

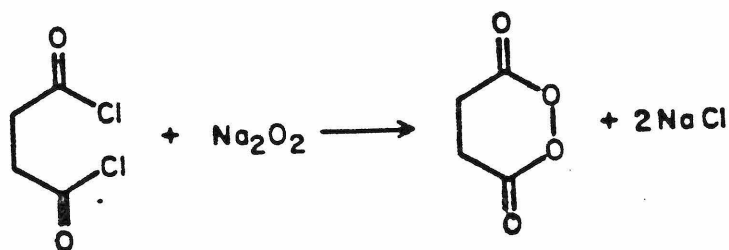
Even for the spd^2 configuration, energy and mean radii differences are considerable. If this were actually the case, it would be difficult to understand how the d orbitals could participate in ground state interactions. One explanation is that electronegative ligands can bring about a contraction of the d orbitals which are sensitive to the effective nuclear charge.⁶⁰⁻⁶⁴ The d orbitals contract in space and drop in energy relative to the s and p orbitals as the charge on the atom increases. Alternatively, calculations⁶⁴ using self consistent field (SCF) wave functions result in less diffuse d orbitals and increasing π overlap. For

example a SCF-MO calculation by Perkins⁶⁵ for $(\text{SiH}_3)_3\text{N}$ indicates π bond stabilization of ca 48 kcal/mole and appreciable electron donation onto silicon. A calculation for the silyl dioxetane system would be particularly interesting for, as mentioned earlier, it could be considered a model for the larger silicone systems.

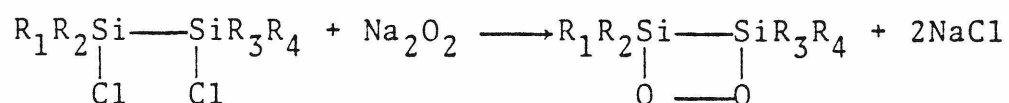
These factors (greater reactivity, reluctance to form stable double bonded adducts, dative $d\pi - p\pi$ bonding, and the influence of the vacant 3d orbitals) will all have an effect on the synthesis and behavior of silyldioxetanes. While these factors should be kept in mind, the magnitude and direction of influence will have to be ascertained in the laboratory rather than by speculation.

Part B. Synthesis and Study of Silyldioxetanes

An immediate problem arises when considering the synthesis of silyldioxetanes. A method analogous to that used for carbon is not possible, as the α -bromohydroperoxide⁶⁶ precursor is prepared from an olefin, and the corresponding silene is nonexistent. Fortunately, this very reluctance of silicon to form doubly bonded species allows synthetic routes unavailable for alkyl dioxetanes. Either of two methods might prove viable. The first is analogous to work done by Dervan⁶⁷ forming cyclic peroxy-compounds by the action of sodium peroxide on dichlorodiketones:

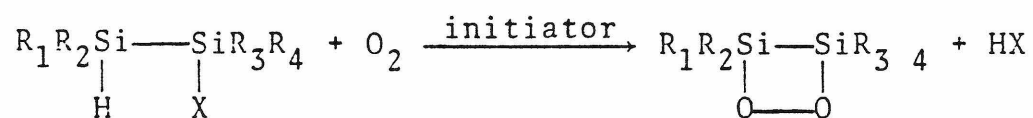


It seems entirely feasible that this scheme could be employed to synthesize the silyldioxetane:



This type of reaction would not be possible with the carbon analogue as chlorine displacement would result in double bond formation; for the silicon system there is no such worry. Too, the $R_4X_2Si_2$ precursor is easily synthesizable⁶⁸ and should be commercially available.

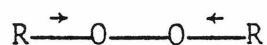
A second possible synthetic route is the autooxidation of the disilyl complex as indicated below:



The reluctance of Si=Si bond formation would again result in ring closure being the preferential reaction. This method seems less promising than the first, however, for two reasons: 1) silicon hydrides are substantially less stable than their alkyl derivatives, and 2) the acid medium generated might induce decomposition via silanol production and subsequent condensation.⁶⁹

The choice of substituents is primarily a question of stability. Brook⁷⁰ and others have demonstrated that compounds containing alternating silicon and oxygen linkages readily rearrange. Also, both triorganosilyl hydroperoxides and bistrisorganosilyl peroxides are known to undergo facile decomposition leading to the more stable siloxane and/or silicone configurations.⁷¹⁻⁷⁴ Primary synthetic efforts should be directed toward making the silyl dioxetane least susceptible to this type of rearrangement. Thus, substituents that stabilize the Si-Si bond would enhance possibilities for a successful synthesis of the peroxide (and, perhaps, entrapment of the initial radical formed--if a two step mechanism is operative). Preparation of 3,3,4,4-tetra-phenylsilyldioxetane is an excellent choice due to the known stabilization of Si-Si bonds by aromatic and vinyl substitution.⁷⁵⁻⁷⁷ The phenyl moiety might also stabilize the initial radical formed from O-O bond cleavage by delocalization of the odd electron in the same way the benzyl radical is stabilized. Admittedly the aromatic group is an atom removed from the radical center, but some oxygen $p\pi$ -silicon- $d\pi$ -phenyl- $p\pi$ conjugation might be possible if rotation around the C-Si bond is not important.

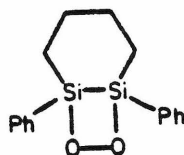
Alternately, the traditional explanation for stabilization effects on O-O bonds in peroxide centers is the ability of substituents to minimize the charge on the opposed dipoles of the two oxygen atoms:⁶⁹



In this light electron withdrawing groups such as methoxy or ethoxy would be expected to enhance peroxide stability. The silyl analogue of cis-diethoxy-1,2,-dioxetane (a known participant in chemiluminescent systems)⁷⁸ is not feasible as the hydride substituents would increase the likelihood of rearrangement, but alkylated ethoxysilyldioxetanes should be fairly stable. Here, though, a delicate balance of stability factors comes into play--electron withdrawing groups will stabilize the O-O linkage, but destabilize the Si-Si bond by increasing the positive charge on silicon. Which factor is more important will have to be determined experimentally.

Steric factors should also be considered--if the increase in reactivity and subsequent cleavage of disilyl complexes is due to the ease of formation of pentavalent silicon through d bonding, bulky substituents will make this route to decomposition less likely. Thus groups like t-butyl or cyclohexyl will "stabilize" the Si-Si moiety by making it less accessible to attack. This has been evidenced with silanols: although variously substituted silanols are known to undergo facile condensation, 1,1,2,2-tetracyclohexyl-1,2-dihydroxydisilane and other sterically hindered species are inert.⁷⁹ Also, naphthyl substituents would lend not only added bulk but also an unsaturated moiety for conjugation⁸⁰ and, therefore, be an excellent choice. A final possibility

is the bicyclic system below:



This could be made from the halogenated complex and Na_2O_2 .⁸¹

Thus synthesis of phenyl-, naphthyl-, t-butyl-, and cyclohexylsilyldioxetanes and combinations thereof should yield a rich variety of silyldioxetanes. This series of compounds could then be studied for energy transfer capabilities and mechanistic considerations. Decompositions could be effected and the various rates compared for substituent and solvent dependencies. If a two step mechanism is operative, substituents should have much less effect on the rate of reaction. If cleavage of the O-O and Si-Si bonds is concerted, unsaturated substituents should markedly influence the rate by participating in the developing π -carbonyl character of the activated complex. Similarly, solvent effects would be minimal if ring opening to a neutral oxy-biradical rather than the polar carbonyl species is rate determining.

Of primary interest is determining whether this reaction yields an electronically excited intermediate via initial silyl carbonyl formation. Thermolysis of the various silyldioxetanes could be done in the presence of fluorescent acceptors such as DPA and DBA to test for chemiluminescence. If evidence were found for this

phenomenon, silyldioxetanes would provide a new and interesting class of compounds for the study of energy generation and transfer, and "photochemistry without light" could be accomplished by the generation of the elusive silylketone moiety. For these reasons preparation and investigation of silyldioxetanes would be an attractive and worthwhile pursuit.

References

1. W. H. Richardson, F. C. Montgomery, M. B. Yelvington, and G. Ranney, J. Amer. Chem. Soc. 96, 4045 (1974).
2. F. McCapra and Y. C. Chang, Chem. Comm. 1011 (1967).
3. T. Goto, "Symposium on the Chemistry of Natural Products," Vol. 5, Butterworth, London, 1968, p. 431.
4. F. McCapra and R. Wigglesworth, J. Chem. Soc. D. 91 (1969).
5. E. H. White, M. W. Cass, T. A. Hopkins, and H. H. Seliger, J. Amer. Chem. Soc. 89, 7148 (1967).
6. D. J. Plant, E. H. White, and W. D. McElroy, Biochem. Biophys. Res. Commun. 31, 98 (1968).
7. F. McCapra, Y. C. Chang, and V. P. Francois, Chem. Comm. 22 (1968).
8. E. H. White, E. Rapaport, T. A. Hopkins, and H. H. Seliger, J. Amer. Chem. Soc. 91, 2178 (1969).
9. W. H. Richardson, F. C. Montgomery, M. B. Yelvington, and H. E. O'Neal, J. Amer. Chem. Soc. 96, 7525 (1974).

10. W. H. Richardson, F. C. Montgomery, and M. B. Yelvington, J. Amer. Chem. Soc. 94, 9277 (1972).
11. N. J. Turro and P. Lechtken, J. Amer. Chem. Soc. 94, 2886 (1972).
12. E. H. White, J. Wiecke, and D. F. Roswell, J. Amer. Chem. Soc. 91, 5194 (1969).
13. T. Cottrell, "The Strength of Chemical Bonds", pp. 270-280, 2nd ed. Butterworth, London (1958).
14. L. Pauling, "The Nature of the Chemical Bond", p. 64, 2nd ed. Cornell Univ. Press, Ithaca, NY (1948).
15. C. Eaton, J. Chem. Soc. 3077 (1950).
16. R. A. Shaw, J. Chem. Soc. 2831 (1957).
17. B. J. Aylett, Adv. Inorg. and Rad. Chem. 11, 255 (1968).
18. J. A. A. Keteelar, Z. Kristallog. 92, 155 (1935).
19. C. Eaborn, "Organosilicon Chemistry", Butterworth, London (1960).
20. L. H. Sommer, "Stereochemistry, Mechanism and Silicon", McGraw-Hill, NY (1965).
21. R. S. Mulliken, J. Am. Chem. Soc. 72, 4493 (1950).
22. R. S. Pitzer, J. Am. Chem. Soc. 70, 2110 (1948).
23. B. E. Douglass and D. H. McDaniel, "Concepts and Models of Inorganic Chemistry", p. 58, Ginn, Boston (1965).
24. R. S. Mullikan, C. A. Rieke, D. Orloff, and H. Orloff, J. Chem. Phys. 17, 1248 (1948).
25. H. H. Jaffé, J. Chem. Phys. 21, 258 (1953).

26. E. H. Eyster, R. H. Gillette, and L. O. Brockway, J. Amer. Chem. Soc. 62, 3236 (1940).
27. L. E. Gusel'nikov, N. S. Nametkin, and V. M. Vdovin, Accts. Chem. Res. 8, 18 (1975).
28. M. J. S. Dewar, D. H. Lo, and C. A. Ramsden, J. Amer. Chem. Soc. 97, 1311 (1975).
29. D. N. Roark and G. J. O. Peddle, J. Amer. Chem. Soc. 94, 5837 (1972).
30. T. J. Barton, G. Marquardt, and J. A. Kilgow, J. Omet. Chem. 85, 317 (1975).
31. C. M. Galino, R. D. Bash, and L. H. Sommer, J. Amer. Chem. Soc. 97, 7371 (1975).
32. W. Ardo, A. Sekiguchi, and R. Migita, J. Amer. Chem. Soc. 97, 7159 (1975).
33. P. B. Valkovich and W. P. Weber, J. Org. Chem. 40, 229 (1975).
34. T. J. Barton and J. A. Kilgour, J. Amer. Chem. Soc. 98, 7231 (1976).
35. T. J. Barton and J. A. Kilgour, J. Amer. Chem. Soc. 96, 7150 (1974).
36. I. M. T. Davidson and J. F. Thompson, Chem. Comm. 251 (1971).
37. N. S. Nametkin, L. E. Gusel'nikov, T. H. Islamov, N. V. Shishkira, and V. M. Vdovin, Dokl. Akad. Nauk SSSR 175, 135 (1967).
38. N. S. Nametkin, T. H. Islamov, L. E. Gusel'nikov, A. A.

- Sobtsov, and V. M. Vdovin, Izv. Akad. Nauk SSSR, Serkhin 90 (1971).
39. N. S. Nametkin, T. H. Islamov, L. E. Gusel'nikov, and V. M. Vdovin, Usp Khim 41, 203 (1972).
40. T. Kh. Islamov, Ph.D. Thesis, Institute of Petrochemical Synthesis, Moscow, 1970.
41. L. E. Gusel'nikov, N. S. Nametkin, T. H. Islamov, A. A. Sobtsov, and V. M. Vdorin, Izv. Akad. Nauk SSSR, Serkhin 84 (1971).
42. K. Kimura and M. Kubo, J. Chem. Phys. 30, 151 (1959).
43. E. A. V. Elsworth and A. J. Downs, J. Chem. Soc. 3516 (1960).
44. L. O. Blockway and F. T. Wall, J. Am. Chem. Soc. 56, 2373 (1934).
45. K. Hedberg, J. Am. Chem. Soc. 77, 6491 (1955).
46. P. H. Kasai and R. J. Myers, J. Chem. Phys. 30, 1096 (1959).
47. A. Almenningen, O. Bastiansen, V. Ewing, K. Hedberg, and M. Troetteberg, Acta Chem. Scand. 17, 2455 (1963).
48. C. I. Beard and B. P. Dailey, J. Amer. Chem. Soc. 71, 929 (1949).
49. D. R. Jenkins, R. Kewley, and T. M. Sugden, Trans. Faraday Soc. 58, 1284 (1962).
50. H. C. Brown, H. Bartholomay, and M. D. Taylor, J. Amer. Chem. Soc. 66, 435 (1944).
51. S. Sujeshi and S. Witz, J. Amer. Chem. Soc. 76, 4631

- (1954).
52. B. J. Aylett, J. Inorg. and Nuc. Chem. 15, 87 (1960).
53. B. J. Aylett and L. K. Peterson, J. Chem. Soc. 4043 (1965).
54. E. A. V. Ebsworth and M. J. Mays, J. Chem. Soc. 3893 (1963).
55. J. F. Brown and P. T. Prescott, J. Amer. Chem. Soc. 86, 1402 (1960).
56. M. G. Townsend, J. Chem. Soc. 51 (1962).
57. M. D. Curtis and A. L. Allred, J. Amer. Chem. Soc. 87, 2554 (1965).
58. H. H. Jaffe, J. Chem. Phys. 22, 1430 (1954).
59. A. G. MacDiarmid, "The Bond to Carbon", p. 10, Dekker, Inc., New York (1968).
60. D. P. Craig and D. W. Magnusson, J. Chem. Soc. 4895 (1956).
61. D. P. I. Craig, A. Maccoll, R. S. Nyholm, L. E. Orgel, and L. E. Sutton, J. Chem. Soc. 332 (1954).
62. D. P. Craig, "Chemical Society, Symposia at Bristol", Chem. Soc. (London), Spec. Publ. 12, 343 (1958).
63. D. P. Craig and C. Zauli, Gazz. Chem. Ital. 90, 1700 (1960).
64. D. W. J. Cruickshank, B. C. Webster, and D. F. Mayers, J. Chem. Phys. 40, 3733 (1964).
65. P. G. Parkins, Chem. Comm. 268 (1967).
66. W. H. Richardson and I. F. Hodge, J. Amer. Chem. Soc.

- 93, 3996 (1971).
67. Peter Dervan, personal communication.
68. H. Gilman, T. C. Wu, H. A. Hartzfeld, G. A. Guter, A. G. Smith, V. V. Goodman, and S. H. Eidt, J. Amer. Chem. Soc. 74, 561 (1952).
69. R. R. Hatt, Can. J. of Chem. 42, 985 (1964).
70. A. G. Brook, Accts. Chem. Res. 7, 77 (1974).
71. W. Hahn and L. Metzinger, Makromol. Chem. 21, 113 (1956).
72. R. A. Pike and L. H. Shaffer, Chem. and Ind. (Rev) 1294 (1957).
73. R. L. Dannley and G. Jalics, J. Chem. Soc. 3848 (1965).
74. A. K. Shubber and R. L. Dannley, J. Org. Chem. 36, 3784 (1971).
75. M. Kumada and K. Tamao, Adv. Organomet. Chem. 6, 55 (1968).
76. H. Sakurai and M. Kira, J. Amer. Chem. Soc. 96, 791 (1974).
77. H. Sakurai, S. Tasaka, and M. Kira, J. Amer. Chem. Soc. 94, 9285 (1972).
78. T. Wilson and P. Shaap, J. Amer. Chem. Soc. 93, 4126 (1971).
79. K. W. Palmer and F. S. Kipping, J. Chem. Soc. 1020 (1930).
80. A. R. Lapley, J. Amer. Chem. Soc. 86, 2545 (1964).
81. D. A. Armitage, Organomet. Chem. 1, 117 (1971).

PROPOSITION 4

A Chemically Induced Dynamic Nuclear Polarization (CIDNP)

Study of Pt(IV) Alkyl Complexes

Interest in transition metal alkyl complexes has increased dramatically in recent years as they have been found to be more abundant and stable than heretofore recognized. In particular thermal decompositions have been studied extensively revealing a variety of decomposition pathways including α ,¹ β ,² and reductive eliminations^{3,4} and homolysis of the carbon metal bonds.⁵ In contrast, although a number of metal-alkyl systems have been studied photochemically, most of the information gleaned has been qualitative in nature; few quantitative mechanistic studies have been made. Furthermore, while it has been generally claimed that photochemical cleavage results in radical formation via homolysis,⁶ there is little evidence to support this speculation and conflicting data are often the case rather than the exception.

In order to gain insight into the mechanism of possible radical reactions, we propose to study the photochemical decomposition of a series of metal-alkyl complexes by the technique of chemically induced dynamic nuclear polarization (CIDNP).⁷⁻¹¹ In this technique the nuclear magnetic resonance spectrum (NMR) is followed during the course of the reaction. A product arising from radical precursors will exhibit a polarized spectrum, resulting in peaks of enhanced absorption (A) or emission (E). In addition to this simple diagnosis, more detailed information, including the history of radical pairs preceding product formation and their dynamic behavior, may be derived from signs of the hyperfine

coupling constants, g factor differences, precursor multiplicities, and signs of the nuclear spin coupling constants.

For reactions run in high magnetic fields, qualitative predictions and interpretation of experimental data may be made on the basis of two rules. This may be exemplified by the pair of radicals a and b with g factors g_a and g_b , $\Delta g = g_a - g_b$, nuclei i and j, and hyperfine coupling constants A_i and A_j . If nucleus i belongs to radical a, the CIDNP spectrum of nucleus i can be coupled to nucleus j with a nuclear spin coupling constant J_{ij} . This can be described by the signs of two quantities Γ_{ne} for net effects (A,E) and Γ_{me} for multiplet effects (E/A, A/E):

$$\Gamma_{ne} = \mu \epsilon \Delta g a_i$$

$$\Gamma_{ne} = + = \text{net absorption, A}$$

$$\Gamma_{ne} = - = \text{net emission, E}$$

$$\Gamma_{me} = \mu \epsilon a_i a_j J_{ij} \sigma_{ij}$$

$$\Gamma_{me} = + = \text{low field part E, high field part A in a multiplet, E/A}$$

$$\Gamma_{me} = - = \text{high field part E, low field part A in a multiplet, A/E}$$

Definitions of parameters are as follows:

$\mu = +$ for a triplet or free precursor. A free precursor derives each of the fragments of the

radical from a different source.

$\mu = -$ for a singlet precursor

$\epsilon = +$ for products from recombination within the original cage

$\epsilon = -$ for products from fragments which escape the original cage

$\Delta g =$ the sign of $(g_i - g)$ where g_i is the g factor for the radical fragment containing nucleus i and g is the factor for the other radical fragment. The g values are obtained from ESR data.

$a =$ the sign of the hyperfine coupling constant. The sign is generally obtained from ESR data on stable free radicals.

$J_{ij} =$ the sign of the nuclear spin coupling constant between nuclei i and j . The sign is generally available from NMR data.

$\sigma_{ij} = +$ if nuclei i and j are originally in the same radical fragment.

$\sigma_{ij} = -$ if nuclei i and j are originally in different radical fragments.

The CIDNP observed will be opposite for products derived from singlet versus triplet precursors and for original cage versus escape products. Furthermore, if the reactant shows substantial polarization, it must necessarily have been reformed from radical species. Therefore, CIDNP can give

evidence for rapid recombination resulting in no net reaction which would explain low quantum yields or "apparent" lack of reactivity.

For this study a series of platinum(IV) complexes of the type $\text{PtR}_3\text{L}_2\text{X}$, PtR_4L_2 and $\text{PtR}_2\text{R}'\text{L}_2\text{X}$ (Table 1)^{12,13} will be investigated using the CIDNP technique. Examination of the configurations of these complexes (Figure 1) would lead one to conclude that reductive eliminations of the type shown in Equation 1 might be facile. This is indeed the case upon

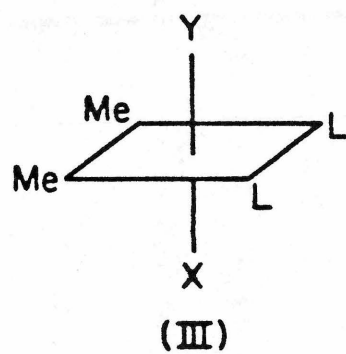
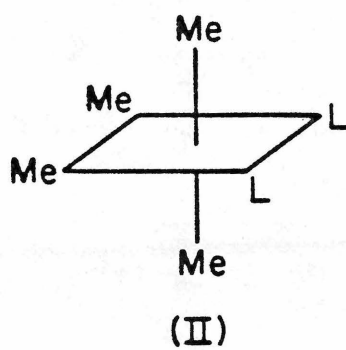
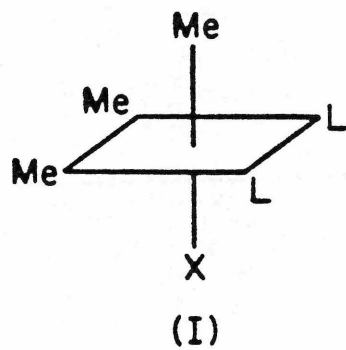


thermal decomposition as indicated by the data in Table 2.^{12,13} Different results, however, can be obtained photochemically: in the photolysis of $\text{PtMe}_3(\text{PMe}_2\text{Ph})\text{I}$ both ethane and methane were observed implying that decomposition did not proceed via a concerted pathway.¹⁴ Similar contrasting modes for decomposition were seen for some platinum(II) complexes. Thermolysis of cis- PtR_2L_2 ($\text{R} = \text{Ph}, \text{C}_6\text{H}_4\text{Me-4}$; $\text{L} = \text{PPh}_3, \text{PMe}_2\text{Ph}, \text{P}(\text{C}_6\text{H}_4\text{Me-4})_3$; $\text{L}_2 = \text{Ph}_2\text{PCH}_2\text{PPh}_2, \text{Ph}_2\text{CH}_2\text{CH}_2\text{PPh}_2$, or $\text{Me}_2\text{PCH}_2\text{CH}_2\text{PMe}_2$) led to concerted reductive elimination of biaryl.¹⁵⁻¹⁷ Photochemical studies of cis- PtR_2L_2 ($\text{R} = \text{CH}_3, \text{CH}_2\text{CH}_3$; $\text{L} = \text{PPh}_3, \text{L}_2 = \text{Ph}_2\text{CH}_2\text{CH}_2\text{PPh}_2$) complexes by two independent researchers, however, showed no evidence of concerted coupling products.^{18,19} Although the complexes studied are not strictly analogous, alkyl derivatives of cis- PtR_2L_2 would also be expected to undergo reductive elimination thermally

Table 1. Pt(IV) Complexes of the Type $\text{PtR}_3\text{L}_2\text{X}$, PtR_4L_2 and $\text{PtR}_2\text{R}'\text{L}_2\text{X}$.

<u>Complex</u>	<u>Configuration</u>
$\text{PtClMe}_3(\text{PMe}_2\text{Ph})_2$	I
$\text{PtClMe}_3(\text{AsMe}_2\text{Ph})_2$	I
$\text{PtBrMe}_3(\text{PMe}_2\text{Ph})_2$	I
$\text{PtBrMe}_3(\text{AsMe}_2\text{Ph})_2$	I
$\text{PtIme}_3(\text{PMe}_2\text{Ph})_2$	I
$\text{PtMe}_4(\text{PMe}_2\text{Ph})_2$	II
$\text{PtMe}_4(\text{AsMe}_2\text{Ph})_2$	II
$\text{PtClMe}_2(\text{COMe})(\text{PMe}_2\text{Ph})_2$	III
$\text{PtClMe}_2(\text{CO)Me}(\text{AsMe}_2\text{Ph})_2$	III
$\text{PtBrMe}_2(\text{COMe})(\text{PMe}_2\text{Ph})_2$	III
$\text{PtBrMe}_2(\text{COMe})(\text{AsMe}_2\text{Ph})_2$	III
$\text{PtBrMe}_2(\text{CH}_2\text{CH}=\text{CH}_2)(\text{PMe}_2\text{Ph})_2$	III
$\text{PtImeEt}_2(\text{PMe}_2\text{Ph})_2$	III
$\text{PtBrMe}_2(\text{CH}_2\text{Ph})(\text{PMe}_2\text{Ph})_2$	III

Figure 1. Configurations for Pt(IV) complexes of the type $\text{PtR}_3\text{L}_2\text{X}$, PtR_4L_2 , and $\text{PtR}_2\text{R}'\text{L}_2\text{X}$.



L = PMe_2Ph or AsMe_2Ph

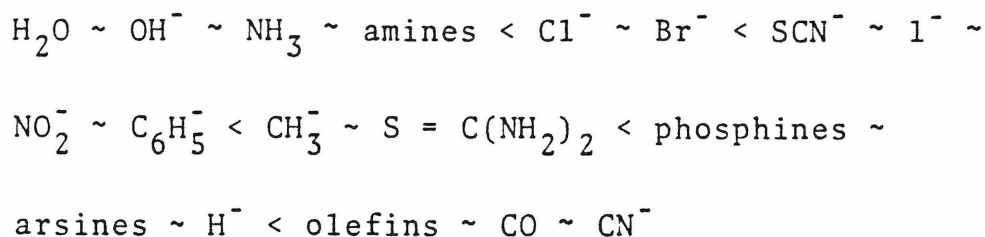
X = Cl, Br, or I, Y = acetyl, benzyl, or allyl

Table 2. Thermal Decomposition Data

Complex	Pyrolysis Temperature (°C)	Gas Evolved	Residue
PtClMe ₃ (PMe ₂ Ph) ₂	170	90% C ₂ H ₆ , 10% MeCl	<u>trans</u> -PtClMe(PMe ₂ Ph) ₂
PtClMe ₃ (AsMe ₂ Ph) ₂	180-190	C ₂ H ₆	Oil
PtBrMe ₃ (PMe ₂ Ph) ₂	160	C ₂ H ₆	<u>trans</u> -PtBrMe(PMe ₂ Ph) ₂
PtBrMe ₃ (AsMe ₂ Ph) ₂	185	C ₂ H ₆	Oil
PtIME ₃ (PMe ₂ Ph) ₂	165	C ₂ H ₆	<u>trans</u> -PtIME(PMe ₂ Ph) ₂
PtMe ₄ (PMe ₂ Ph) ₂	160	C ₂ H ₆	<u>cis</u> -PtMe ₂ (PMe ₂ Ph) ₂
PtMe ₄ (AsMe ₂ Ph) ₂	165	C ₂ H ₆	<u>cis</u> -PtMe ₂ (AsMe ₂ Ph) ₂
PtClMe ₂ (COMe)(PMe ₂ Ph) ₂	140	(CH ₃) ₂ CO	<u>trans</u> -PtClMe(PMe ₂ Ph) ₂
PtClMe ₂ (COMe)(AsMe ₂ Ph) ₂	130-135	(CH ₃) ₂ CO	<u>trans</u> -PtClMe(AsMe ₂ Ph) ₂
PtBrMe ₂ (COMe)(PMe ₂ Ph) ₂	125	(CH ₃) ₂ CO	<u>trans</u> -PtBrMe(PMe ₂ Ph) ₂
PtBrMe ₂ (COMe)(AsMe ₂ Ph) ₂	130-140	(CH ₃) ₂ CO	<u>trans</u> -PtBrMe(AsMe ₂ Ph) ₂
PtBrMe ₂ (CH ₂ Ph)(PMe ₂ Ph) ₂	135	C ₂ H ₆ , C ₂ H ₅ -Ph	not identified

as the ease of elimination has been shown to be R = acetyl > allyl > ethyl > methyl > [$^2\text{H}_3$]methyl > benzyl > phenyl > trifluoromethyl.⁴ Thus, very different modes of decomposition are possible depending on the method of initiation.

In the thermolysis of the platinum(IV) complexes, the trans effect was seen to influence labilization in the expected way. The order of increasing effect is generally considered to be²⁰



The trans influence is also reflected in Pt-C bond distances, weaker bonds being evidenced when the trans ligand Cl^- is replaced by Br^- and I^- .²¹ These effects should not be as important for photochemically induced decomposition, however. Here the respective excited state populated upon irradiation should be of primary importance with respect to ligand dissociation. For example excitation into a $\sigma - \sigma^*$ transition should result in fragmentation of this bond and expulsion of the specific ligand thus bonded. If relaxation to a state of lower energy occurs, preferential loss of a particular ligand will be seen regardless of increasingly energetic excitations.

The varied complexes proposed for study (and possibly deuterated analogues) should give specific information as to

what groups are preferentially eliminated. This should be easily detected from CIDNP data. Wavelength dependent study would aid in elucidation of the nature of the electronic transitions involved and allow speculation as to the molecular orbital scheme for this interesting class of compounds. Traditional photochemical techniques could also be employed to complement data obtained from the CINDP studies outlined above.

References

1. F. S. D'yachkovskii and N. E. Krushch, Zh. Obsch. Khim. 41, 1779 (1971).
2. G. M. Whitesides, J. F. Gaasch and E. R. Stedronsky, J. Am. Chem. Soc. 94, 5258 (1972).
3. M. F. Semmelhack and L. Ryons, Tetrahedron Lett. 2967 (1973).
4. M. P. Brown, R. J. Puddephatt and C. E. E. Upton, J. Chem. Soc. Dalton 2457 (1974).
5. G. M. Whitesides, E. J. Panek and E. R. Stedronsky, J. Am. Chem. Soc. 94, 232 (1972).
6. A. Hudson, M. F. Leppert, P. W. Lednor and B. K. Nicholson, J. Chem. Soc., Chem. Commun. 966 (1974).
7. S. H. Pine, J. Chem. Ed. 49, 664 (1972).
8. B. Kaptein, J. Chem. Soc., Chem. Commun. 732 (1971).
9. H. R. Ward, Accts. Chem. Res. 5, 18 (1972).
10. R. G. Lawler, Accts. Chem. Res. 5, 25 (1972).
11. J. K. S. Wan, Adv. in Photochem. 12, 283 (1980).

12. J. D. Ruddick and B. L. Shaw, J. Chem. Soc. A 2969 (1969).
13. M. P. Brown, R. J. Puddephat, C. E. E. Upton and S. W. Lavington, J. Chem. Soc., Dalton 1613 (1974).
14. Unpublished results, P. Slusser.
15. P. S. Braterman, R. J. Cross and G. B. Young, J. Chem. Soc., Dalton 1892 (1977).
16. P. S. Braterman, R. J. Cross and G. Brent Young, J. Chem. Soc., Chem. Commun. 627 (1975).
17. P. S. Braterman, R. J. Cross and G. B. Young, J. Chem. Soc. Dalton, 1306 (1976).
18. P. W. N. M. Van Leeuwen, C. F. Roobeek and R. Huis, J. Organomet. Chem. 131, 467 (1977).
19. R. Pierantozzi, C. McLaren and G. L. Geoffrey, unpublished results.
20. K. F. Purcell and J. C. Kotz, Inorganic Chemistry, W. B. Saunders Co., Philadelphia, 1977, 703.
21. Ibid, 704.

PROPOSITION 5

Characterization of Some Chlorate and Nitrate Reductases

Nitrate reductases have been isolated from both microorganisms¹ and higher plants.² This enzyme catalyzes the reduction of NO_3^- to NO_2^- via electron donor molecules such as NADH and NADPH. Two main types of nitrate reductases, eukaryotic and prokaryotic, may be distinguished on a phylogenetic basis.³ The principal distinction between these are the incorporation of flavin adenosene dinucleotide in the eukaryotic type and the respective forms of the iron groups involved in electron transport for each. All nitrate reductases, however, have been shown to require molybdenum for their formation and activity although characterization of the specific metal site is wanting.¹

For both eukaryotic and prokaryotic types, chlorate represents an alternative and competitive substrate.³ Some but not all species will also effect chlorate to chlorite reduction. Enzymes that reduce both substrates have been designated type A while those that reduce nitrate only as type B.⁴ Some bacteria, e.g., Aerobacter aerogenes and A. denitrificans contain both types of enzymes while others, e.g., A. aerogenes strain L-III-1 or Pseudomonas putida have only type B.³ Type A enzymes have been shown to reduce bromate as readily as chlorate (where tested) and iodate slowly or not at all.⁵ These enzymes are particulate and very sensitive to azide or cyanide.⁶ Inhibition by the former (K_i $0.3-2 \times 10^{-6}$ M) is reversible and competitive with nitrate and may indicate that each is bound to the same

metal site. Effects of cyanide are not completely reversible, and kinetics are non-competitive when cyanide reacts before nitrate. Activation energies for type A enzymes for the reduction of nitrate are moderate (7.4-12.0 KJ). Type B enzymes are often soluble and are relatively insensitive to azide or cyanide.⁷ For these ions chlorate is a mixed non-competitive and competitive inhibitor. Large activation energies (24.3 KJ) are found for nitrate reduction.

A third class of enzymes presumed to be related to nitrate reductases has been discovered by Pichinoty and Piechaud.^{6,8-11} Isolated from some bacteria e.g., *Hafnia* (6/63) sp., *Proteus vulgaris* and *Providencia stuarti*, this enzyme reduces chlorate but not nitrate. The reasons for this specificity are not clear and lead to interesting speculation as to the nature of the three types of enzymes. Two possible explanations of this unique reactivity are immediately obvious: either the molybdenum environment is different in each case and/or a different molybdenum redox couple is responsible for reduction. Structural differences seem likely in the case of type A and type B enzymes as they show dissimilar behavior with regard to reactions with cyanide and azide. The effects of these substrates has yet to be determined for the chlorate reducing enzymes, precluding structural speculations. Since the redox potential for $\text{NO}_3^-/\text{NO}_2^- \rightarrow \text{NO}_3^- - \text{INO}_2^-$ is .420 V and that of $\text{ClO}_3^-/\text{ClO}_2^-$ is .600 V, the lack of chlorate reduction by types A and B enzymes is not a

reflection of the reducing capabilities of the molybdenum site. If these are similar for all three types of enzymes, perhaps different redox couples e.g., MoVI/MoV and MoV/MoIV are operative in the respective catalytic pathways. Characterization of the enzymes from Aerobacter aerogenes, A. dentifricans, A. aerogenes strain L-III-1, Pseudomonas putida, Proteus vulgaris, and Providencia stuarti would be interesting and informative. Structural determinations and enzyme characterizations could be made by X-ray absorption edge and EXAFS, electrochemical, and EPR studies. Determination of the electron transfer mechanism would be elucidated by reaction with inorganic redox reagents.

The application of X-ray absorption spectroscopy has confirmed and elaborated ideas about the molybdenum sites in nitrogenase,^{12,13} xanthine oxidase,¹⁴ and sulfite oxidase.¹⁵ This technique could easily be extended to study the nitrate reductase and nitrate reductase related enzymes. The edge region is particularly informative as the presence of a low energy feature is indicative of a molybdenyl functionality. Also, the exact position of absorption reflects the oxidation state of molybdenum; oxidized and reduced samples of the enzymes could be analyzed for indication of the active redox couple(s). Furthermore, since edge regions reflect the molybdenum environment, similarities or lack thereof would be informative in regard to enzyme structure. This qualitative picture would be complemented in detail by the EXAFS region

of the spectrum. The key parameters derivable from this region are the number of scattering atoms of a certain type and the distance of these scatterers from the molybdenum. Thus structural components and bond orders may be evaluated for the immediate environment. In some cases, atoms beyond the first coordination sphere may also be determined. The presence of heavy metal atoms such as iron or a second molybdenum held closely and rigidly with respect to the absorbing molybdenum by a bridging ligand has a significant effect. Thus a haem group interaction might also be seen for these enzymes. Moreover, since EXAFS measurements should be sufficiently sensitive to detect an enzyme-substrate complex, should there be two absorbers with overlapping spheres (e.g., molybdenum and iron), the two sets of data would complement each other. Thus, absorption edge and EXAFS data should give a highly specific picture of the local environments of these enzymes allowing conclusive evidence as to their structures.

EPR spectroscopy can also be informative as to the nature of the surrounding ligands and the oxidation states of the metal. EPR results illustrative of important trends and potentially relevant to molybdenum enzymes are given in Table 1.¹⁶ Although there is no single complex whose parameters are identical to those for an enzyme, some of the trends are informative. In general g values close to 2.0023 correlate to small A values ($^{95,97}\text{Mo}$); these are attributable

Table 1. EPR of Selected Molybdenum(V) Models.

Complex	g	A^a	B_x	B_y	B_z	A_x^a	A_y^a	A_z^a	shfs ^e	Reference
MoO(SC ₆ H ₅) ₄ ⁻	1.990	33	1.979	1.979	2.019	22	22	56		Boyd <u>et al.</u> , (1978)
MoOCl[S ₂ P(i-C ₃ H ₇) ₂] ₂	1.966	41							$A_p=26$	Chen <u>et al.</u> , (1979)
MoO[S ₂ P(i-C ₃ H ₇) ₂](OSC ₆ H ₅) ₄	1.976	37							$A_p=19$	Stiefel <u>et al.</u> , (1977)
MoOCl(C ₉ H ₇ NS) ₂ ^b	1.969	42	1.948	1.950	2.003	42	22	63		Spence <u>et al.</u> , (1978)
MoOCl[SC(CH ₃) ₂ CH ₂ CH ₂ N(CH ₃)CH ₂ N(CH ₃)CH ₂ CH ₂ S]	1.966	41	1.940	1.949	2.006	42	17	65		Spence <u>et al.</u> , (1978)
MoOCl[SC(CH ₃) ₂ CH ₂ NHCH ₂ CH ₂ NHCH ₂ C(CH ₃) ₂ S]	1.970	42	1.944	1.958	2.011	40	25	61		Spence <u>et al.</u> , (1978)
MoOCl(C ₉ H ₇ NO) ₂ ^c	1.952	47								Chen <u>et al.</u> , (1979)
MoOCl(C ₅ H ₇ O ₂) ₂ ^d	1.939	53								Chen <u>et al.</u> , (1979)
MoO(NCS) ₅ ⁻²	1.935	50	1.928	1.928	1.944	38	38	76	$A_N=2.2$	Garif'yanov <u>et al.</u> , (1964) Rayabchikov <u>et al.</u> , (1966)
Mo(NHSC ₆ H ₄) ₃	1.988	38							$A_N=2.1$ $A_H=6.4$	Gardner <u>et al.</u> , (1978) Stiefel <u>et al.</u> , (1977)
Mo[S ₂ CN(C ₂ H ₅) ₂](NHSC ₆ H ₄) ₂	1.990	38							$A_N=2.4$ $A_H=7.4$	Pariyadath <u>et al.</u> , (1976) Stiefel <u>et al.</u> , (1977)
Mo[S ₂ CN(C ₂ H ₅) ₂] ₄ ⁺	1.979	37								Nieuwport (1974)
Xanthine Oxidase	1.977	34	1.951	1.956	2.025	37	24	41	$A_H=12$	Bray & Meriwether (1966)
Sulfite Oxidase	1.979	51	1.968	1.968	2.000	46	46	63	$A_H=10,12$	Cohen <u>et al.</u> , (1971)
Nitrate Reductase (<u>E. coli</u>)	1.983		1.964	1.985	1.999				$A_H=9-12$	Bray <u>et al.</u> , (1976)

^a 95,97Mo hyperfine splitting in gauss; ^b the ligand is thiooxine; ^c the ligand is oxine; ^d the ligand is acetylacetonate (acac); ^e ligand superhyperfine splitting in gauss for ³¹P, ¹⁴N or ¹H.

to increased covalent bonding. Furthermore, sulfur spin-orbit coupling can also lead to higher g and lower A ($^{95,97}\text{Mo}$) values, the only biologically relevant molecule (O,N,S) to do so. Therefore, g and A values are rough measures of the number of sulfur atoms in the coordination sphere. The EPR spectrum should also be informative as to the redox couple involved for each enzyme. For example, nitrate reductase obtained from Escherichia coli K12 was shown to cycle between Mo(V) and Mo(VI) states¹⁷ while the Chlorella vulgaris enzyme cycle involved Mo(IV) and Mo(V).^{18,19} Differences in the redox couples could explain the specificity of the enzymes in question.

Molybdenum undoubtedly functions as the terminal electron donor for the nitrate and chlorate reductases, as the redox potential of the haem iron (-0.060 V) falls between those for chlorate (+0.600) and nitrate (+0.425 V) and NAD(P)H (-0.315 V). While E° values for molybdenum couples in the protein bound states are not known for eukaryotic nitrate reductases, measured values for the Mo(VI)/Mo(V) couple in prokaryotic systems vary between -0.200 V and -0.400 V.²⁰ Since E° values are not known for the enzymes in question, these could be measured by cyclic voltammetry. This would also be instructive for deduction of type and number of redox states available to the enzyme. A series of experiments could then be conducted to examine the mechanism of electron transfer for these enzymes by inorganic redox

reagents. Depending on the exact potentials measured, typical reagents such as FeEDTA^{2-} ($E^\circ = .120 \text{ V}$) and Co(phen)_3^{3+} ($E^\circ = .370 \text{ V}$) might be reacted. Since it has been suggested that the molybdenum center of nitrate reductases is in a hydrophobic region of the protein,²¹ dramatic rate differences should be evidenced by hydrophobic e.g., Co(phen)_3^{3+} and hydrophilic e.g., FeEDTA^{2-} types of inorganic reagents. These experiments should elucidate the mechanism of oxidation and reduction operable in these enzymes. Furthermore, they will provide information concerning the accessibility and nature of the redox centers and the rate of intramolecular electron transfer.

The experiments proposed should elucidate the structure of the active molybdenum site, the potential and redox states operable, and the mechanism of electron transfer for each enzyme studied. This information would allow speculation as to the remarkable specificity evidenced by these enzymes in particular and to understanding the class of nitrate reductases as a whole.

References

1. E. J. Hewitt, Plant Biochemistry, D. H. Northcote, Ed., University Park Press, Baltimore, Maryland 1974.
2. L. E. Schrader, G. L. Ritenour, G. L. Eilrich and R. H. Hageman, Plant Physiol., 43, 930 (1968).
3. E. J. Hewitt and B. A. Notton, "Nitrate Reductase Systems in Eukaryotic and Prokaryotic Organisms,"

Molybdenum and Molybdenum Containing Enzymes, M.

Coughlan, ed., Pergamon Press, Oxford, England, 273 (1980).

4. F. Pichinoty, Biochim. Biophys. Acta 89, 378 (1964).
5. C. A. Fewson and D. J. P. Nicholas, Biochim. Biophys. Acta 49, 335 (1961).
6. F. Pichinoty, Arch. Mikrobiol. 68, 51 (1969).
7. F. Pichinoty, Bull. Soc. Franch Physiol. Veg. 12, 97 (1966).
8. F. Pichinoty, Bull. Soc. Chem. Biol. 47, 1526 (1965).
9. M. Piechaud, J. Ping, F. Pichinoty, E. Azdelay and L. LeMinor, Ann. Inst. Pasteur 112, 24 (1967).
10. F. Pichinoty and M. Piechaud, Ann. Inst. Pasteur 114, 77 (1968).
11. F. Pichinoty, Arch Mikrob. 68, 51 (1969).
12. S. P. Cramer, K. O. Hodgson, W. O. Gellum and L. E. Mortenson, J. Am. Chem. Soc. 100, 3398 (1978).
13. S. P. Cramer, K. O. Hodgson, W. O. Gellum, L. E. Mortensen, E. I. Stiefel, J. R. Chisnell, W. J. Brill and V. K. Shah, J. Am. Chem. Soc. 100, 3814 (1978).
14. T. D. Tullius, D. M. Kurtz, Jr., S. D. Conradson and K. O. Hodgson, J. Am. Chem. Soc. 101, 2776 (1979).
15. S. P. Cramer and K. O. Hodgson, Prog. Inorg. Chem. 25, 1 (1979).
16. E. I. Stiefel, "Structures and Spectra of Molybdoenzyme Active Sites," Molybdenum and Molybdenum

Containing Enzymes, M. Coughlan, ed., Pergamon Press, Oxford, England, 80 (1980).

17. S. P. Vincent and R. C. Bray, Biochem. J. 171, 639 (1978).
18. L. Solomonson, "Nitrogen Assimilation in Plants," Proc. Long. Ashton Symp. E. J. Hewitt and C. V. Cutting, eds., Academic Press, N.Y. and London, in press.
19. E. J. Hewitt, B. A. Notton and C. D. Gardner, Biochem. Soc. Trans. (in press).
20. R. J. P. Williams, "Advances in the Chemistry of Coordination Compounds," Proc. VI Sympos. Internal. Conf. Coordination Chemistry, S. Kirschner, ed., Detroit (1961).
21. C. D. Gardner, M. R. Hyde, F. E. Mabbs and V. I. Routledge, Nature, 252, 579 (1974).